ORNL/TM-2015/646

Design and Demonstration of a Material-Plasma Exposure Target Station for Neutron Irradiated Samples

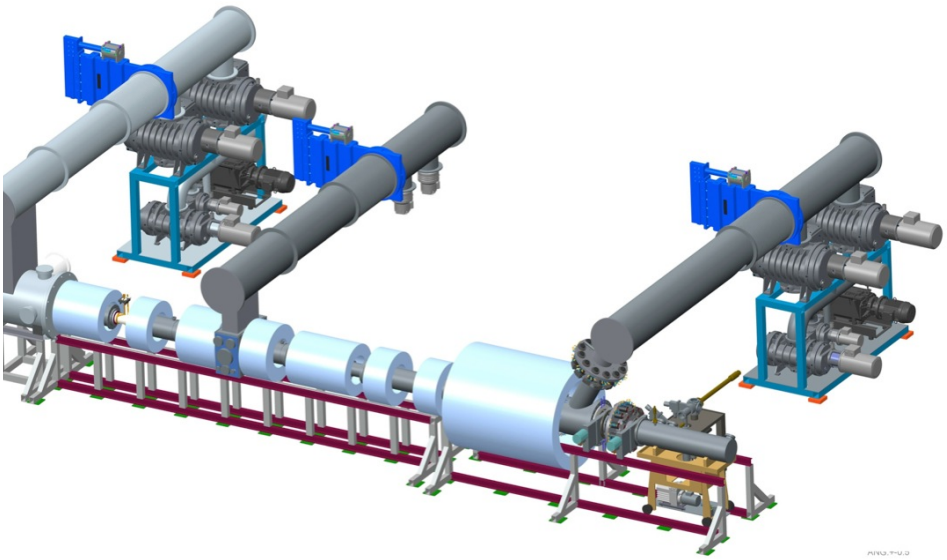

J. Rapp
A.M. Aaron
G.L. Bell
T.W. Burgess
R.J. Ellis
D. Giuliano
R. Howard
J. Kiggans
T. Lessard
E.K. Ohriner
D.E. Perkins
V.K. Varma

October 20, 2015

OAK RIDGE NATIONAL LABORATORY
MANAGED BY UT-BATTELLE FOR THE US DEPARTMENT OF ENERGY

ORNL/TM-2015/646

LOIS 7033

Design and Demonstration of a Material-Plasma Exposure Target Station for Neutron Irradiated Samples

J. Rapp
A.M. Aaron
G.L. Bell
T.W. Burgess
R.J. Ellis
D. Giuliano
R. Howard
J. Kiggans
T. Lessard
E.K. Ohriner
D.E. Perkins
V.K. Varma

October 20, 2015

Prepared by
OAK RIDGE NATIONAL LABORATORY
Oak Ridge, TN 37831-6283
managed by
UT-BATTELLE, LLC
for the
US DEPARTMENT OF ENERGY
under contract DE-AC05-00OR22725

CONTENTS

1. INTRODUCTION 1
2. NEUTRONICS CALCULATIONS 3
   2.1 BACKGROUND AND DESCRIPTION OF HFIR 3
      2.1.1 Specifics of the HFIR Irradiations 5
      2.1.2 Assessment of Displacement Damage Levels 8
   2.2 RESULTS OF SIMULATED IRRADIATION OF MATERIALS FOR USE IN MPEX 8
   2.3 DISCUSSION OF NEUTRONICS CALCULATIONS 10
3. MATERIAL FLOW ANALYSIS AND IRRADIATION CAPSULE DESIGN 12
   3.1 DETAILS FOR CAPSULE IRRADIATION AT HFIR AND POST IRRADIATION HOT CELL WORK 12
      3.1.1 MPEX Irradiation Capsule 12
      3.1.2 Post Irradiation Shipping and Hot Cell Work 17
   3.2 RADIOLOGICAL FACILITY TO SUPPORT MPEX AND SPECIMEN STORAGE 18
      3.2.1 Specimen Material Flow Discussion 19
      3.2.2 Creation of a Radiological Facility (RF) for 7625 19
      3.2.3 Handling and Storage of MPEX Samples 21
      3.2.4 Nuclear Materials Accountability 23
      3.2.5 Costs associated with the 7625 Radiological Facility re-designation 23
4. DESIGN OF TARGET STATION AND ANCILLARIES 25
   4.1 TARGET DESIGN INTRODUCTION 25
   4.2 TARGET STATION DESIGN REQUIREMENTS 25
      4.2.1 Design Alternatives 26
   4.3 MPEX TARGET 28
      4.3.1 Target Design 28
      4.3.2 Target Puck design 30
      4.3.3 Target Puck Holder 32
   4.4 TARGET EXCHANGE CHAMBER 35
   4.5 DIAGNOSTIC CHAMBER 39
   4.6 TARGET INTRODUCTION INTO TEC AND THE GLOVE BOX DESIGN 41
      4.6.1 Contamination Control 43
   4.7 PROTOTYPING OF THE TARGET 44
5. ENRICHED TUNGSTEN MATERIAL PROCESSING 45
6. REFERENCES 49

APPENDIX A. ACTIVITIES BY NUCLIDE FOR FIVE LIKELY MATERIALS IRRADIATED IN HFIR AND COOLED FOR AT LEAST TWO YEARS A-3

APPENDIX B. DOSE EQUIVALENT RATES (MREM/HR) FOR SEVERAL MPEX MATERIAL SAMPLES AS A FUNCTION OF COOLING TIME, THAT WERE IRRADIATED IN THE HFIR CENTRAL FLUX TRAP FOR 10 CYCLES. B-2

APPENDIX C. DIFFERENCES IN SNS AND HFIR IRRADIATIONS C-2

APPENDIX D. MPEX SYSTEM SAFETY ISSUES OPERATING NEAR A MAGNETIC FIELD D-2

APPENDIX E. ALTERNATIVE APPROACH FOR LINEAR MOTION OF THE TARGET INTO PMI CHAMBER E-2

LIST OF FIGURES

Fig. 1 The HFIR core, showing inner and outer fuel elements composed of many fuel plates. Target sites in the flux trap region are seen in the center. 4
Fig. 2.The HFIR reactor system with main irradiation site features indicated 5
Fig. 3. Histogram (in 252 neutron energy groups) of the neutron spectrum in an elemental tungsten sample irradiated in HFIR in the flux trap region at the core midplane. 6
Fig. 4. Neutron spectra in a HFIR flux trap target inside or outside of a Gd thermal neutron shield. 7
Fig. 5. MPEX radioactive material flow diagram 12
Fig. 6. Cross-sectional view of the MPEX PFC irradiation vehicle 13
Fig. 7. Axial view of the trefoil footprint, trefoil target layout, and the proposed TTRRH layout 14
Fig. 8. Temperature Contour Plot (°C) for the 700°C and 1200°C cases 15
Fig. 9. Radial cross-section of the HFIR 16
Fig. 10. Sugarman shipping cask 18
Fig. 11. Storage vault wall cross section 22
Fig. 12. MPEX sample storage container design concept 22
Fig. 13. Metal jars used to house irradiated MPEX samples 22
Fig. 14. Overall layout of the MPEX system 26
Fig. 15. Components that interface with TEC 27
Fig. 16. Target design for MPEX 29
Fig. 17. Target puck and target puck holder assembly 29
Fig. 18. Target puck assembly 30
Fig. 19. Cross-sectional view of the target puck showing the water flow through copper channels 31
Fig. 20. Temperature of the target versus thickness of tungsten back plate and grafoil 31
Fig. 21. Temperature Profile of the Target Puck in Plasma 32
Fig. 22. Cooling lines connections on the Target Puck Holder 33
Fig. 23. 15 degree target puck holder showing puck, tungsten cover and copper base 34
Fig. 24. Flow channels for the 15 degree target puck holder 34
Fig. 25. Target Exchange Chamber 35
Fig. 26. Schematic of the Layout of PMI, TEC and Diagnostic Chambers 36
Fig. 27. Target attached to the telescoping arm fully extended 37
Fig. 28. Target located inside the PMI chamber 38
Fig. 29. Telescoping actuator showing the target cooling lines 38
Fig. 30. Rail System for TEC transfer 39
Fig. 31. Diagnostic chamber and TEC interface 40
Fig. 32. Clam Shell Actuation in the Diagnostic Chamber 40
Fig. 33. Vacuum Cart for target transport 41
Fig. 34. Vacuum cart interfacing with TEC during target change out 42
Fig. 35. Vacuum cart and Glove Box interface 43
Fig. 36. 3D Printed and Fabricated Target Puck 44
Fig. 37. SEM analysis of W-182 powder 45
Fig. 38. Cold pressed tungsten to 55% density and sintered tungsten to 67% density 46
Fig. 39. Graphite die and tungsten pellets after hot-pressing to density of 90% (left) and 93% (right). 47
Fig. 40. Canned tungsten pellets in stainless steel 47
Fig. 41: Broken tungsten sections in a matrix of steel. 48

LIST OF TABLES

Table 1. Summary of Simulated Irradiations for 10 HFIR Cycles of Candidate MPEX Sample Materials and Representative Dose Rates after Two Years of Cooling 9
Table 2. Activities (Bq/g) for top active nuclides and total activity in W targets at Discharge (after 10 cycles irradiation) and after two years of cooling 11
Table 3. Summary of results for the MPEX rabbit 14
Table 4. MPEX candidate materials and activity after 2 year decay period 16
Table 5. Calculated HC-3 and RQ values for estimated PFC materials 20

1. INTRODUCTION

Fusion energy is the most promising energy source for the future and one of the most important problems to be solved progressing to a commercial fusion reactor is the identification of plasma facing materials compatible with the extreme conditions in the fusion reactor environment. The development of plasma material interaction (PMI) science and the technology of plasma facing components are key elements in the development of the next step fusion device in the United States, the so-called Fusion Nuclear Science Facility (FNSF). All of these PMI issues and the uncertain impact of the 14 MeV neutron irradiation have been identified in numerous expert panel reports to the fusion community. The 2007 Greenwald report [1] classifies reactor plasma facing materials (PFCs) and materials as the only Tier 1 issues, requiring a ". . . major extrapolation from the current state of knowledge, need for qualitative improvements and substantial development for both the short and long term."

The Greenwald report goes on to list 19 gaps in understanding and performance related to the plasma-material interface for the technology facilities needed for DEMO oriented R&D and DEMO itself. Of the 15 major gaps, six (G7, G9, G10, G12, G13) can possibly be addressed with ORNL's proposal of an advanced Material Plasma Exposure eXperiment [1]. Establishing this midscale plasma materials test facility at ORNL is a key element in ORNL's strategy to secure a leadership role for decades of fusion R&D. That is to say, our end goal is to bring the "signature facility" FNSF home to ORNL.

This project is related to the pre-conceptual design of an innovative target station for a future Material-Plasma Exposure eXperiment (MPEX). The target station will be designed to expose candidate fusion reactor plasma facing materials and components (PFMs and PFCs) to conditions anticipated in fusion reactors where PFCs will be exposed to dense high temperature hydrogen plasmas providing steady state heat fluxes of 5-20 MW/m2 and ion fluxes up to 1024 m-2s-1. Since PFCs will have to withstand neutron irradiation displacement damage up to 50 dpa, the target station design must accommodate radioactive specimens (materials to be irradiated in HFIR or at SNS) to enable investigations of the impact of neutron damage on materials. Therefore, the system will have to be able to install and extract irradiated specimens using equipment and methods to avoid sample modification, control contamination, and minimize worker dose. Included in the design considerations will be an assessment of all the steps between neutron irradiation and post-exposure materials examination/characterization, as well as an evaluation of the facility hazard categorization. In particular, the factors associated with the acquisition of radioactive specimens and their preparation, transportation, experimental configuration at the plasma-specimen interface, post-plasma-exposure sample handling, and specimen preparation will be evaluated.

The report is structured as follows:

Neutronics calculations to determine the dose rates of the samples were carried out. Those calculations give information about the radioactivity of the samples after irradiation in HFIR or at SNS. The calculations were performed for a large number of potential plasma facing materials. Cool-down periods were determined to reduce the dose rates to levels, which are acceptable for handling the materials in glove boxes. All calculations were done for 12mm diameter and 1mm thick target samples. This is the largest size target feasible to be irradiated in the so-called flux trap of HFIR (In order to reduce uncertainties in the PMI experiments the exposed target surface area should be considerably larger than the total surface area including shadowed surfaces due to mounting of the target in MPEX).

A Material Flow analysis was carried out. This includes the whole lifecycle of a target specimen from irradiation, cool-down, shipping to the hot-cells, opening of the irradiation capsules, transfer from hot-cells to location of MPEX and storage in building 7625. As part of this flow analysis also a design of the irradiation capsule to be used in HFIR was done. In addition the requirements for handling radioactive specimen in building 7625 were elaborated and discussed.

A pre-conceptual design of the target station for exposure of neutron-irradiated samples to fusion reactor relevant plasmas was completed. This design includes the target holder, the target exchange chamber, the diagnostic chamber and the glove box. The design process is documented and design choices are explained.

2. NEUTRONICS CALCULATIONS

The assessments of the neutronics include the calculated induced radioactivity and resulting radiation dose rates of a variety of potential fusion reactor plasma-facing materials e.g., tungsten. The scientific code packages Monte Carlo N-Particle (MCNP) and Standardized Computer Analyses for Licensing Evaluation (SCALE) were used to simulate irradiation of the samples in HFIR. This included the generation and depletion of nuclides in the material and the subsequent composition, activity levels, gamma radiation fields, and resultant dose rates as a function of cooling time. A challenge of the MPEX project is to minimize the radioactive inventory in the preparation of the samples and the sample dose rates for inclusion in the MPEX facility.

Unfortunately, due to the lack of a fusion-relevant intense neutron source, the maximum experimental 14 MeV neutron exposure levels achieved to date (~0.01 DPA) are about four orders of magnitude below what will be required in a demonstration fusion reactor. A high fluence accelerator-based 14 MeV neutron source, the International Fusion Materials Irradiation Facility (IFMIF)[3] is currently in the engineering validation and engineering design activities phase. However, its realization is very uncertain. Computational modeling and experimental studies indicate the initial displacement damage structures for fission, 14 MeV D-T fusion, and spallation neutrons are similar.[4,5,6] This suggests fission reactors can continue to be used for fundamental studies of radiation-induced microstructural and mechanical properties of candidate fusion reactor materials.

This assessment will mainly focus on irradiation of plasma-facing materials with the High Flux Isotope Reactor (HFIR)[7-13], which can reach high DPA levels.

This will enable investigations of the impact of neutron damage on materials properties, behavior, and performance. The target exchange system of the MPEX device must be able to install and extract irradiated specimens using equipment and methods to avoid sample modification, to control contamination, and to minimize worker dose. Design considerations will include an assessment of all the steps between neutron irradiation and post-exposure materials examination/characterization, as well as an evaluation of the facility hazard categorization. In particular, the factors associated with acquisition of radioactive specimens and their preparation, transportation, experimental configuration at the plasma-specimen interface, post-plasma-exposure sample handling, and specimen preparation for detailed materials characterization will be evaluated, and the results will be integrated into the target station design.

To that end, material samples are to be irradiated in HFIR or SNS to damage levels of at least 10 DPA. This paper focuses on the proposed irradiation of sample materials in the HFIR flux trap target region under total neutron flux irradiation levels of about 4.0×10^{15} n/cm^2/s with a large fast flux component. The scientific code packages Monte Carlo N-Particle (MCNP 5.151) [16] and Standardized Computer Analyses for Licensing Evaluation (SCALE6.1.2)[17, 18] were used in sample irradiation simulations. Some comparisons to the results of simulated material sample irradiations in SNS will also be shown. Based on health physics good practices, for safe handling of sample disks in a glove box, the dose equivalent rate per sample disk would be less than 100 μSv/hr (10 mrem/hr) at a distance of 0.30 m (1 ft) from a suitably cooled irradiated sample.

2.1 BACKGROUND AND DESCRIPTION OF HFIR

It is a beryllium-reflected, light-water–cooled and –moderated, flux-trap-type reactor that uses uranium highly enriched in 235U as the fuel and provides one of the highest steady-state neutron fluxes of any research reactor in the world. The HFIR central flux trap target region (a 12.70-cm [5-in]-diameter hole) forms the center of the core and is typically used for isotope production or material irradiation

experiments. The fast flux (> 0.1 MeV) in this region exceeds 1.1 × 1015 n/cm2/s. The thermal neutron flux in the flux trap region can exceed 2.5 × 1015 n/cm2/s.

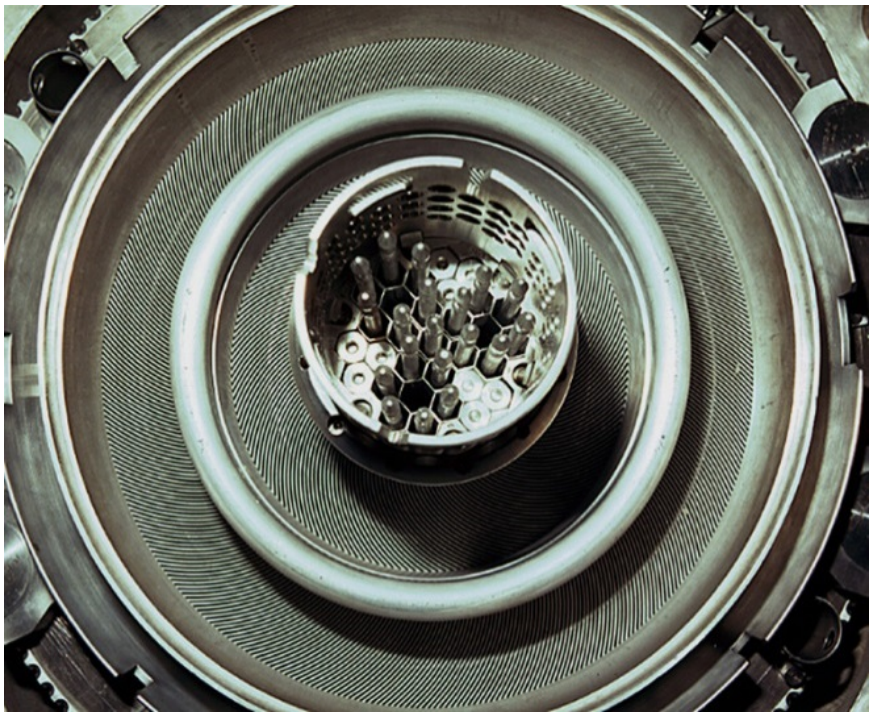

Fig. 1 The HFIR core, showing inner and outer fuel elements composed of many fuel plates. Target sites in the flux trap region are seen in the center.

The fuel region is composed of two concentric fuel elements (Fig. 1) made up of involute-shaped fuel plates: the inner fuel element (IFE) contains 171 fuel plates, and the outer fuel element (OFE) contains 369 fuel plates. The involute design of the fuel plates provides constant-width coolant channels between adjacent plates. The HFIR fuel (U_3O_8-Al cermet) is nonuniformly distributed along the arc of the involute to minimize the radial peak-to-average power density ratio. A burnable poison (B_4C) is included in the inner fuel element primarily to reduce the negative reactivity requirements of the reactor control plates. A typical highly enriched uranium (HEU) core loading in HFIR is 9.4 kg of ^{235}U and 2.8 g of ^{10}B. Fig. 2 also shows the numerous target irradiation locations in the flux trap target (FTT) region within the fuel elements.

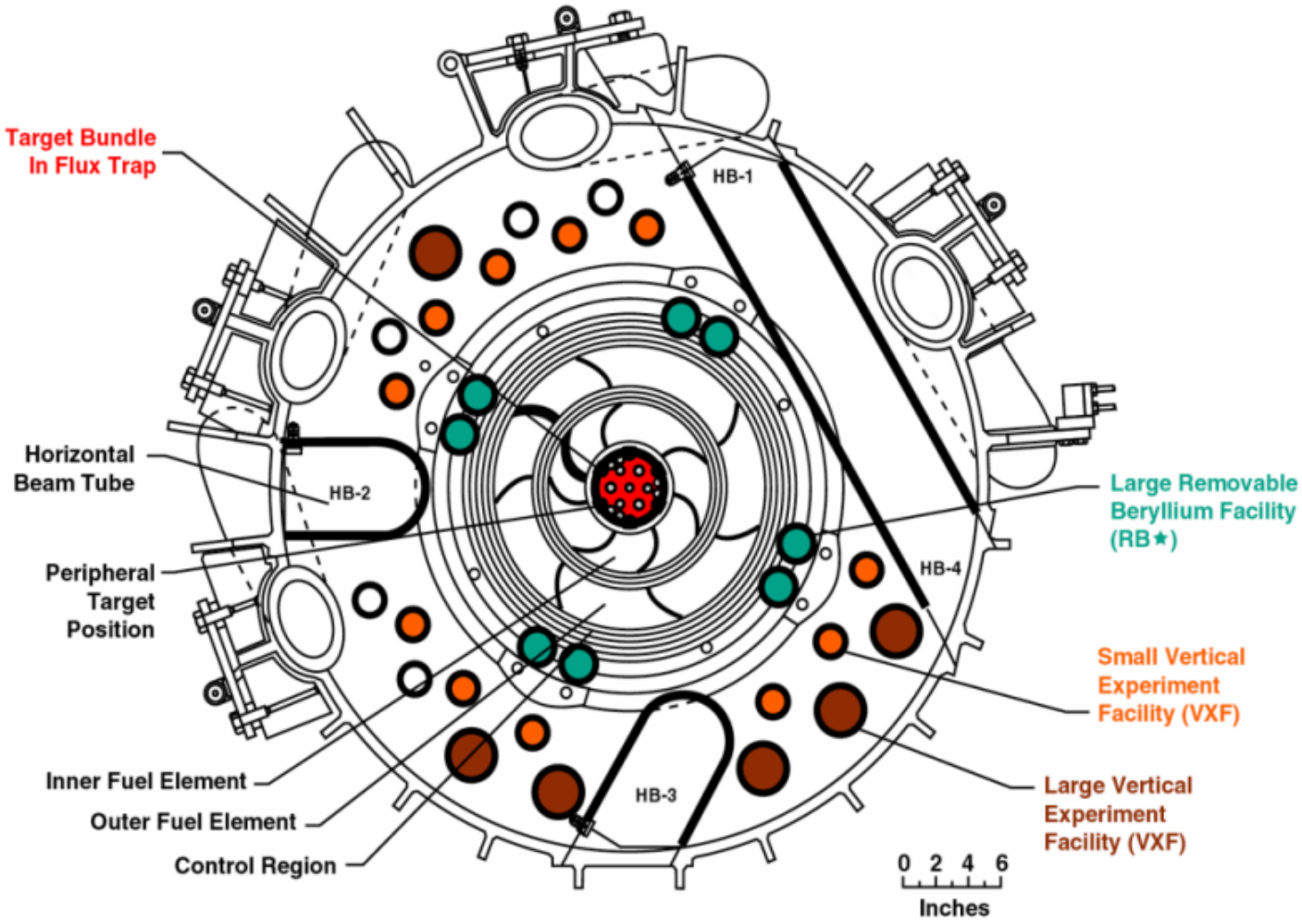

Fig. 2.The HFIR reactor system with main irradiation site features indicated

The irradiation of the material samples for MPEX is planned to take place in a specially designed facility that will replace three of the 31 target sites in the flux trap region. The samples for irradiation will be placed axially at the HFIR midplane to utilize the maximized neutron flux at that location.

2.1.1 Specifics of the HFIR Irradiations

A HFIR cycle normally consists of full-power operation at 85 MW (thermal) for a period of 22 to 26 days (depending on the experiment and reactivity load of the irradiation targets in the reactor), followed by an end-of-cycle outage of two to three weeks for refueling, control plate change-out (every several years), calibrations, maintenance, and inspections. The irradiation of the material samples for MPEX is planned to take place in a specially designed facility that will replace three target sites in the flux trap region. The irradiated samples will be placed axially at the HFIR mid-plane to utilize the maximized neutron flux at that location. Numerous experimental material irradiations have been completed in HFIR[11, 12, 19]. Some of

the experimental results related to displacement damage and material structural changes have been published in these and other studies.[20]

Fig. 3 shows the neutron flux spectrum in an elemental tungsten sample at the mid-plane of a target location, as calculated in detailed tally calculations using MCNP 5.151.[21] The spectrum is presented as a histogram (in 252 neutron energy groups) with flux per lethargy along the linear y-axis and neutron energy along the logarithmic x-axis. The displacement damage accumulated in the irradiated sample is dominated by the fast-neutron fluence and the high intermediate-energy neutron fluence. The major characterizations of the neutron energy are thermal ($E < 0.625$ eV) – the thermal neutron flux is 2.22×10^{15} n/cm^2/s, intermediate ($0.1 \text{ MeV} \geq E > 0.625$ eV) – the intermediate neutron energy flux is 1.33×10^{15} n/cm^2/s, and fast ($E > 0.1$ MeV) neutron energy – the fast neutron flux is 1.17×10^{15} n/cm^2/s.

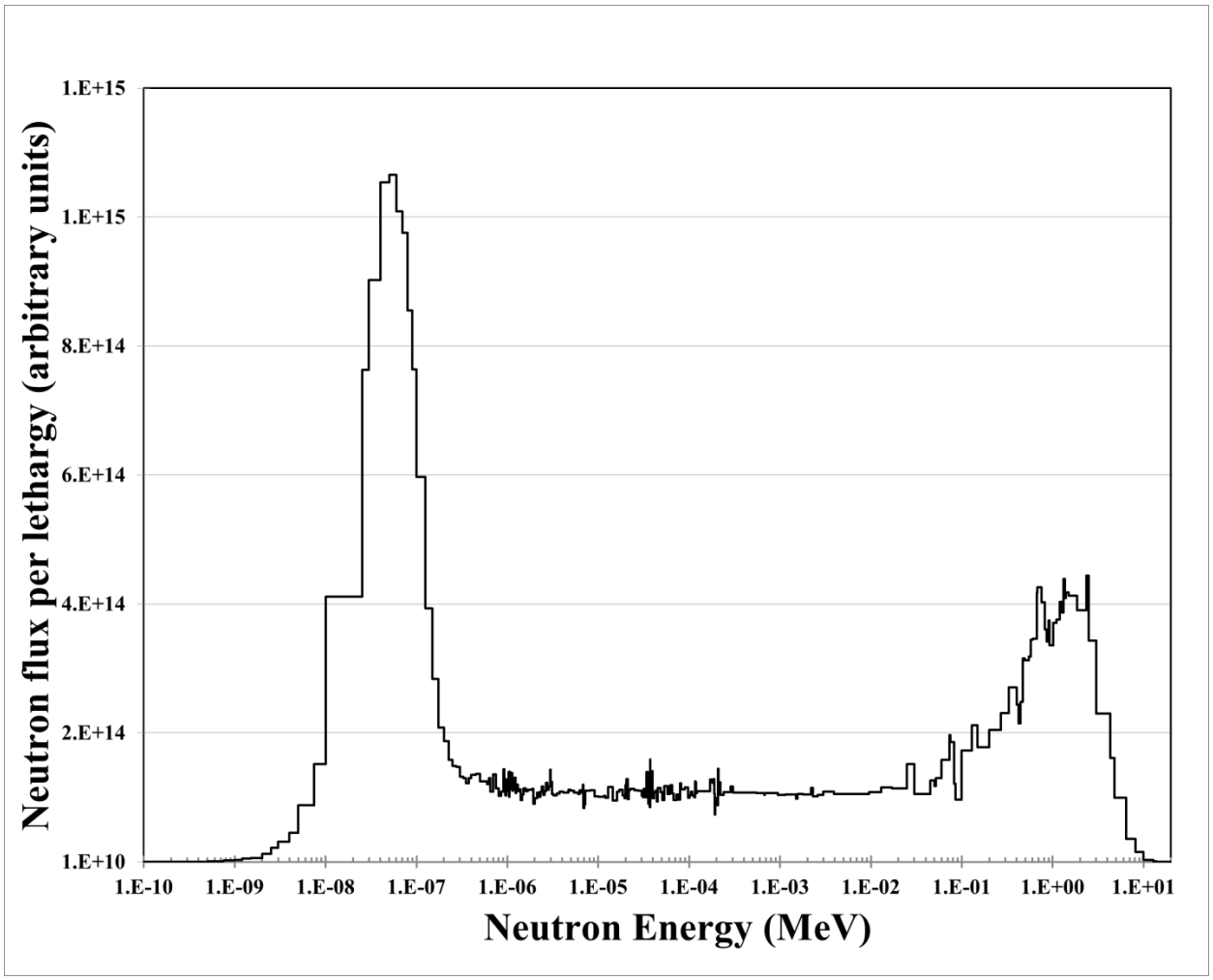

Fig. 3. Histogram (in 252 neutron energy groups) of the neutron spectrum in an elemental tungsten sample irradiated in HFIR in the flux trap region at the core midplane.

A fusion neutron spectrum will lead to different transmutants (mainly Re and Os isotopes) than the HFIR neutron spectrum, in irradiation reactions with tungsten for example. Also, a fusion neutron spectrum would result in a lower He/DPA ratio. The effects of the DPA level can be investigated and the chemical effects of the different transmutants and He levels can be studied separately. The thermal neutron

components in the HFIR neutron spectrum is large and causes many transmutations to Re and Os and high activity levels.

As used in irradiations in the HFIR flux trap region, Gd thermal neutron shields can be utilized to remove the thermal neutron flux impinging on the tungsten targets. Fig. 4 shows the effect Gd shields have on the relevant neutron spectrum. As seen in the figure, most of the thermal neutrons and a large portion of the neutron flux in the intermediate energy range are removed from the neutron spectrum.

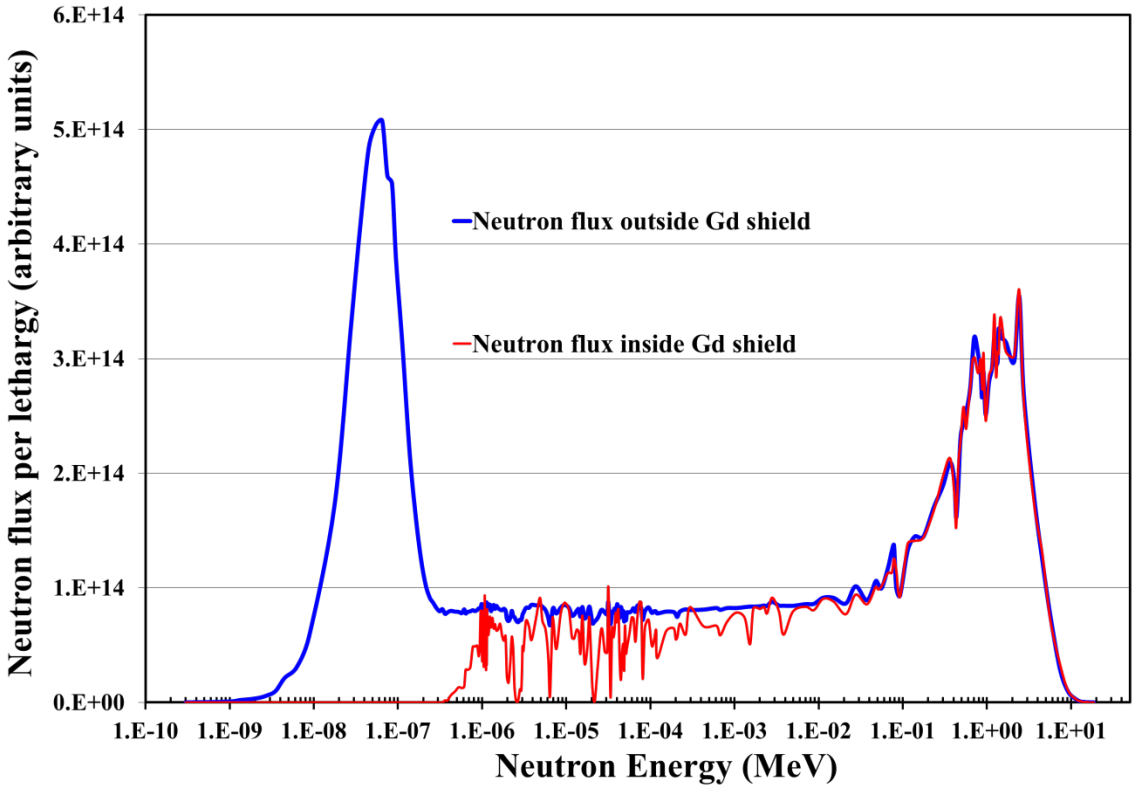

Fig. 4. **Neutron spectra in a HFIR flux trap target inside or outside of a Gd thermal neutron shield.**

Current experience with the use of Gd shields in irradiation rabbits in single sites in the HFIR flux trap region is that the shields are viable for about two HFIR cycles. In order for Gd shields to be effective for 10 or more HFIR cycles the thickness of the shields will need to be increased considerably, which would require a design of a capsule for smaller material specimens (~6 mm diameter). Since Gd is a strong thermal neutron absorber, the reactivity load of a cylindrical shield is proportional to its circumference. If the reactivity load of the Gd shield is to great, the length of the HFIR cycle could be reduced, which would be expensive for the experiment as penalties would be incurred

2.1.2 Assessment of Displacement Damage Levels

As discussed in the introduction, it is important to have MPEX sample materials available with displacement damage between 10–50 DPA of structural damage. The displacement damage phenomena considered in this work are based on the Norgett, Robinson, and Torrens (NRT) formalism.[22] In a crystalline material, a displacement cascade can be considered a series of collisions that is initiated when an atom, known as "the primary knock-on atom" (PKA), is hit by a high-energy neutron (in this case) and then recoils with a certain amount of kinetic energy that is dissipated in secondary, tertiary, etc., collisions. The NRT formalism presents the total level of displaced atoms (in DPA) produced by a PKA with kinetic energy E_{PKA} as shown in Equation (1) 23.

$$\nu_{NRT} = 0.8\ T_d(E_{PKA}) / 2E_d \qquad (1)$$

E_d is the displacement threshold energy; T_d (a function of E_{PKA}) is the available damage energy; and the factor 0.8 is an efficiency factor that accounts for realistic atomic scattering (as compared to hard sphere collisions). In applying Equation (1), the level of displacement damage accumulated in the samples undergoing HFIR fast flux irradiation was estimated using an MCNP code methodology with F4 tallies with the total damage cross section, MT=444. This tally, in conjunction with the proper normalization for the neutron flux in the sample, yields the total available damage energy (T_d) for displacement damage[24, 25].

The methods and related DPA information described in Ref. 24 were used in earlier studies[11] concerning HFIR fast neutron irradiations. The value of the DPA level is determined using Equation (1) with the appropriate choice of E_d. Values of E_d generally depend on material structure, crystal planes/directions, and grain size. E_d generally ranges from ~20 to ~40 eV for most metals and alloys used in structural applications.[23] Alloys and mixtures have a net E_d based on the elements in their composition, the crystalline structure, and the direction of the incident neutrons.

The American Society for Testing and Materials (ASTM) in a table of E_d values, recommends values for E_d for tungsten and similar elements in the 90 eV range. Generally, experimental determinations for E_d tend to be lower than ASTM values. Refs. 25 and 26 also discuss several values of E_d for tungsten. For the irradiation of tungsten samples in the high fast-flux environment in the HFIR flux trap region, the rate at which displacement damage accumulates was determined to be 1.0±7% DPA per HFIR cycle, when an effective E_d of 42 eV[26, 27, 28] is considered. For the simulated irradiations discussed in this paper, it was assumed the samples are irradiated in HFIR for 10 cycles, giving an expected displacement damage level of 10 DPA for the irradiated tungsten. The Monte Carlo relative error for the displacement damage in DPA is about ±7% based on the tally statistics from the appropriate MCNP case outputs.

2.2 RESULTS OF SIMULATED IRRADIATION OF MATERIALS FOR USE IN MPEX

Fig. 5 shows the short-term (cooling time) relation between the specific activity (in Ci/g) of a variety of tungsten samples of different compositions and varying levels of displacement damage (by length of irradiation in HFIR). The calculations account for the 24-25 day HFIR cycles (at power) with several weeks being shut down for the maintenance of the reactor system between cycles. The different behavior between natural tungsten and tungsten enriched in ^{182}W are seen in the curves. Generally, natural tungsten undergoing fast fluence neutron irradiation transmutes with irradiation time to rhenium and osmium, along with many high specific activity radionuclides.

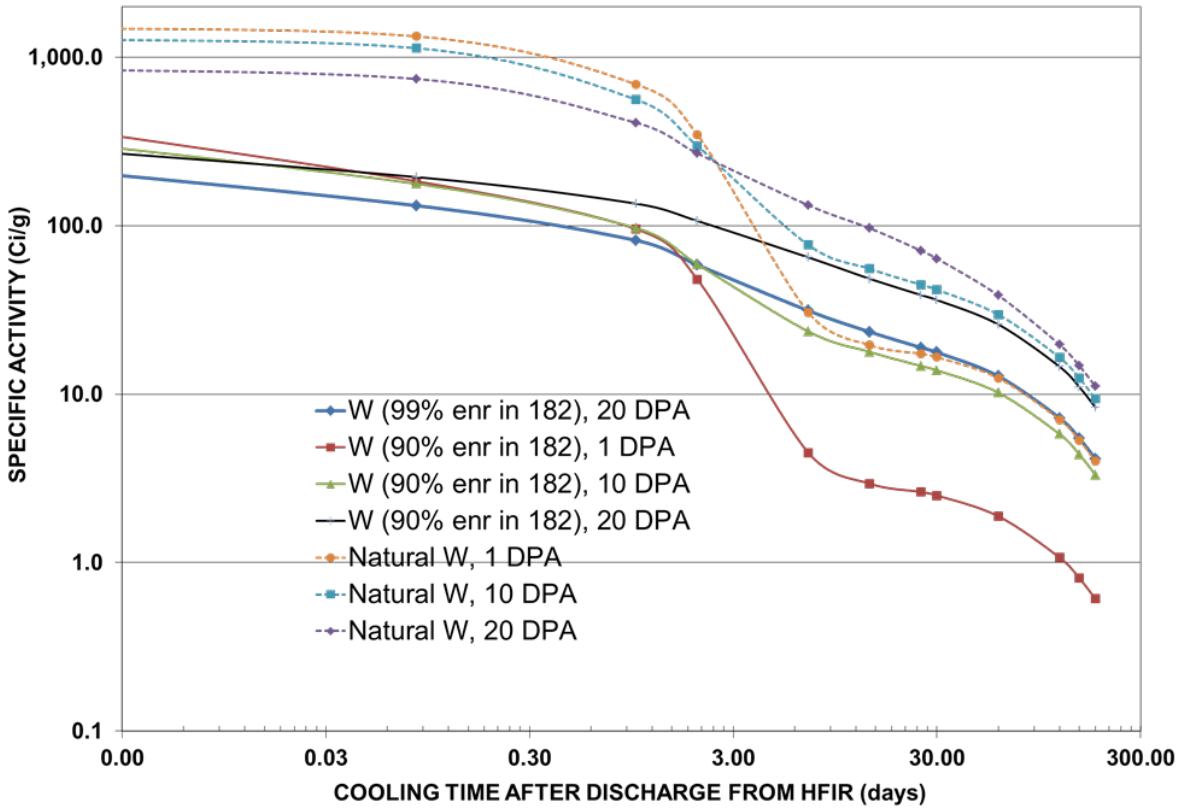

Fig. 5. Specific activities of tungsten samples as function of composition and DPA damage and exposure in HFIR

For example, Fig. 5 shows that at about half a year after discharge, the specific activity for a 20 DPA (~20 cycle) 99%-enriched tungsten sample is approximately the same as for a one DPA (one cycle) natural tungsten sample. Also shown is an interesting short-term effect that tungsten samples irradiated for fewer HFIR cycles actually have higher specific activities than samples irradiated for longer times, because for longer irradiations, certain high-activity radionuclides are transmuted reducing their activity in the samples.

Table 1. Summary of Simulated Irradiations for 10 HFIR Cycles of Candidate MPEX Sample Materials and Representative Dose Rates after Two Years of Cooling

Material	Brief Description of Material	Density (g/cc)	Mass/Disk (g)	Disk Dose Rate (μSv/hr at 0.30 m)	Percentage uncertainty (1σ) in the disk dose rates
C	Carbon as graphite	2.23	0.252	2.13E-06	±1.5E-02%
SiC	Standard SiC	3.21	0.363	6.11E-05	±2.4E-02%
Li-7	Li enriched to 100% Li7	0.53	0.060	3.30E-02	±6.8E-03%
Be	Natural Be	1.85	0.209	1.62E-01	±7.9E-03%

Li	Natural Li	0.53	0.060	8.51	±6.8E-03%
Mo-La_2O_3	1 wt% La_2O_3	10.18	1.151	14.9	±8.0E-03%
Mo	Natural Mo	10.22	1.156	14.9	±7.9E-03%
W_enr99%	99 wt% W-182	19.25	2.177	88.6	±2.7E-02%
W_enr90%	90 wt% W-182	19.25	2.177	108.1	±2.6E-02%
W-SiC	Natural W with 50 wt% SiC	11.23	1.270	190.0	±2.4E-02%
WC	Natural W with 50 at% C (6.127 wt% C)	15.63	1.768	287.8	±2.4E-02%
W-TiC	Natural W with 0.80 wt% Ti	18.71	2.116	358.2	±2.4E-02%
W-La_2O_3	Natural W with 1 wt% La_2O_3	19.12	2.162	364.2	±2.4E-02%
W-Re	Natural W with 20 at% Re (20.14 wt% Re)	19.30	2.183	364.6	±2.6E-02%
W-Rh	Natural W with 3 at% Rh (1.7 wt% Rh)	19.20	2.172	366.0	±2.4E-02%
W-K	Natural W with 100 appm K (0.12 wt% K)	19.20	2.175	371.3	±2.4E-02%
W_nat	Natural W	19.25	2.177	371.4	±2.4E-02%
W-Fe	Natural W with 0.9 wt% Fe	19.00	2.149	435.5	±2.3E-02%
W-Pd	1.5 at% Pd (0.87 wt% Pd)	19.20	2.172	1285.8	±1.6E-02%
W-Ta-TiC	Natural W with 1 wt% TiC; 10 wt% Ta	18.48	2.090	1521.9	±2.6E-02%
W-Ta10	Natural W with 10 wt% Ta	18.96	2.144	1565.2	±2.6E-02%
Ta-W10	Ta with 10.1 wt% W	16.69	1.917	7245.7	±2.4E-02%
Ta	Natural Ta	16.69	1.888	10477.2	±2.6E-02%

Tungsten samples are a prime focus of this work but an extensive list of possible fusion reactor plasma-facing materials was established and assessed.Table 1 presents a summary of the detailed investigation of more than 20 possible mpex test samples. The densities are indicated for the alloy or mixture of interest. All of the sample dose rates and related properties are based on samples of standard size: 1.2 cm in diameter and 1 mm thick. The dose equivalent rates (μsv/hr) are calculated using the scale/mavric (monaco with automated variance reduction using importance calculations) [17] Monte Carlo radiation shielding sequence in conjunction with 57-group gamma source intensity distributions calculated using origen. The scale/mavric sequence is based on the cadis (consistent adjoint driven importance sampling) methodology. The gamma-ray strength (accounting for gamma intensity, photons/s, from the source for gammas with energy greater than 10 kev) and the gamma spectrum representing the gamma source from the appropriate sample disks (per g of the sample material) for each particular cooling time were entered as input to scale/mavric. Scale/mavric performed monte carlo radiation transport simulations to determine the dose equivalent rate (μsv/hr) at specified locations, starting from the material sample disks. Dose rate determinations were performed with scale/mavric using the ansi standard (1977) flux-to-dose-rate response data.

2.3 DISCUSSION OF NEUTRONICS CALCULATIONS

The dose equivalent rates listed in Table 1 at a nominal distance of 0.30 m (1 ft) from the various HFIR-irradiated samples span a large range in strengths. These differences are due to the generation and depletion of radionuclides during multiple cycles in HFIR. The dose rate is due to the gamma-energy

distribution for gamma rays more energetic than 10 keV. Table 1 tabulated comparative results for a nominal cooling time of two years. The time behavior of the gamma-source radionuclides that contribute to the gamma radiation and the dose rate determines how the sample dose rates change with time.

After two years of cooling, tungsten enriched to 99 wt% in ^{182}W has an associated 0.30-m (1-ft) dose rate of just under 90 μSv/hr. This meets the dose rate criterion mentioned earlier to allow safe handling by staff of the samples that will go into MPEX. However, the natural tungsten sample at the same cooling time gives rise to a dose rate of about 370 μSv/hr which is clearly too high according to the established glove box rules. The tungsten enriched to 99 wt% in ^{182}W is beneficial for short cooling times and it can also allow for dedicated experiments to study the effect of transmutation on (a) thermal conductivity and (b) hydrogen retention separately from the material displacement damage. The remaining materials that have been investigated for use as possible MPEX test samples have a wide range of behaviors and associated dose rates after irradiation. Many materials will meet the < 100 μSv/hr criterion if enough cooling time is available.

Table 2. Activities (Bq/g) for top active nuclides and total activity in W targets at Discharge (after 10 cycles irradiation) and after two years of cooling

Natural Tungsten				Tungsten enriched to 99wt% in W-182			
	At end of irradiation (Bq/g)		After 2 yrs of cooling (Bq/g)		At end of irradiation (Bq/g)		After 2 yrs of cooling (Bq/g)
re188	2.17E+13	w185	1.81E+09	w183m	7.33E+12	w185	7.28E+08
w187	1.64E+13	re188	1.20E+08	re186	6.37E+11	w181	2.31E+07
w183m	2.24E+12	w188	1.19E+08	w185	6.14E+11	re188	1.79E+06
re186	2.18E+12	ir192	6.94E+06	re188	3.34E+11	w188	1.77E+06
os189m	1.92E+12	w181	6.12E+06	w187	2.63E+11	ir192	1.01E+05
w185	1.52E+12	pt193	2.24E+06	os189m	3.19E+10	ta182	8.92E+04
re188m	5.83E+11	ir194	1.63E+05	re188m	8.98E+09	os185	5.38E+03
os191m	3.61E+11	os194	1.63E+05	os191m	5.31E+09	ir194	2.34E+03
os191	2.18E+11	os185	3.76E+04	os191	3.20E+09	re186	4.27E+02
ir191m	2.18E+11	ta182	2.38E+04	ir191m	3.20E+09	re184	2.76E+02
w188	1.67E+11	re186	2.19E+03	w185m	3.02E+09	hf181	8.55E-01
Total	**4.79E+13**	**total**	**2.06E+09**	**total**	**9.24E+12**	**total**	**7.55E+08**

Table 2 presents a comparison in the nuclidic activities for natural tungsten, (irradiated for 10 cycles in HFIR) with the same for tungsten enriched to 99 wt% in ^{182}W. Total activity for natural tungsten for zero cooling is about five times greater than for tungsten enriched in ^{182}W. It is about three times greater after two years of cooling.

APPENDIX A tabulates the specific activities of five likely MPEX test materials, irradiated for 10 HFIR cycles in the flux trap target region, and cooled for at least two years. APPENDIX B shows curves of the dose equivalent rates at a distance one ft away from the sample disks, for a number of MPEX test materials irradiated for 10 cycles in HFIR and then cooled for three years. 0 shows a comparison of a similar irradiation scenario: two years of continuous irradiation in an SNS beam, vs. two years (nominally 14 HFIR cycles) irradiation in the HFIR flux trap region.

Material flow analysis and irradiation capsule design

A target station is being designed for MPEX to hold single 12 mm diameter PFC specimens. These specimens will be pre-irradiated in the HFIR to an exposure of 50 DPA (max) neutron damage. Specimens will be affixed to a target station and will be exposed to plasmas supplied by MPEX. Specimen characterization and analysis will be performed at the experiment site. Sealed sources for diagnostics instrumentation should be discussed with appropriate facility safety personnel to ensure radiological material inventory limitations are not violated. Some sample erosion will be expected (non-fixed contamination hazard), but no further activation products are expected to be produced from plasma exposure.

A closed 'radioactive material flow' was developed to support the MPEX facility that spans form extraction from the HFIR to depletion in MPEX. This process demands consideration from various systems including: radioactive shipments from radioactive facilities, hot cell facility work plans, site preparation to accept radioactive material at the MPEX site, radioactive material balance and inventory controls, and a viable waste disposal system. Fig. 5 illustrates the flow diagram. This document describes the proposed system to address these issues.

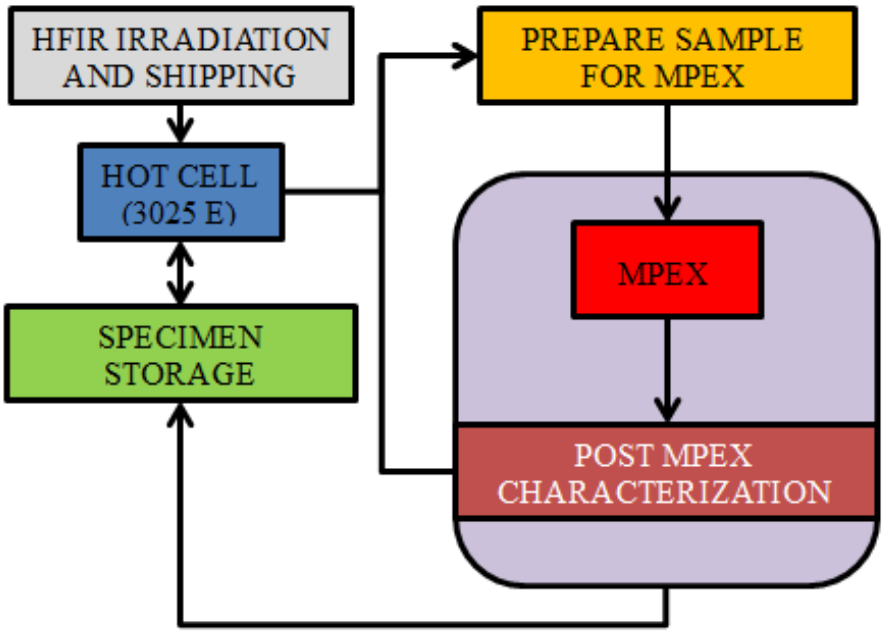

Fig. 5. MPEX radioactive material flow diagram

2.4 DETAILS FOR CAPSULE IRRADIATION AT HFIR AND POST IRRADIATION HOT CELL WORK

The following describes details for capsule irradiation at HFIR and post irradiation hot cell work.

2.4.1 MPEX Irradiation Capsule

The design of the irradiation capsule is discussed in the following subsections.

2.4.1.1 Capsule Design

An irradiation vehicle design for the PFC candidate materials was developed in support of the MPEX target station LDRD. This capsule (i.e. “rabbit”) design allows for, at most, 10 disk specimens with a diameter of 12 mm (maximum). The MPEX rabbit has an aluminum housing, a molybdenum holder with a diameter that can be varied and optimized to achieve the desired specimen irradiation temperature. Inside the holder are the specimens in two rows of five specimens stacked ‘end to end’. The tungsten specimens are located inside the holder with the flat sides of the discs parallel to the axis of the rabbit (or holder) in order to obtain more uniform temperatures. This allows a total of 10 specimens to be inserted in a single rabbit in two rows of five specimens each. The two rows of five specimens will be separated by SiC spacers with a spring that will press the specimens into the holder walls for better thermal contact. The rabbit will be filled with helium for maximum heat transfer. An alternative design would be to stack the specimens flatly; putting the radial surface in contact with the capsule holder. This design was rejected because it imparted relatively large radial temperature gradients (as much as 10%) on the specimen.

An axial cross-section of the design is shown in Fig. 6. These capsules will be irradiated in the HFIR flux trap to utilize the high flux to accelerate neutron damage in the materials. MCNP modeling estimated the number of irradiation periods to reach nominal neutron damage (10 dpa) will be 10 HFIR cycles (roughly two years).

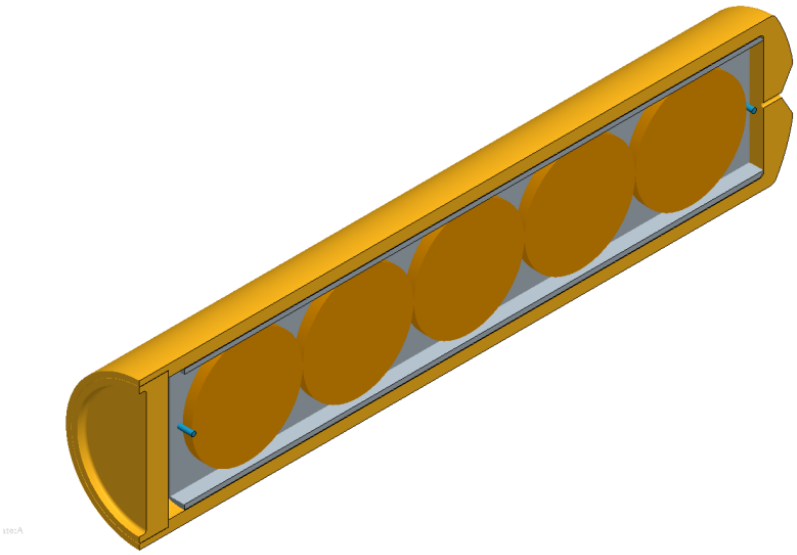

Fig. 6. Cross-sectional view of the MPEX PFC irradiation vehicle

The dimensions of the MPEX rabbit are given in drawing S14-01-RHH01. The total length of the rabbit design is 7.07 cm and the outside diameter is 1.59 cm, as this rabbit will be irradiated inside a trefoil holder; a newly developed capability for irradiating larger bore rabbit capsules like the MPEX rabbit in the target region of the HFIR. The trefoil occupies the space of three target positions in the HFIR flux trap and has an open diameter of 1.77 cm. Fig. 7 demonstrates the trefoil rabbit holder concept.

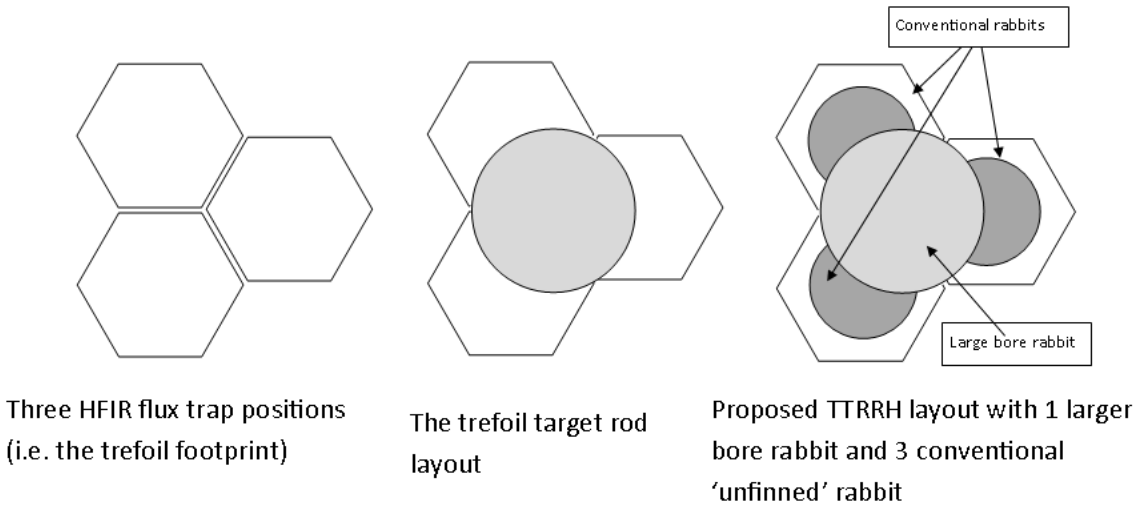

Fig. 7. Axial view of the trefoil footprint, trefoil target layout, and the proposed TTRRH layout

Several cases were analyzed to understand the capsule performance; given that a range of temperatures may be required by the MPEX (700°C as the minimum case and 1200°C as the maximum case). The holder outer diameter was varied to increase bulk specimen temperature. Table 3 details the capsule performance (i.e. specimen bulk temperature as a function of holder diameter). Fig. 8 shows representative temperature contour plots for the MPEX specimens

Table 3. Summary of results for the MPEX rabbit

Holder diameter (mm)	Housing/Holder gap (mm)	T-avg (°C)	T-min/T-max (°C)
13.28	0.0275	700	678/708
13.27	0.0325	750	727/759
13.20	0.0675	1074	1047/1084
13.20	0.0675	1035	1008/1044
13.17	0.0825	1201	1173/1211
13.10	0.1175	1467	1435/1478
13.00	0.1675	1759	1724/1770

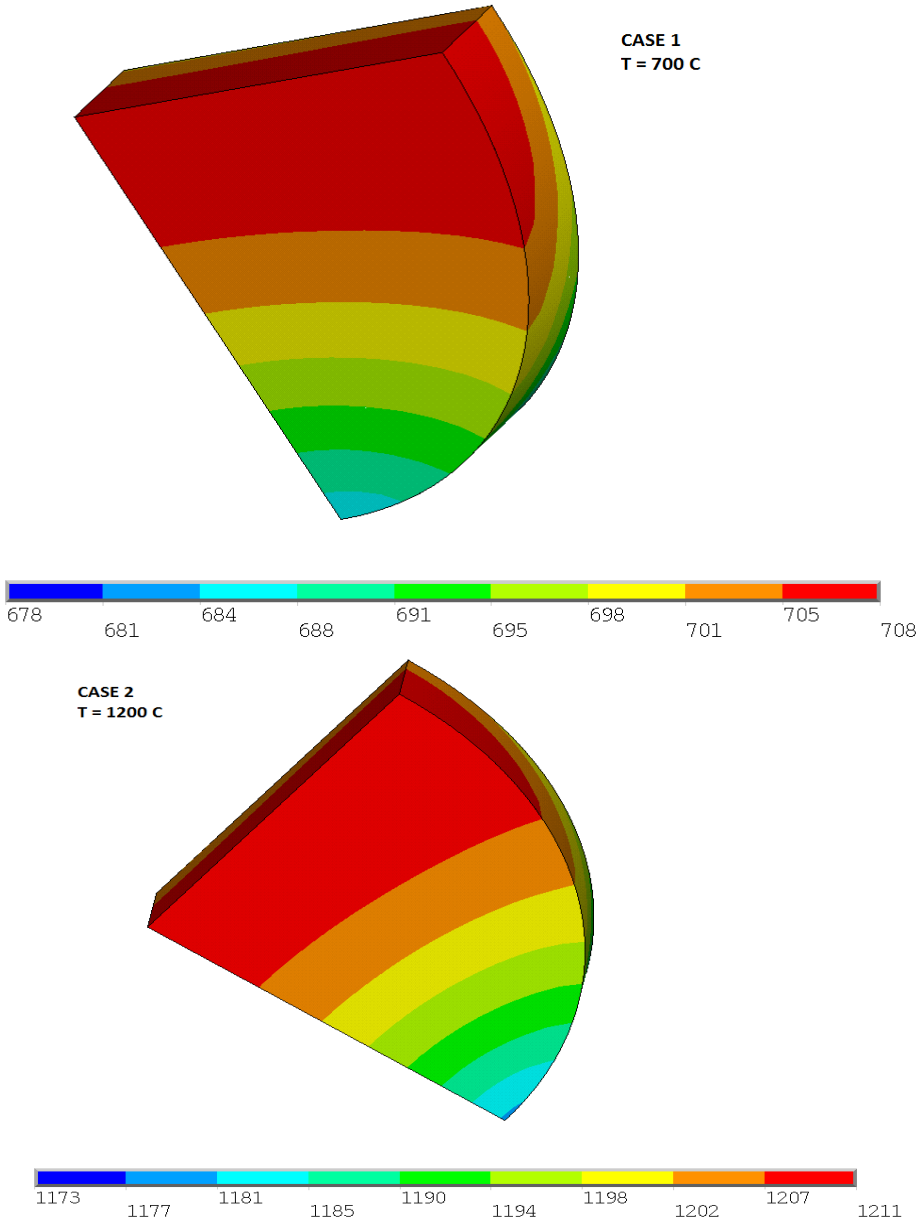

Fig. 8. Temperature Contour Plot (°C) for the 700°C and 1200°C cases

2.4.1.2 Alternative Designs

The HFIR has two facilities to perform materials irradiations that require fast neutron flux (E>1MeV); the flux trap and removable beryllium region (Fig. 9). The flux trap is being utilized for the design described in the previous section, but the reflective beryllium (RB*) region provides unique capabilities that may be used for irradiating PFCs. Namely, this region provides the capability for actively controlling the PFC specimen region, where the previous design is passively controlled. Moreover, the RB* sites can employ a thermal neutron shield, such as gadolinium, to attenuate the neutron fluence and reduce the thermal neutron damage effects on the specimen material.

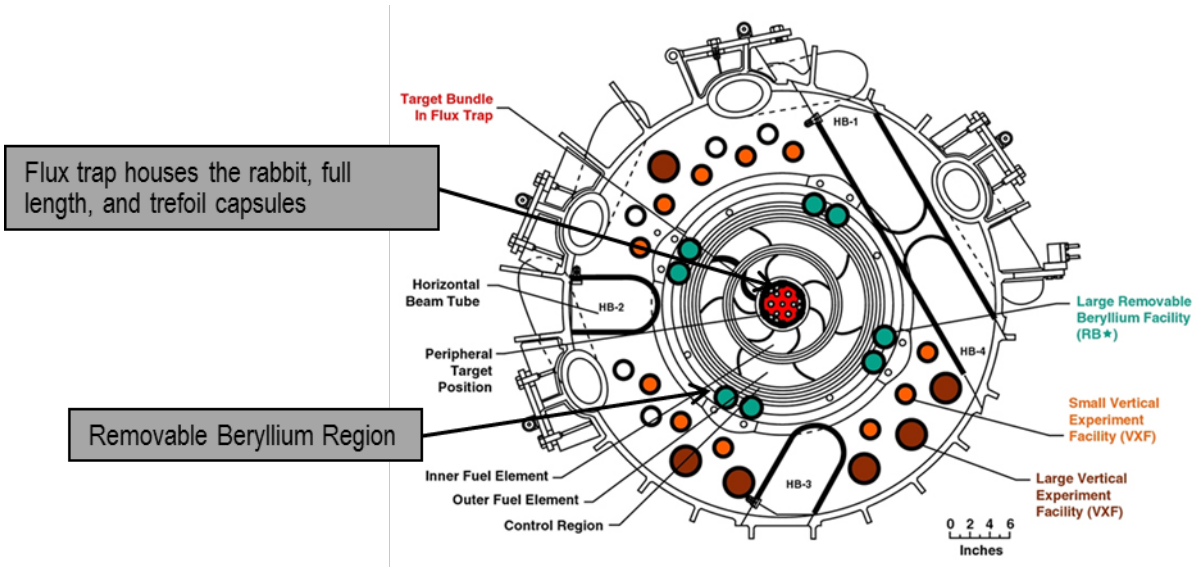

Fig. 9. Radial cross-section of the HFIR

The major drawbacks to the RB* facility is cost. The HFIR employs a policy of charging programs for operating cycle reduction; with incurred cost that are not trivial (~$15k/day lost). Placing experiments into the RB* sites inherently reduce the effectiveness of the removable beryllium and leads to cycle reduction. Moreover, the gadolinium shield will also absorb neutrons and lead to reduction in cycle length. Also, given the high flux in this region, the gadolinium will lose its effectiveness in roughly six cycles. Therefore, the PFC samples are limited to around 0.8 dpa, unless a replaceable shield is developed to support the irradiation campaign.

2.4.1.3 End of Irradiation Logistics

Once the irradiation schedule is completed, the capsules will remain in the HFIR pool for another two years (minimum) to allow the shorter lived isotopes to decay away and reduce the overall specimen activities. Table 4 details the candidate materials for MPEX and the maximum activity details for the material (assumes 10 specimens, or a single capsule, of each candidate material). This exercise is beneficial from both the shipping and handling standpoints because the capsules can be sent to a hot cell facility without violating shipping hazard category 3 limitations, and after the allotted decay period, the specimens can be manipulated for reasonable amounts of time in a glove box.

Table 4. MPEX candidate materials and activity after 2 year decay period

Decay Daughters	MPEX Candidate Material					Total Activity (Ci)
	99 wt% W-182	Natural W	10 wt% Ta-W	1 wt% La2O3-W	20 wt% Re-W	
	Activity (Ci)					
W-181	6.25E-04	1.65E-04	1.51E-04	1.63E-04	1.31E-04	5.43E-02
Ta-182	2.41E-06	6.42E-07	6.65E-03	6.34E-07	5.09E-07	2.93E-01
W-185	1.97E-02	4.88E-02	4.57E-02	4.83E-02	4.00E-02	8.91E+00
Os-185	1.46E-07	1.02E-06	9.32E-07	1.01E-06	5.17E-06	3.64E-04
Re-188	4.84E-05	3.24E-03	2.95E-03	3.20E-03	2.65E-03	5.32E-01

W-188	4.79E-05	3.21E-03	2.92E-03	3.17E-03	2.63E-03	5.27E-01
Ir-192	2.73E-06	1.88E-04	1.71E-04	1.85E-04	5.39E-04	4.78E-02
Pt-193	0.00E+00	6.05E-05	5.51E-05	5.98E-05	2.22E-04	1.75E-02
Ir-194	6.33E-08	4.41E-06	4.02E-06	4.36E-06	1.61E-05	1.27E-03
Os-194	0.00E+00	4.41E-06	4.02E-06	4.36E-06	1.61E-05	1.27E-03

2.4.2 Post Irradiation Shipping and Hot Cell Work

A shipping infrastructure between the HFIR and the ORNL hot cell facilities is already in place and well understood. Activation analyses on an 'as built' capsule basis will be generated after each unique capsule irradiation schedule is completed, and this data is provided to the Research Reactor Division to facilitate the shipment. The hot cell that is most suitable for performing the post-irradiation disassembly ORNL Irradiated Materials Examination and Testing (IMET) Facility in building 3025E. It is a two-story block and brick structure with a two-story high bay that houses six heavily shielded cells and an array of sixty shielded storage wells. It includes the Specimen Prep Lab (SPL) with its associated laboratory hood and glove boxes, an Operating Area, where the control and monitoring instruments supporting the in-cell test equipment are staged, a utility corridor, a hot equipment storage area, a tank vault room, office space, a trucking area with access to the high bay, and an outside steel building for storage. Applications specific to the facility include: physical and mechanical properties testing, examination of irradiated materials, irradiated specimen storage, and sample preparation.

The Sugarman S-10-* casks (Fig. 10) are suitable shipping packages for the capsule, and all loading/unloading and shipping documentation (instructions, transportation limitations, etc.) are in active use.

Fig. 10. Sugarman shipping cask

All work at the IMET facility must be approved by facility management. The disassembly of similar 'rabbit' style capsules is routine at the IMET facility, but any special instructions, considerations or non-routine work must be proceduralized. The work must be provided to the hot cell operations team and must be scheduled through the facility 'plan of the day' (POD). Also, any special tooling used to perform non-routine tasks must be inserted into the hot cell bank, and will be subject to safety screening to ensure all work and tools do not violate the site Safety Analysis Report (SAR). The IMET facility is a Hazard Category (HC) 3 nuclear facility that must maintain a material balance area (MBA). The activation analysis data provided for shipment is also used by IMET personnel. As stated earlier, short term and (potential) long term storage of specimens can occur in the IMET facility, but arrangements for this concession must be established by the facility management.

The mature shipment infrastructure from a hot cell to a destination radiological facility is also in place and readily used. Small lead containers, secured in shipping drums, will be used to transfer the specimens form one site to the other. If long term storage has occurred between the initial shipment from HFIR, a subsequent decay calculation or extrapolation of the older values will need to be performed to ensure the destination MBA does not erroneously reflect the actual amounts of activated material.

2.5 RADIOLOGICAL FACILITY TO SUPPORT MPEX AND SPECIMEN STORAGE

The following subsections will discuss the material specimen handling and storage.

2.5.1 Specimen Material Flow Discussion

A workflow for handling and storage of the irradiated/plasma exposed materials must be developed to ensure adequate safe measures, inventory controls, and experimental rigor. Prior to the specimens arrival at the MPEX site, this location must have all safeguards and required infrastructure in place and all work control must be approved and in use. Given the specimens will be radioactive; the MPEX location must be designated as a Radiological facility. Moreover, a distinct storage location must be identified to house the PFC materials when they are not being used in MPEX. Finally, a controlled area will be established to contain any work that may require radioactive work.

In accordance with the ORNL ALARA policy, the material flow plan must minimize radioactivity exposure to personnel. Therefore, the workflow will require that only one specimen be handled outside the storage location at a time. Essentially, the MPEX technical staff will receive a bulk shipment of specimens from the hot cell facility, and store them into the storage site. Once a researcher requests an order for a specimen, the staff will obtain the single specimen and process it for insertion into MPEX (in a glovebox). After the plasma exposure experiment is completed, the necessary analysis and characterization will be performed, and the specimen will be returned to the storage location. An inventory system should be implemented to track the location of the specimen at all times (i.e. storage facility, glovebox, MPEX, etc.). This system should be robust enough to not allow for any two specimens to be located at the same location at the same time. This will support the ALARA program as well as reducing the likelihood of losing specimen traceability by mixing up samples.

2.5.2 Creation of a Radiological Facility (RF) for 7625

MPEX will be located in building 7625 at the ORNL reservation, and this site is the preferred storage location for the irradiated PFC materials. In order to accommodate the radioactive material, building 7625, or a designated space in the building, must be re-designated for that purpose. Two designation categories are available for this purpose: the Radiological Facility (RF) and the Accelerator Facility (AF). After initial discussions with ORNL ES&H, it was decided to designate this space as an RF since the RF designation provides the adequate environment, work, and safety controls for the MPEX, and the RF guidelines more closely suit the expected work.

The Land Use Committee must be notified in order to establish a radiological hazard facility. Furthermore, special documentation for the site must be established to move forward with the site reclassification. ORNL SBMS requires a multi-disciplined team (e.g., Facility Management, facility research organizations, Facility Safety, Fire Protection Engineering, Nuclear Criticality Safety, Emergency Management, Radiological Protection, Transportation and Waste Management Division, and operation personnel) be established to identify radiological inventory through reviews of existing facility documentation, facility walk-downs, and interviews, etc.

The next action item is to identify what radiological materials and the quantity limitations associated with said materials and the HC/ EPA) Reportable Quantity (RQ) limitations must be calculated. Based on the isotopic breakdown of PFC materials in Table 5, the percent of HC-3 and RQ limits are calculated in Table 5.

As shown in Table 5, the estimated limits are far below the maximum amounts allowed for a Radiological Facility. Note that by October 2016, the HC-3 TQs in DOE-STD-1027 will be superseded by updated HC-3 TQs but the EPA RQs will not change. As such, as of October 2016, the HC-3 sum of fractions for this inventory is projected to be 0.67% making the values reported in Table 5 conservative. Further Guidance for establishing this necessary documentation can be found in SBMS (Establishing and Maintaining Facility Hazard Categorization Documents).

Table 5. Calculated HC-3 and RQ values for estimated PFC materials

Isotope	Activity (Ci)	HC-3 TQ (Ci)	HC-3 Ratio	40 CFR 302.4 RQ (Ci)	RQ Ratio
W-181	5.43E-02	1.30E+04	4.18E-06	1.00E+02	5.43E-04
Ta-182	2.93E-01	6.20E+02	4.73E-04	1.00E+01	2.93E-02
W-185	8.91E+00	1.38E+03	6.46E-03	1.00E+01	8.91E-01
Os-185	3.64E-04	1.10E+03	3.31E-07	1.00E+01	3.64E-05
Re-188	5.32E-01	2.20E+04	2.42E-05	1.00E+03	5.32E-04
W-188	5.27E-01	2.80E+02	1.88E-03	1.00E+01	5.27E-02
Ir-192	4.78E-02	9.40E+02	5.09E-05	1.00E+01	4.78E-03
Pt-193	1.75E-02	2.40E+04	7.29E-07	1.00E+03	1.75E-05
Ir-194	1.27E-03	1.42E+04	8.94E-08	1.00E+02	1.27E-05
Os-194	1.27E-03	8.20E+01	1.55E-05	1.00E+00	1.27E-03
			0.89 % HC-3 limit		98.0% RQ limit

Once the radiological inventory limits are fully understood (i.e. actual material compositions and bounding activity limits are established) further documentation detailing the radiological inventories for the RF must be generated by the appropriate Nuclear Facility Safety personnel. However, the 98% RQ limit (i.e. low radiation facility threshold) dictates the 7625 site should be designated as a RF. Divisions responsible for radioactive materials in a facility are required to use the Radioactive Material Inventory System (RMIS) for the tracking of radioactive materials within a facility. A facility specific inventory system may be used in lieu of RMIS provided:

- Facility specific spreadsheets/software that can be used to verify compliance with radioactive material inventory hazard categorization requirements is utilized

- The CFM grants approval for the use of the alternate spreadsheet/software application.

Software/spreadsheets used with this procedure shall be used in accordance with SBMS subject area: Software Quality Assurance. For facilities that use the RMIS, Nuclear and Radiological Protection Division (NRPD) personnel maintains the software quality assurance records.

Necessary space and resources to manage the radiological hazards and waste must also be identified in order to establish the 7625 RF. This exercise can be performed by performing a Preliminary Hazard Screening (PHS). The objective of the PHS is to describe the current operations and how the facility is divided into structures, systems, subsystems, and specific

process areas. It will also identify the Controlled Area with the RF, and Radioactive Materials area, Radiation Area, etc.

- Controlled Area: any area to which access is managed by or for DOE to protect individuals from exposure to radiation and/or radioactive material.
- Radioactive Material Area: any area within a controlled area, accessible to individuals, in which items or containers of radioactive material exist and the total activity of radioactive material exceeds the applicable values detailed in 10 CFR 835.
- Radiation Area: any area, accessible to individuals, in which radiation levels could result in an individual receiving an equivalent dose to the whole body in excess of 0.005 rem in 1 hour at 30 centimeters from the source or from any surface that the radiation penetrates.

Further guidance for performing a PHS and details pertaining to these special areas can be found in SBMS and 10 CFR 835, respectively. Note that work controls for all spaces not designated for radiological work will not be affected by the re-designation of the facility. For example, 4500S and 4508 are RFs, but radiological work is not done the whole of these buildings. Certain laboratories, facilities, etc. such as the Low Activation Materials Development and Analysis (LAMDA) facility is designated as a Controlled Area and have special work and inventory controls that are specific to that space.

2.5.3 Handling and Storage of MPEX Samples

The MPEX target station has the capacity to handle only single specimens at a time, which warrants leaving the balance of specimens in a Controlled Area. A preliminary design for a storage vault was completed to address both the radiological hazards and inventory considerations for the RF. Because the samples are radioactive, they must be stored in a shielded vault to reduce the potential of exposing the staff that work in close proximity to the specimen storage location. The shielded vault was designed with the use of the radiation transport code Monte Carlo N Particle version X (MCNPX) to optimize the shielding thickness. The storage vault was designed as a lead filled steel structure.

MCNPX verified that an equivalent shielding thickness of 15.2 cm of steel will be required to reduce the dose rate to 1.5 mrem/hour when measured at a distance of 30 centimeters, from the surface of the container, assuming a maximum of 100 targets are stored in the storage vault. Using lead filled steel, the container will be able to be smaller and lighter. The thickness required for lead filled steel will be 2.6 cm of steel and 5.2 cm of lead totaling 7.8 cm of total wall thickness as shown in Fig. 11.

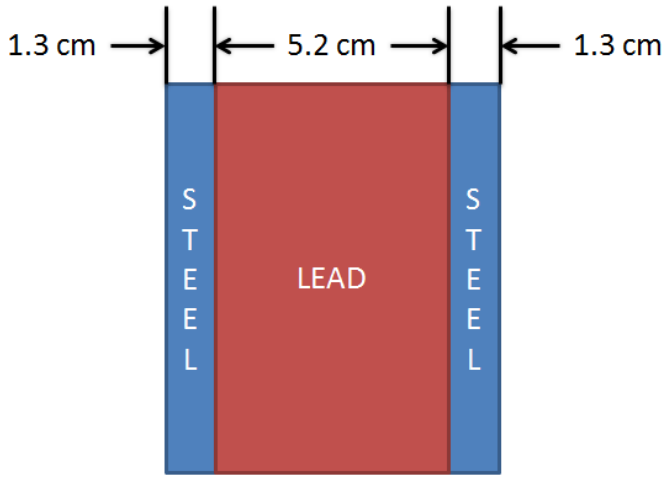

Fig. 11. Storage vault wall cross section

The storage vault has been designed with 10 individually shielded shelves. Each shelf has a lead brick mounted on the front and back of the shelf as shown in Fig. 12. The shelves will contain a specific inventory of MPEX specimens that are contained in metal jars similar to those seen in Fig. 13. Unique identification will be scribed on these metal jars provide specimen traceability. The lead bricks ensure that the worker whom is retrieving the target from the vault will only be exposed to the unshielded radiation given off by the targets on the shelf that has been opened (during the short period of time that they are retrieving the desired target). Additionally the door of the storage vault has been designed to swing to a 90° position and shield any additional workers from the radiation given off by the targets on the shelf. These design aspects will effectively reduce the short-term occupational radiation exposure by over 90%.

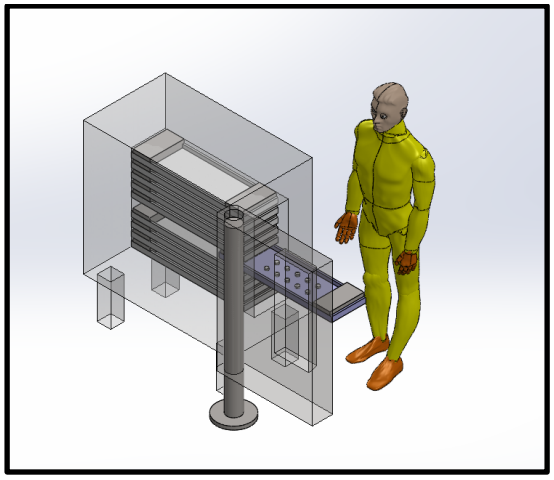

Fig. 12. MPEX sample storage container design concept

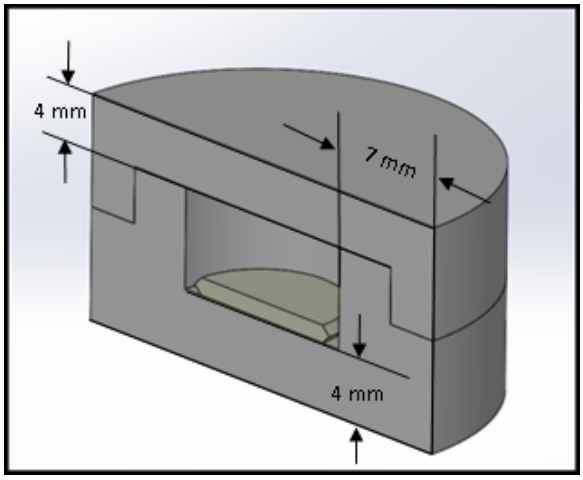

Fig. 13. Metal jars used to house irradiated MPEX samples

This heavily shielded container may be placed in any location that can support the vault's mass. Considerations for personnel who may be stationed for long periods of time in close proximity to the vault were also taken into account. The shielding attenuates the radiation field to 0.1 mrem/hour at 1.23 meters. The additional shielding provided by metal jars further attenuates the dose rate roughly 15%, or 0.085 mrem/hour at 1.23 meters. Therefore, a worker placed at a

permanent work station at this distance will be exposed to 18% the annual DOE dose rate in a year's time (2080 hours/year).

Similarly, the MPEX machine will be designated as a controlled area. Both the storage vault and the MPEX machine must have an established set of boundaries that consist of partitions, walls, or other physical boundaries. Furthermore, a boundary or line must be established to designate the machine as a Radiation Area while MPEX is operating.

2.5.4 Nuclear Materials Accountability

The MPEX is expected to employ some nuclear materials during the operation of the machine. This list includes deuterium, tritium, and ^{6}Lithium (may exist in some of the irradiated sample materials). Lithium samples are being investigated for this work, but the program will require natural lithium (i.e. 97% ^{7}Lithium) is used if this material is selected for investigation. If more than 100g of deuterium is expected to be used for the operation of MPEX, this material must be treated as an accountable quantity. Therefore, establishing any deuterium limits and reclamation/exhaust processes associated with the MPEX and target station must be addressed and implemented before the experiment can be used. Also, accountable quantities of deuterium require an MBA area and all necessary supporting personnel (safeguards and security, two MBA managers, etc.). There are no limits for tritium use; however, a controlled exhaust process must also be employed for this nuclear material. Further guidance on nuclear materials accountability can be found in SBMS.

2.5.5 Costs associated with the 7625 Radiological Facility re-designation

Services provided by the ES&H and Land User Committee to support the reclassification of the designated facility are covered by ORNL overhead, however, some cost will be incurred from other subject matter experts and other designated personnel for their interactions during the designation process (i.e. multi-disciplined teams to identify radiological inventory, completion of PHS, etc.). Developing a waste handling and disposal plan will be a one-time cost and should be relatively routine. However, processing the waste (any swabs, PPE, depleted sample materials, etc.) will be have a considerable associated cost. A solution for mitigating the spread of contamination must also be identified. Upon exiting a controlled area, personnel must be required to verify no contamination is present on their person. This can be performed using sophisticated equipment such as a Personnel Contamination Monitor (PCM) to perform surveys of a worker's hands and feet, but cost upwards of $100k. Other solutions, such as Geiger counters, may be used to perform the same task and cost a fraction of the PCM. For the MPEX application, both systems may be used, but the lower cost and simplicity of the Geiger counter should be the preferred option.

An exhaust stack will likely be required for the 7625 facility; given the MPEX will utilize tritium and deuterium. Facilities at ORNL and Y12 with similar requirements were used to estimate the cost of constructing a viable structure. The cost to build a stack 24 in. in diameter, 60 ft. tall with a flow of 4000 cfm is estimated to be $200k. Other associated infrastructure for the structure includes purchasing a shrouded probe and associated piping and a sampling station with mass flow meter, that are estimated to cost $15k. Lastly the estimated personnel operating burden

(analysis costs, sampling labor costs, and instrumentation and control costs) is estimated to be $70k yearly. Therefore, the total initial estimated cost for the stack structure is $217k, with an annual $70k operating cost.

General Radiological Control Technician (RCT) support is not guaranteed and it is recommended that the MPEX program retain the services of at least one RCT to support the experiment (equivalent to one FTE). If nuclear materials accountability is necessary, a minimum burden of 0.3 FTE is required to support the activity. Implementing the destination site into an RF will initiate many hurdles for the work culture at that location. Considerations and costs associated with items such as reflowing workspace and building accessibility, segregation of ventilation and building utilities, etc. may be incurred by MPEX program and will be non-trivial.

3. DESIGN OF TARGET STATION AND ANCILLARIES

The following sections detail the target station and ancillary designs.

3.1 TARGET DESIGN INTRODUCTION

The MPEX facility is being developed at ORNL to study the material effects of plasma facing components at the diverters for future fusion devices such as Fusion Nuclear Science Facility (FNSF) or DEMO. A preconceptual design of the target design for such a facility is the focus of this LDRD research. Following were the requirements for the target design.

1) Ability to withstand a Gaussian plasma heat flux with a peak value of ^{10} MW/m^2 and ion fluxes up to 10^{24} m^{-2}s^{-1} at the center of the target.
2) Design a target that is disc shaped with a diameter of 10 mm and a thickness of 1mm
3) Ability to handle neutron-irradiated targets from a reactor. The target handling system should be capable of handling radioactive components.
4) After plasma exposure, the surface of the target needs to be analyzed quickly without any exposure to air (oxygen). Hence, the target needs to be transported to a diagnostic chamber for analysis while maintaining vacuum.
5) There should be active cooling of the target when exposed to plasma. The center of the target has to be maintained at 1200°C and ±5mm from the target center the temperature should not deviate more than 30°C.
6) The target holder should accommodate both a target that is orthogonal to the plasma as well as a target that is at 15° to plasma direction.
7) The target is be maintained at 10^{-6} Pa after it has been retrieved from plasma chamber.

Minimize the time taken for diagnostics after the plasma exposure is completed.

3.2 TARGET STATION DESIGN REQUIREMENTS

The MPEX system consists of plasma generators, plasma heaters, confining superconducting magnets and vacuum components. A schematic of the layout of the MPEX is given in Fig. 14. The only portion of the overall MPEX design that the LDRD project focuses on is the design of the Target Exchange Chamber (TEC) and how it interfaces with the Plasma Material Interaction chamber (PMI). The TEC is the chamber that houses the target and all the interconnections need to handle the target. PMI refers to the chamber that sits inside the magnetic field where the target it introduced to expose it to plasma. The TEC also has to interface with a diagnostic system situated away from the magnetic field in another room. This document will detail the selection criteria of the target, the design of the target puck, target handling and target change out, target transfer to diagnostic facility, and finally the diagnostic facility design.

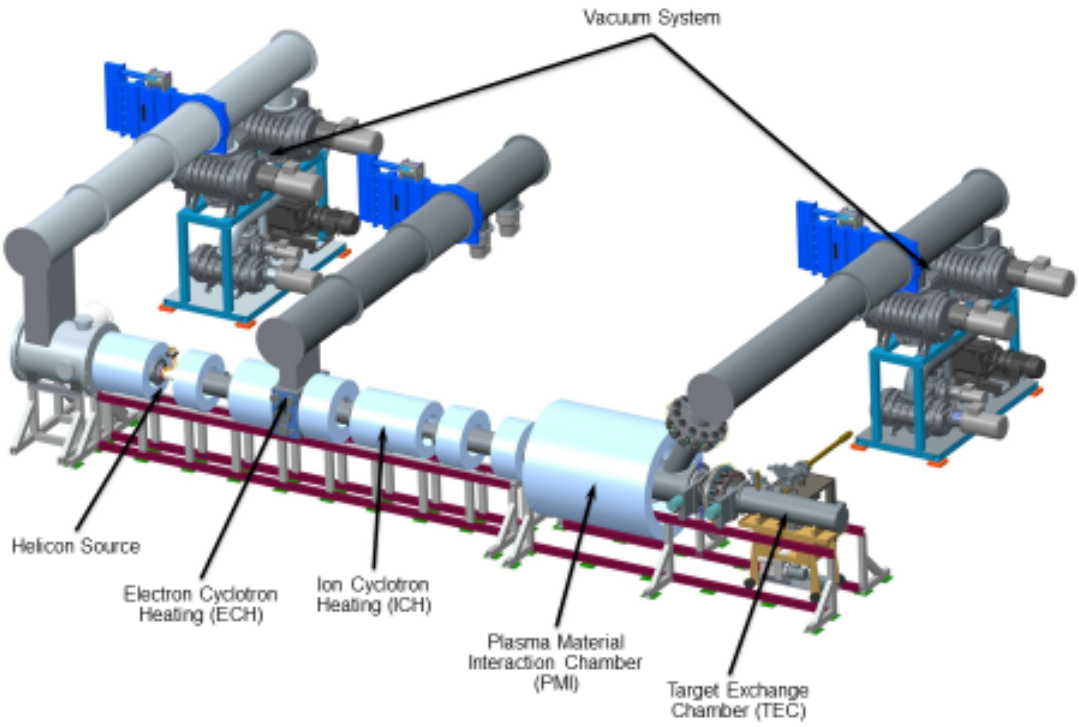

Fig. 14. Overall layout of the MPEX system

The design of the TEC and the components that make it largely depends on the functionality of the TEC chamber design. Couple of design requirements and equipment functionalities drove the decision making process for the TEC chamber. Listed are the questions that needed to be answered that affected the design of TEC.

1) Can the diagnostic equipment be permanently mounted to the TEC?
2) Are the TEC and PMI chambers attached to each other with a quick disconnect capability or attached securely with bolts?
3) If the two chambers are connected with bolts, can a long translating arm for transferring the target to and from the PMI chamber be sufficient?
4) Should a vacuum suitcase be used for transferring samples to the diagnostic chamber?

Will a superconducting magnet be used for the MPEX system?

3.2.1 Design Alternatives

To address these above questions various design options were suggested. The various options provide a combination of alternative designs that may or may not satisfy all the requirements. See Fig. 15 showing the various components that interface with TEC.

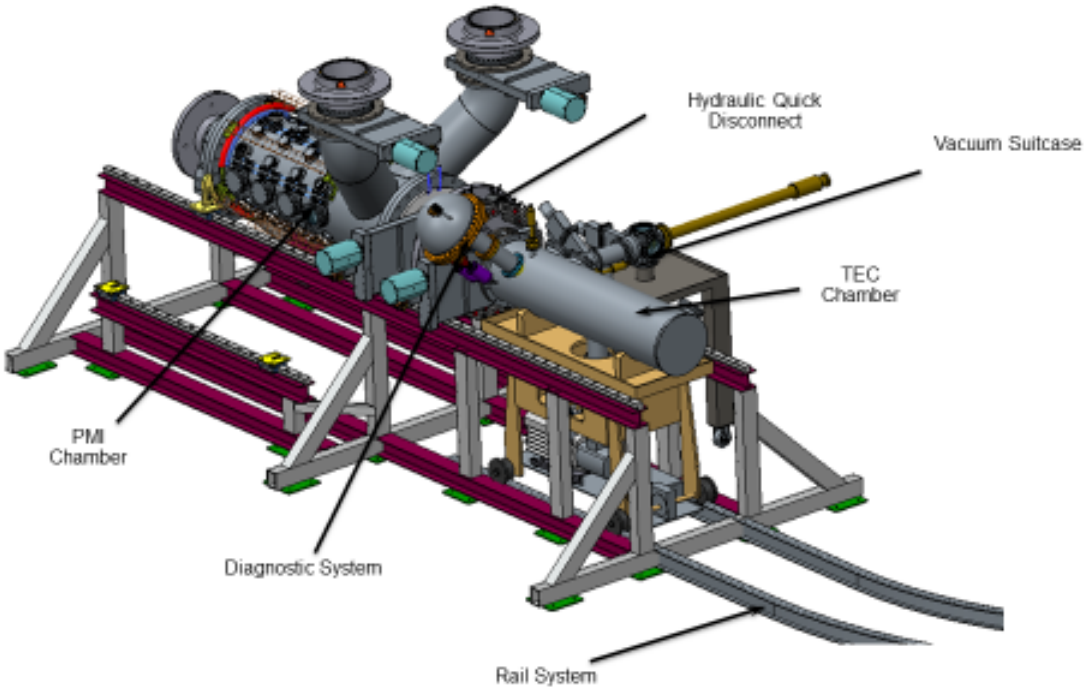

Fig. 15. Components that interface with TEC

Option 1– Automated Vacuum Suitcase to transfer target for diagnostics.

In this option the TEC and PMI are connected with bolts. The target is extended into the PMI chamber and retracted after plasma exposure. The securing of the target and disassembly of the target from the extending base plate has to be performed remotely/robotically. A vacuum suitcase interfaces with the TEC whereby the target is transferred into the suitcase robotically. Also, the vacuum suitcase then will have to disengage from TEC and move to the location of the diagnostic facility.

Although this approach frees personnel from most of the target handling thereby minimizing his/her exposure to high magnetic field and potential radioactive sources it really complicates the design (see APPENDIX D). Performing all these tasks robotically near a high magnetic field where sensors and electrical motors that do not function very well or have to be shielded is a very challenging task. It might also make the target handling prohibitively expensive with very many components that can potentially fail. Hence, this option was not pursued any further.

Option 2– Automated disconnection between PMI and TEC. Entire TEC chamber is taken to diagnostic facility for analysis.

In this approach using a hydraulic disconnect mechanism, and using dual gate valves, the two chambers are isolated once the plasma exposure of target is complete and target retracted. The target is never removed from the target holder on the extending arm. TEC chamber is mounted on

a cart that is on rails enabling it to be moved away from the magnetic field to another room that is magnetically isolated from the super-conducting magnets. The TEC also has an in situ vacuum pump that pumps the atmosphere inside TEC to bring it down to 10^{-6} millibar.

This method easily allows for quick disconnection between TEC and PMI chambers. No personnel are need near the TEC to retract the target. The entire TEC is moved by rail and interfaces with the diagnostic chamber. Here again using dual valves and a hydraulic quick disconnect, the target and the diagnostic chamber are connected. New targets are introduced or old targets removed manually in the diagnostic room. Personnel exposure to a high magnetic field is thereby greatly reduced. This method was chosen as the preferred approach for this project.

Option 3– Long arm for target handling. Manual removal of sample for diagnostics.

Using a long arm was an approach that could potentially remove personnel from a high magnetic field during target insertion into the plasma chamber (See APPENDIX E). Once the target is retracted and sufficiently brought away from the magnetic field, a person using manipulators removes the target into a vacuum suitcase. The vacuum suitcase is then taken to the diagnostic chamber where again using manipulators, the target is positioned for diagnostics.

This approach will have difficulty making turns to transfer the TEC to another room for target diagnostics, due to the long arm. Hence, a vacuum suitcase is the only possible solution. This method requires personnel to handle the target many times and possibility contaminate the target during transfer between various vacuum containments. Every time before a target transfer is made, one has to wait for the chambers to be sufficiently pumped down before valves can be opened. This option will take more time compared to other options being considered.

Option 4– No Super conducting magnet and diagnostics mounted directly on TEC.

MPEX would like to have a superconducting magnet for generating the magnetic field. But, superconducting magnets are costly and once turned ‘ON’ cannot be turned ‘OFF’ quickly. Another less costly option is to use water cooled copper coil magnets. These can be turned ‘ON’ and “OFF’ more easily. Although this option will allow working near the TEC when the magnets are turned ‘OFF’, it was not pursued further since super conducting magnets is the preferred option for better confinement of the plasma.

Based on the options discussed above, *Option 2* was the preferred choice which included an automated hydraulic disconnect between TEC and PMI chambers, a separate diagnostic room, rails for transferring the target, and superconducting magnets. More details of this design will be discussed in later sections of this report.

3.3 MPEX TARGET

The MPEX target system consists of a target, a target puck, and a target holder. Each of the individual components is discussed in this section.

3.3.1 Target Design

Target for MPEX is a frustum of a cone with a base diameter of 12 mm, top diameter of 10 mm, and thickness of 1 mm (see Fig. 16). Initially many materials were under consideration, but

finally five materials with varying percentages of Tungsten Isotope were selected. The selected materials were: 99 wt% W-182, Natural W, 10 wt% Ta-W, 1 wt% La_2O_3-W, and 20 wt% Re-W. All these targets will be fabricated by sintering correctly proportioned powdered tungsten into the desired disc shape.

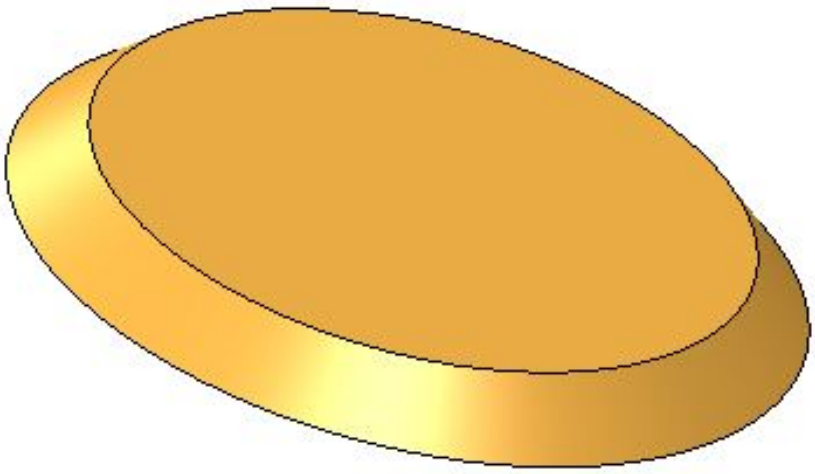

Fig. 16. Target design for MPEX

Fig. 17. shows the configuration of the target puck and the target puck holder. The target puck holder houses the copper water cooled elements which is in contact with the target puck and the cooling channel in contact with the tungsten shield. The target puck holder is fixed to a telescoping arm for exposing target to plasma in the PMI Chamber.

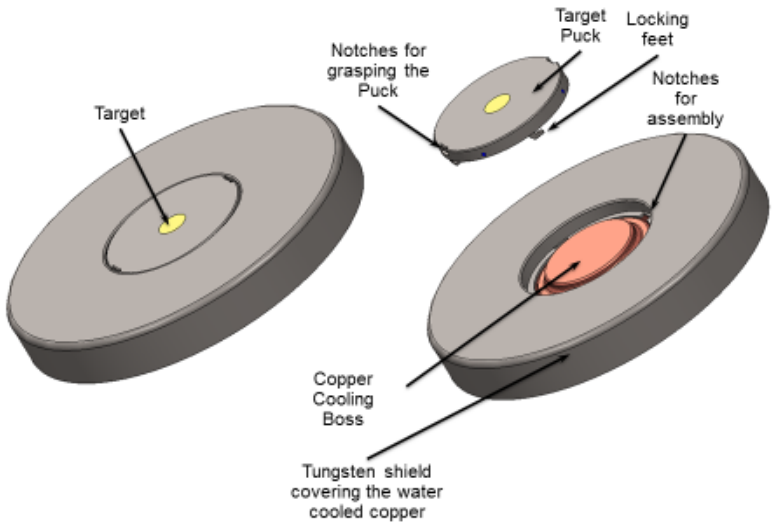

Fig. 17. Target puck and target puck holder assembly

3.3.2 Target Puck design

Target puck is the component that houses the target. Since the target has to be periodically replaced, the cooling channels have to be contained inside the target puck holder copper boss and the target puck interfaces with this boss.

The target puck consists of the target, grafoil, tungsten retainer and the target securing base (See Fig. 18). The grafoil compresses and ensures a good contact between the target and the tungsten retainer, which is in contact with the water cooled copper boss. The thickness of the grafoil and the tungsten retainer affected the temperature of the target. The plasma flux on the tungsten was modeled as ringed regions with differing heat fluxes. Integrating the Gaussian distribution of the plasma flux, these regions closely approximated the plasma heat flux on the tungsten target and the target puck holder.

An aim of the target design is to maintain a uniform temperature on the target. The target center has to be maintained at 1200°C while the difference along the rest of target (±5 mm) has to be kept as low as possible. Since the only heat removal for the target is through water running through the copper in the target puck holder all the thermal resistance and conductivity of the various layers that make up target puck has an influence on the final target temperature.

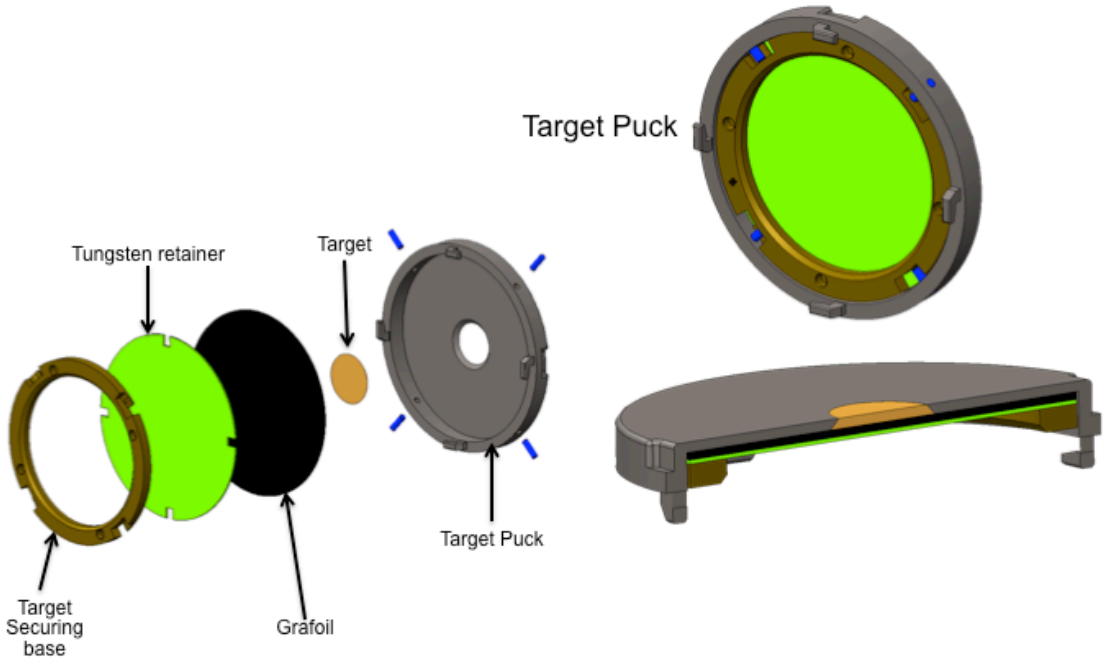

Fig. 19. Target puck assembly

The water flow in and around the target through the copper channels is as shown in Fig. 20. It was found through simulation that a thickness of 0.38mm for tungsten retainer and 0.5 mm for grafoil resulted in the center tungsten target temperature of 1200º C and no melting of copper and only 17º C rise in water temperature (see Fig. 21 and Fig. **22**)

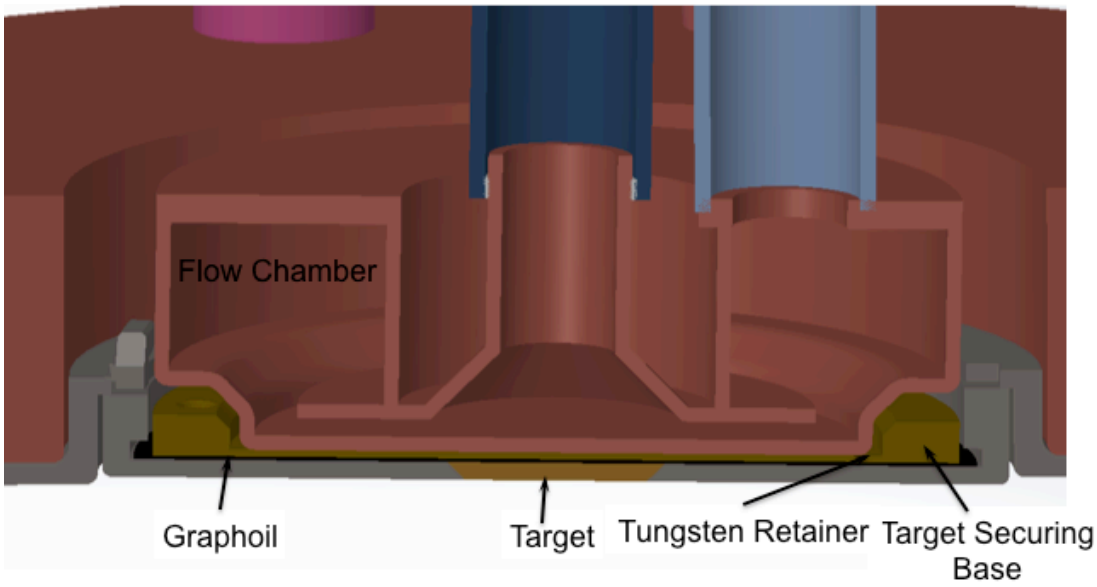

Fig. 20. Cross-sectional view of the target puck showing the water flow through copper channels

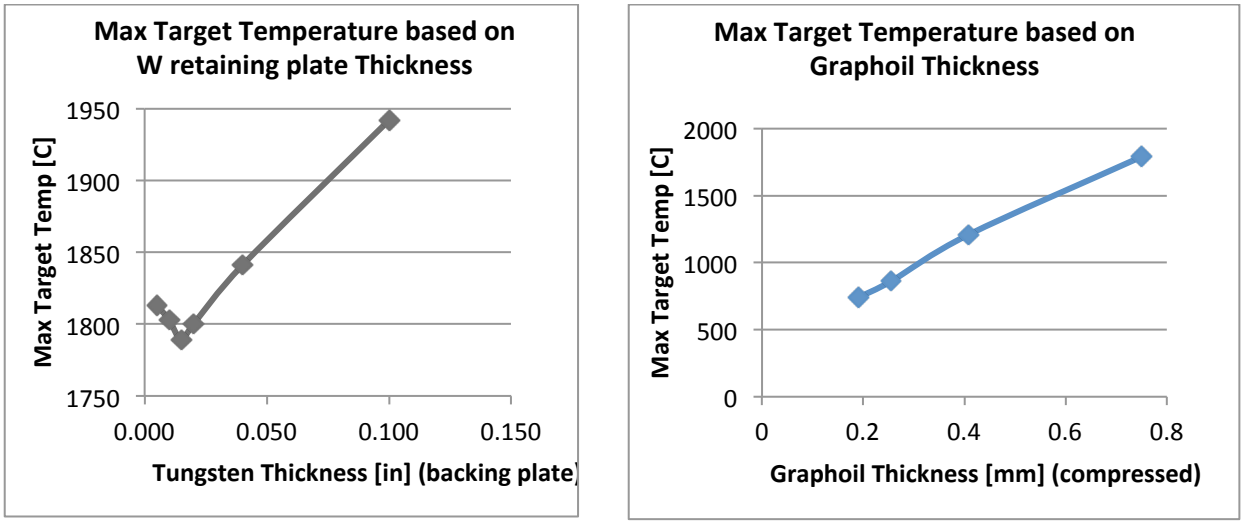

Fig. 21. Temperature of the target versus thickness of tungsten back plate and grafoil

The temperature profile of the Target Puck is show in

Fig. 22. As you can see, one area of the puck gets hotter compared to the other side probably due to the 1° slope of the target puck's top face. The target puck has this feature to ensure that when the plasma is hitting the target there are no arcing near where there is a transition between the target puck and the target puck holder. The plasma completely misses the gap between the two assembled items. Also, the variation of the temperature on the target is kept < 40° C. More optimization of the geometry of the target puck will follow when detailed modeling, simulation and component testing will be performed during detailed design stage.

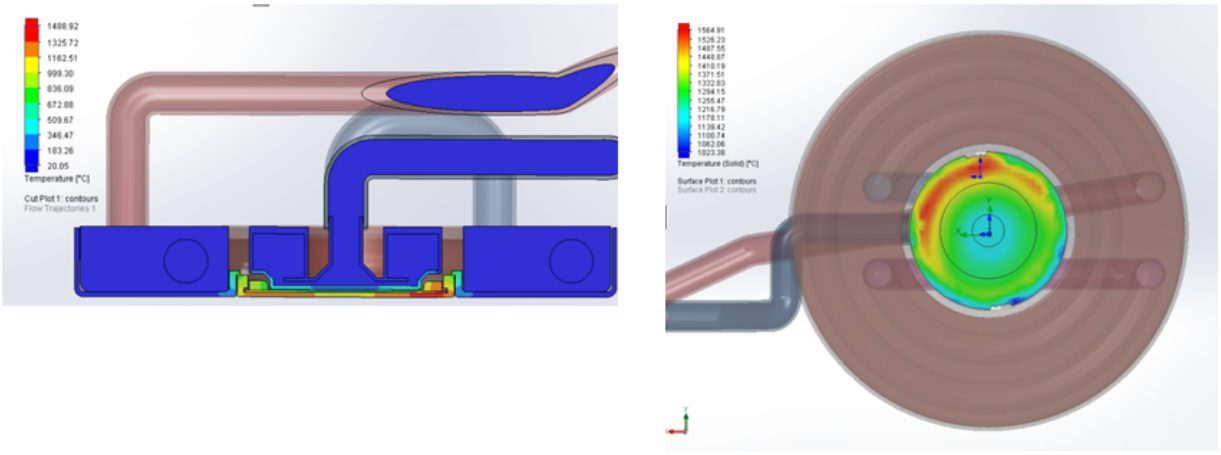

Fig. 22. Temperature Profile of the Target Puck in Plasma

3.3.3 Target Puck Holder

The target puck holder is connected to the TEC through the telescoping arm. The cooling lines reach the copper base of the target puck holder. The puck holder has a diameter of 12 cm. This is greater than the diameter of the MPEX plasma which has a diameter of 10 cm. The larger diameter is to capture any stray plasma and prevent it from hitting other parts of the PMI chamber. The Target puck holder has an outer skin layer of tungsten with a copper base that houses the cooling water lines (see Fig. 23). The cool water comes directly to the center of the puck hitting right under the target. From here the water is directed to the inner ring and finally to the outer ring (shielding part of the target assembly) where it is directed out of the target after flowing almost 330 degrees in the annular ring.

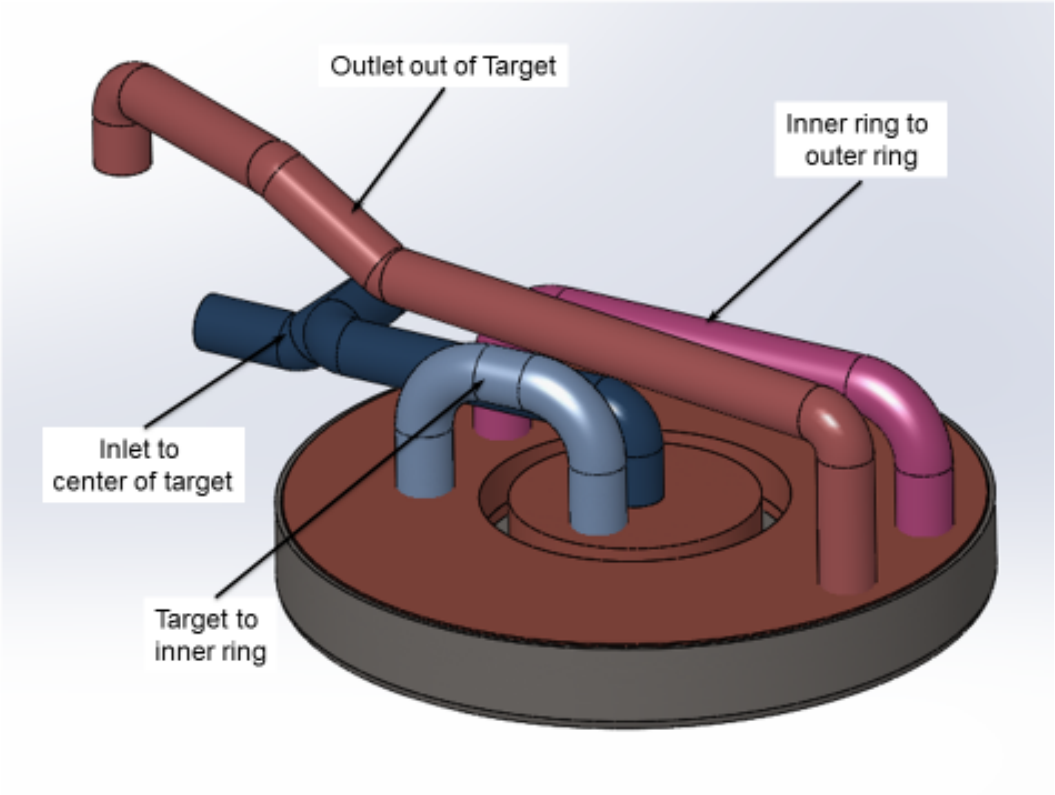

Fig. 23. Cooling lines connections on the Target Puck Holder

In case of a target design that is at 15°, the flow pattern is slightly different. Fig. 25 shows the copper base and tungsten cover for the 15° target puck holder. The dimension of the target holder is much bigger (15.1 cm x 40.3 cm) to accommodate for the 10 cm diameter plasma incident on the target at 15°. The size is larger than the plasma size to ensure that the target holder captures most of the plasma and prevent it from hitting other regions of the PMI chamber. The shape of the target holder is rectangular instead of disc shaped design for the normal (90°) target. The tungsten cover provides protection for the copper from direct contact with plasma. The copper base carries cooling water lines to maintain temperature of the target at 1200°C. The removable target puck design is same for the 15° and the 90° target allowing them to be interchangeably used.

Fig. 24 shows the cooling water lines that are routed along the length of the target compared to the concentric cooling lines for the 90° target. There is an array of upper water channels that cool the top surfaces of the target, which join at the farther end to form a plenum for the return hot water. A separate cold water line feeds the boss where the target puck is directly in contact with the copper (see Fig. 26). This increased water flow in this region helps remove heat where there is largest heat flux. Water returning from the puck region combines with water coming down the central part of the target and flows down to the return plenum. Since the plasma is hitting the top surface of the target holder, the cold water lines are offset to the top surface of the copper base.

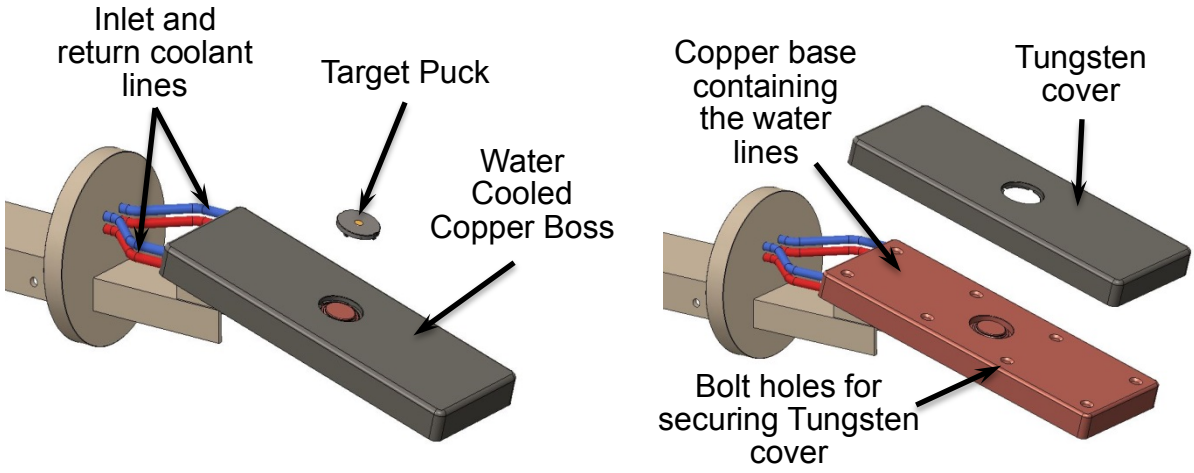

Fig. 25. 15 degree target puck holder showing puck, tungsten cover and copper base

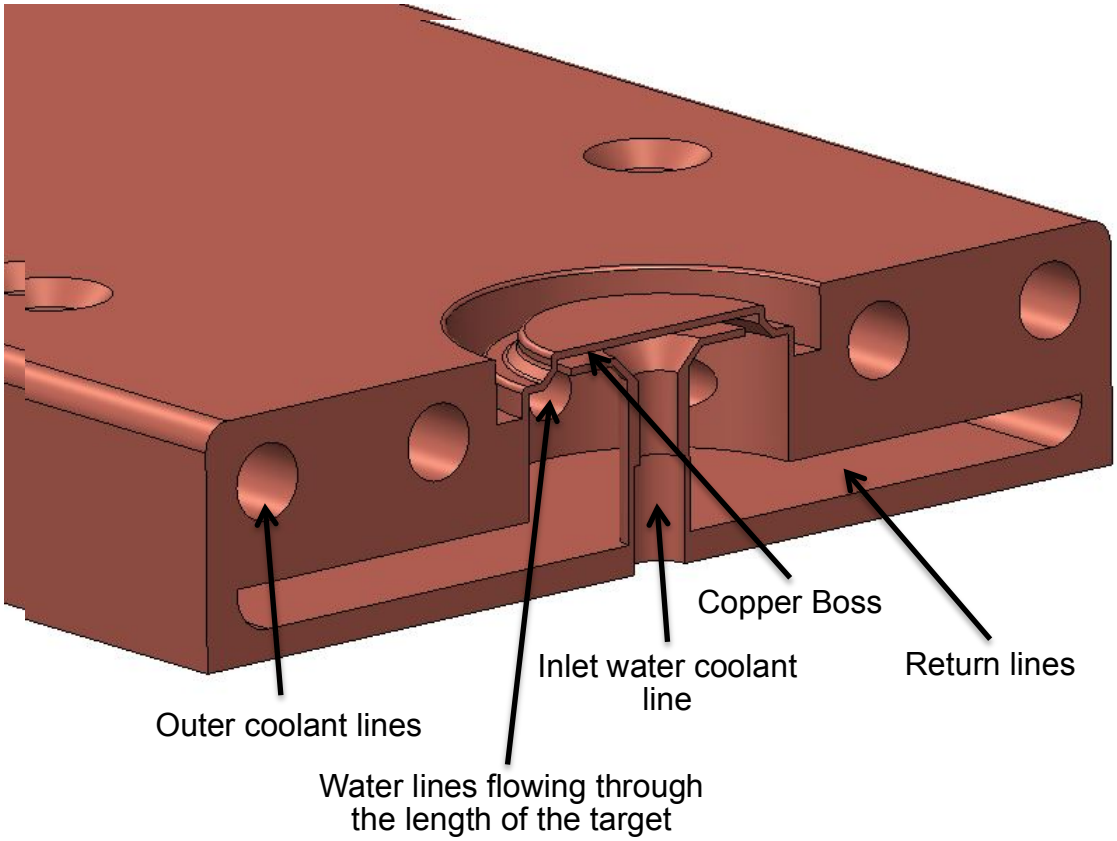

Fig. 26. Flow channels for the 15 degree target puck holder

3.4 TARGET EXCHANGE CHAMBER

The target exchange chamber is the cylindrical chamber with in internal diameter of 0.35 m and a length of 1.47 m that houses the target. It has a telescoping arm to extend the target into the PMI chamber. Fig. 27 shows the target exchange chamber connected to the PMI chamber.

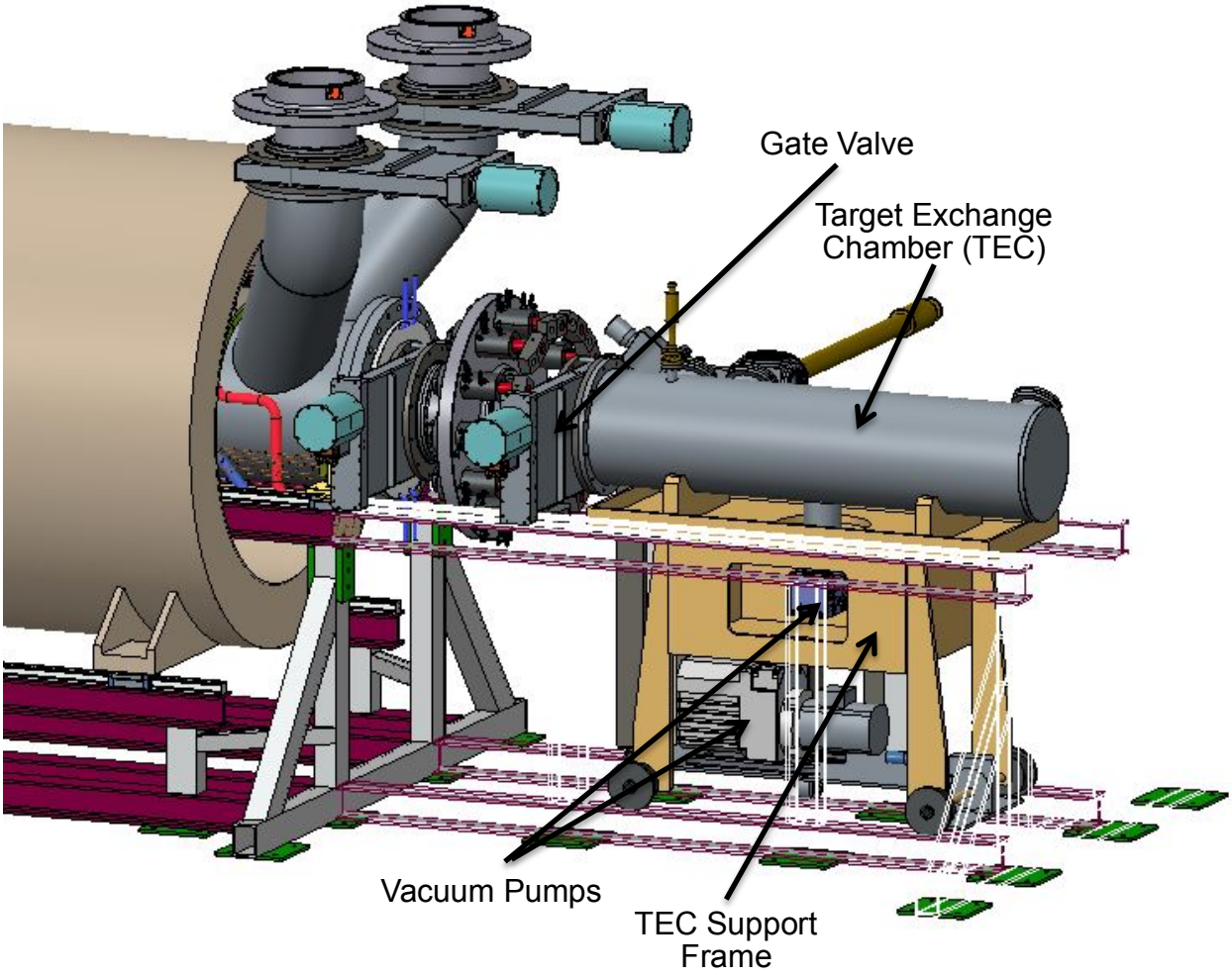

Fig. 27. Target Exchange Chamber

The TEC is designed to be on rails so that it can be disconnected from PMI chamber and taken to an area with low magnetic field for target diagnostics. Fig. 28 shows the PMI chamber in two positions: 1) TEC connected to the PMI and 2) TEC connected to the Diagnostic Chamber. The rail system helps transfer the target after plasma exposure without having to use a vacuum cart. The vacuum cart is used for transferring targets from glove box to TEC and back. Even though vacuum cart can interface with TEC when connected to PMI chamber, there is no need to change the target at this location close to the magnetic field. A decision to change or reuse the target is made after a diagnostic has been performed on the target.

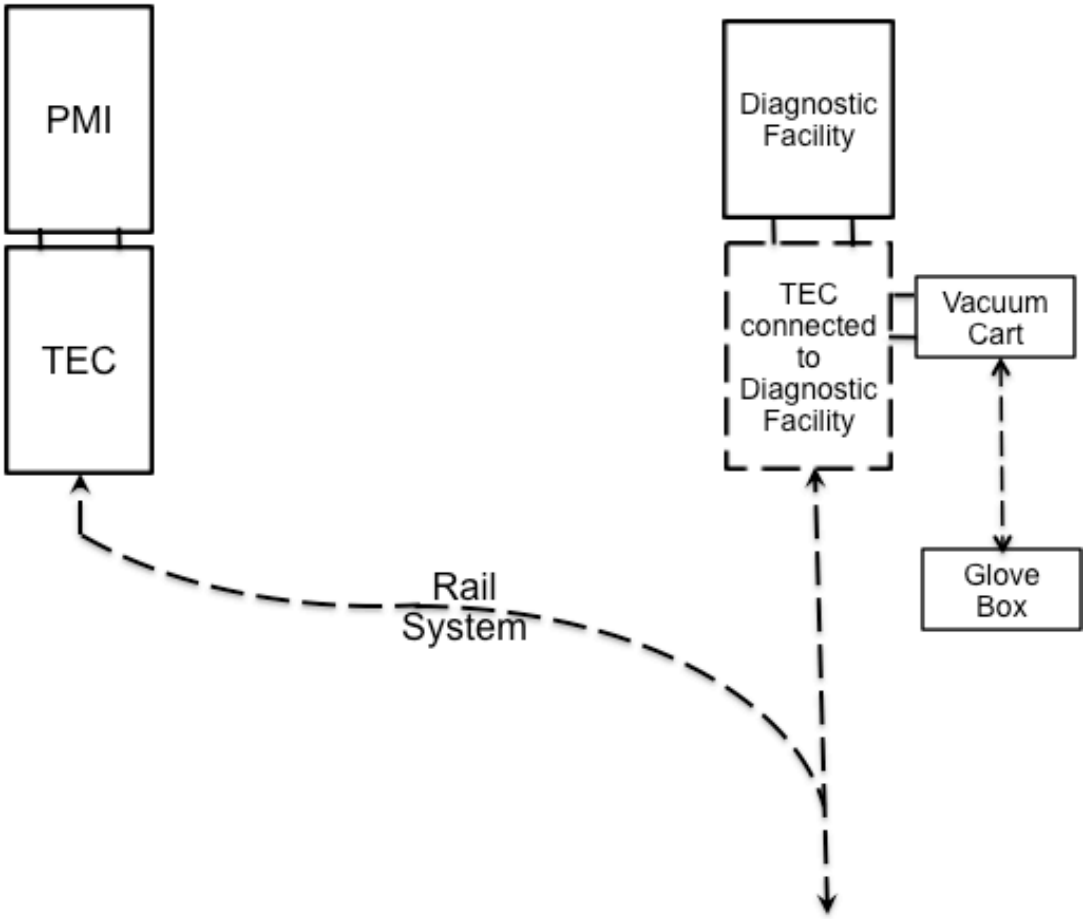

Fig. 28. Schematic of the Layout of PMI, TEC and Diagnostic Chambers

A three stage telescoping system made of 316 Stainless Steel sliders and ceramic wheels provides the linear extension[1] for the target arm (see Fig. 29). With ceramic wheels, the chamber can be in vacuum minimizing the off-gassing since no lubricating grease is used in the translating slides. The actuator for this linear slide will be a pneumatic (not electric) motor, to allow it to operate in close proximity to magnetic field. Also, to extend the arm, a push pull chain is used. The push pull chain uses stainless steel with aluminum bronze sprocket to avoid galling between moving parts in a vacuum environment[2]. A vacuum rotary joint[3] is used to couple the pneumatic motor[4] to the push-pull chain drive[5]. An extension of 1.6 meters is achieved by the telescoping slide.

The TEC also houses both a roughing (36 m^3/hr Duo 35 Rotary Vane pump) and a high vacuum pump (936 m^3/hr HiCube 300 Turbo pump)[6]. Since the pumps needs to operate close to high magnetic field of 0.1 Tesla, an iron enclosure is made around the pumps to shield it from the magnetic field. An EM

[1] http://www.tpa-us.com/index.html --tsq43 series
[2] http://www.framo-morat.com/usa/
[3] https://www.pfeiffer-vacuum.com/productPdfs/PF224010-T.en.pdf
[4] http://www.parker.com/literature/Pneumatics%20Division%20Europe/PDE-Documents/Rotary_Actuators_Platform_Catalogue_PDE2613TCUK.pdf
[5] http://www.framo-morat.com/usa/LinearChain_size25.html
[6] https://www.pfeiffer-vacuum.com/en/products/pumping-stations/turbo-pumping-stations/

radiation calculation needs to be performed to determine the actual thickness of the iron required for this magnetic shielding. The TEC is brought down to 10^{-6} millibar pressure as soon as it is isolated from the PMI chamber to reduce redeposition of elements on the target surface. Since the targets handled in MPEX are radioactive, the cart also needs to house a HEPA filter. The exhaust from the vacuum pumps is routed through this HEPA filter. Since the radioactivity of the target and the constituent elements are going to be low, it should be permissible to exhaust the air from the accredited HEPA filter directly into the building. The TEC chamber is on rails so that it can be moved to another building that is magnetically isolated from the superconducting magnets. This adjacent building will be magnetically isolated to house diagnostic equipment that is sensitive.

Since the extended arm is going to be a cantilevered load at the end of the arm, there is possibility for vibration of the target. To minimize this vibration the target, when extended, slides on to a ramp fixed in the PMI chamber. The ramp also provides a travel stop for the target to ensure that it is positioned correctly every time at the same location in the PMI chamber (see Fig. 30).

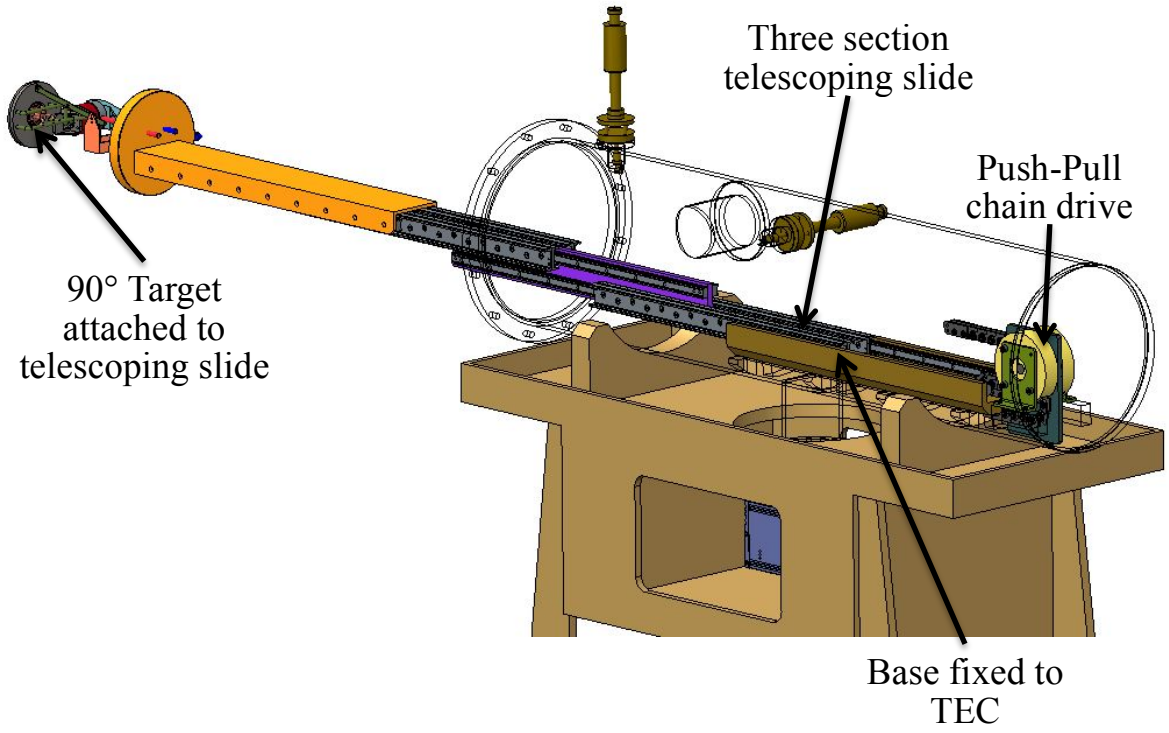

Fig. 29. Target attached to the telescoping arm fully extended

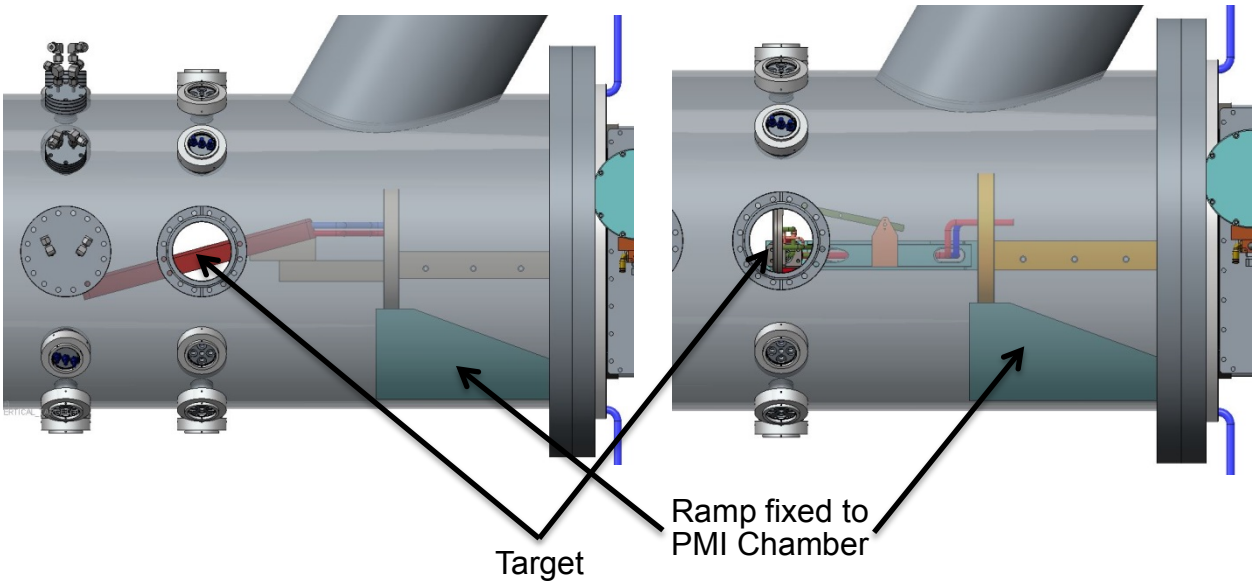

Fig. 30. Target located inside the PMI chamber

The cooling lines for the target run along the top of the linear slide connecting to the target puck holder (see Fig. 32). The lines have a fixed length that is attached to the TEC and a portion that moves with the telescoping arm using cable tray/hose carrier design. Finally the coolant lines terminate at the end of the TEC through a water vacuum feedthrough connection. Water lines leaving the TEC to the chiller are disconnected when TEC is being moved to the diagnostic room. The chilled water temperature is maintained at 15° C.

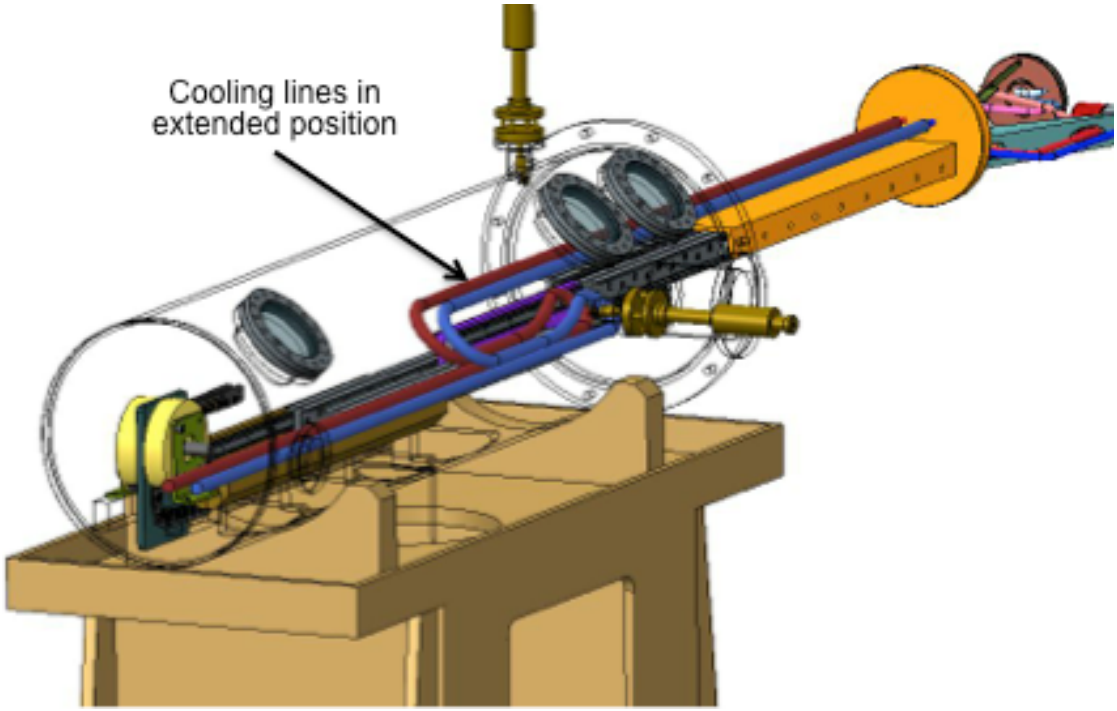

Fig. 31. Telescoping actuator showing the target cooling lines

3.5 DIAGNOSTIC CHAMBER

Once the target is exposed to plasma, it is important to measure the surface properties of the exposed surface. This has to be performed before any re-deposition of material takes place. If the target is maintained in a non-vacuum environment, the target surface will incur deposition of the material not present after plasma exposure. This will corrupt the results of the material characterization of an irradiated sample exposed to plasma. To ensure that the target surface is pristine, soon after the target is retracted, the PMI gate valves are closed to isolate the TEC. The vacuum pump on the TEC cart is started immediately to reduce the pressure inside the TEC chamber to $10^{-}7$ mbar.

The TEC chamber is taken to a diagnostic room by a rail system (see Fig. 32). The umbilicals providing cooling water are disconnected while the electrical and pneumatic connections remain connected to the cart as it is being moved to an adjacent building. A trough or a festoon system is employed by the rail transfer system for all the power delivery. The diagnostic chamber is a fixed piece of equipment that has similar interfaces as the PMI chamber with dual gate valves and a hydraulic coupling. This allows for easy coupling of the TEC chamber and the diagnostic chamber (see Fig. 33). Since the diagnostic chamber is fixed and has its own vacuum pump connection, it will be maintained at 10^{-6} millibar pressure a priori. The hydraulic couplings are actuated to attach TEC to the diagnostic chamber. Once the TEC pressure also reaches 10^{-6} millibar, the gate valves can be opened. The telescoping target can now be extended into the diagnostic chamber. Fig. 33 shows a generic XPS system, although it could be any of the surface diagnostic equipment.

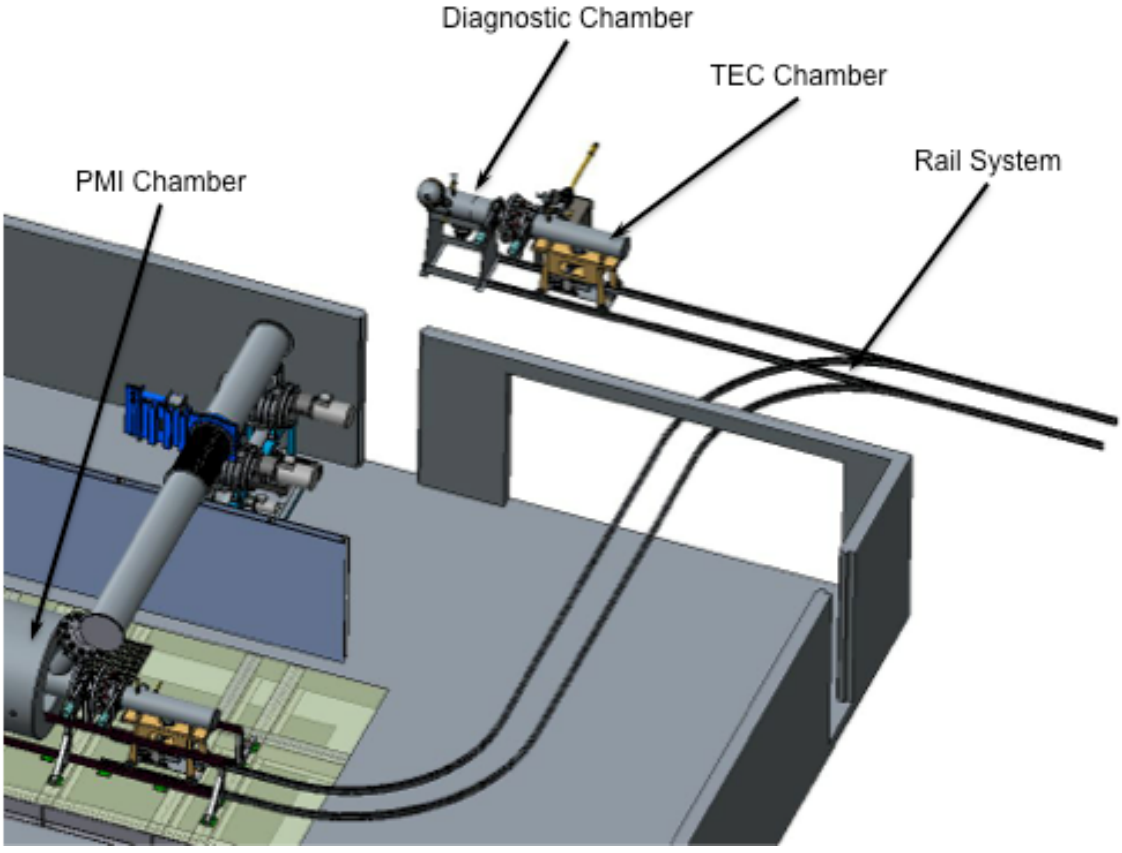

Fig. 32. Rail System for TEC transfer

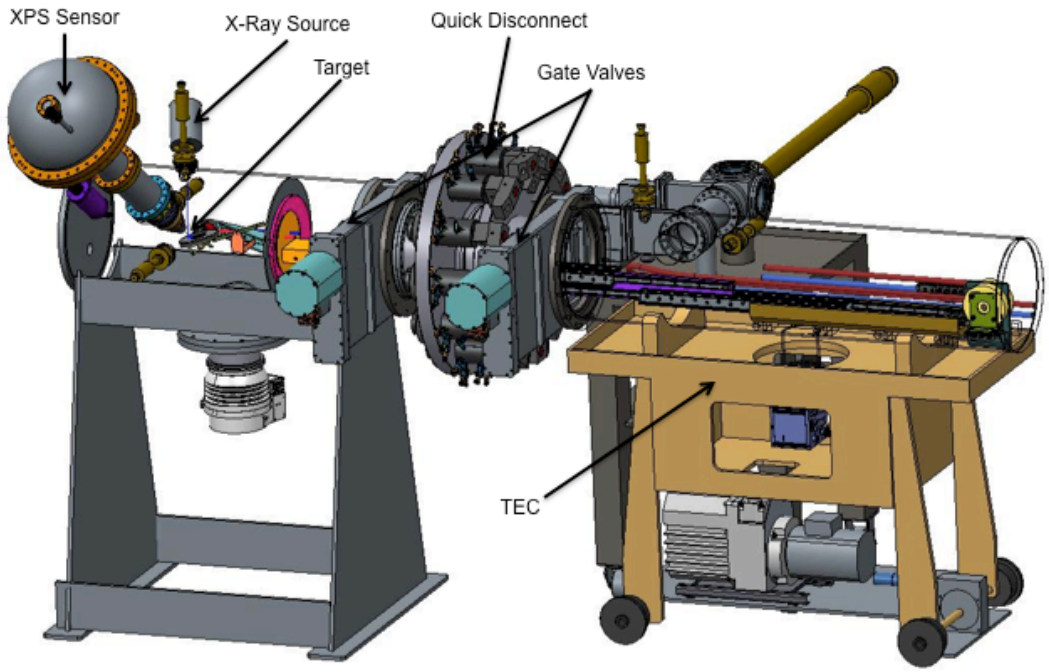

Fig. 33. Diagnostic chamber and TEC interface

Since the XPS system operates at vacuum close to 10^{-9} millibar, and since the hoses carrying the coolant to the target is flexible corrugated stainless tubing, it will be difficult to main this high vacuum in both TEC and diagnostic chamber. Hence, the TEC will be maintained at 10^{-6} millibar while the diagnostic chamber will be maintained at 10^{-9} millibar. To isolate these two chambers a clamshell sealing mechanism that seals against the tungsten plasma dump is proposed (see Fig. 34).

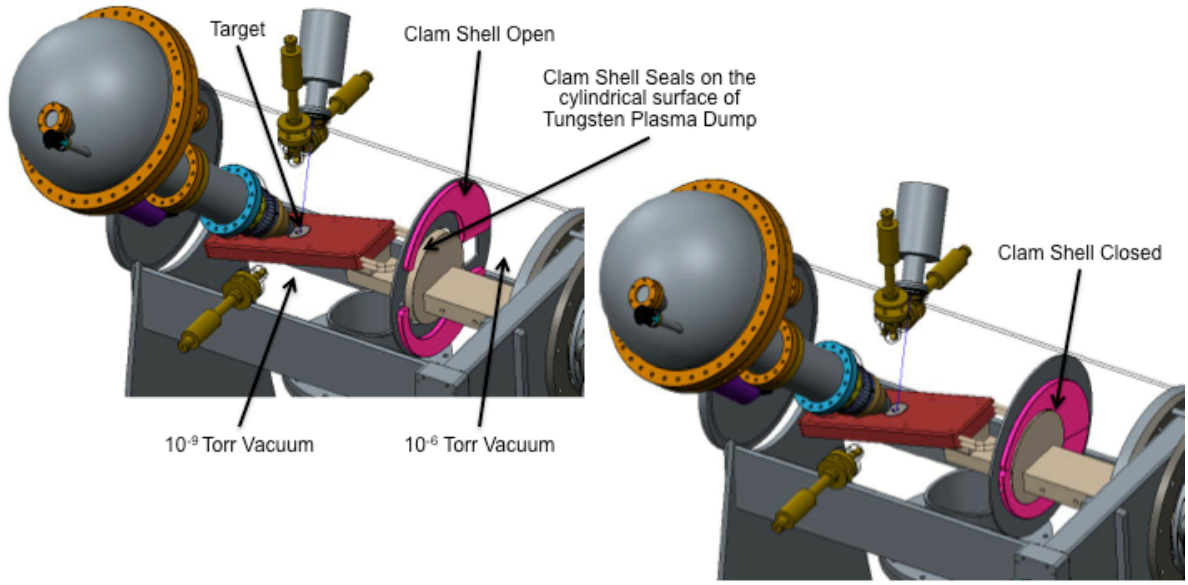

Fig. 34. Clam Shell Actuation in the Diagnostic Chamber

The clamshell's are built into the diagnostic chamber and uses a knife-edge seal to achieve this seal. Fig. 34 shows the opened and closed configuration of the clamshell. During the diagnostics, TEC vacuum pump will be running and maintaining a vacuum of 10^{-6} mbar in the TEC chamber.

3.6 TARGET INTRODUCTION INTO TEC AND THE GLOVE BOX DESIGN

Targets are introduced into TEC through vacuum port at the side of the chamber. Using vacuum interlocks and manipulators, the target is secured on the target holder. A vacuum cart is used to introduce new targets into TEC or remove existing targets from TEC. Fig. 35 shows a vacuum cart with manipulator.

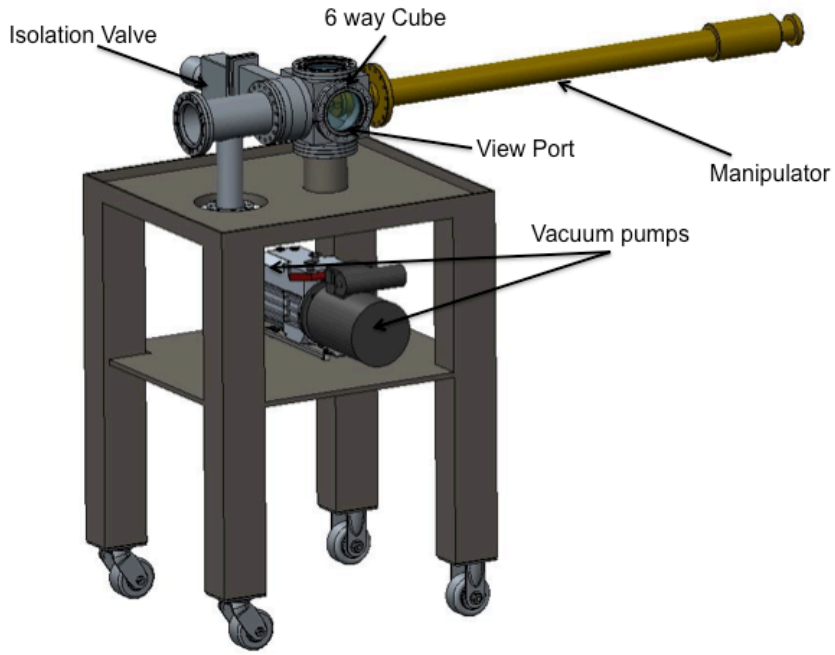

Fig. 35. Vacuum Cart for target transport

The vacuum cart houses a vacuum cube[7] with windows on all six sides. Three sides of the cube have windows while the other three sides have manipulator, support structure and a vacuum gate valve. A roughing pump (rotary vane Duo 5 with 5 m^3/hr. speed) and a high vacuum pump (turbo HiCube 80 with 241 m^3/hr. speed)[8] are also are housed in this cart. This allows tubing connections and the target to be at the same vacuum as TEC when targets are introduced into the chamber. The isolation gate valve is used to ensure that between transfers, the target can be kept in a vacuum atmosphere.

A Powerprobe[9] with a long linear stroke with capability to elevate the sample and a port aligner for angular alignment is used for target transfer .The end effector will be a recessed plate for the cylindrical puck (50mm ϕ).

[7] http://www.lesker.com/newweb/flanges/fittings_cf_crosses.cfm?pgid=cube
[8] https://www.pfeiffer-vacuum.com/en/products/pumping-stations/turbo-pumping-stations/
[9] http://www.lesker.com/newweb/sample_manipulation/sample_transfer/linear_rotary_motion/eppseries.cfm

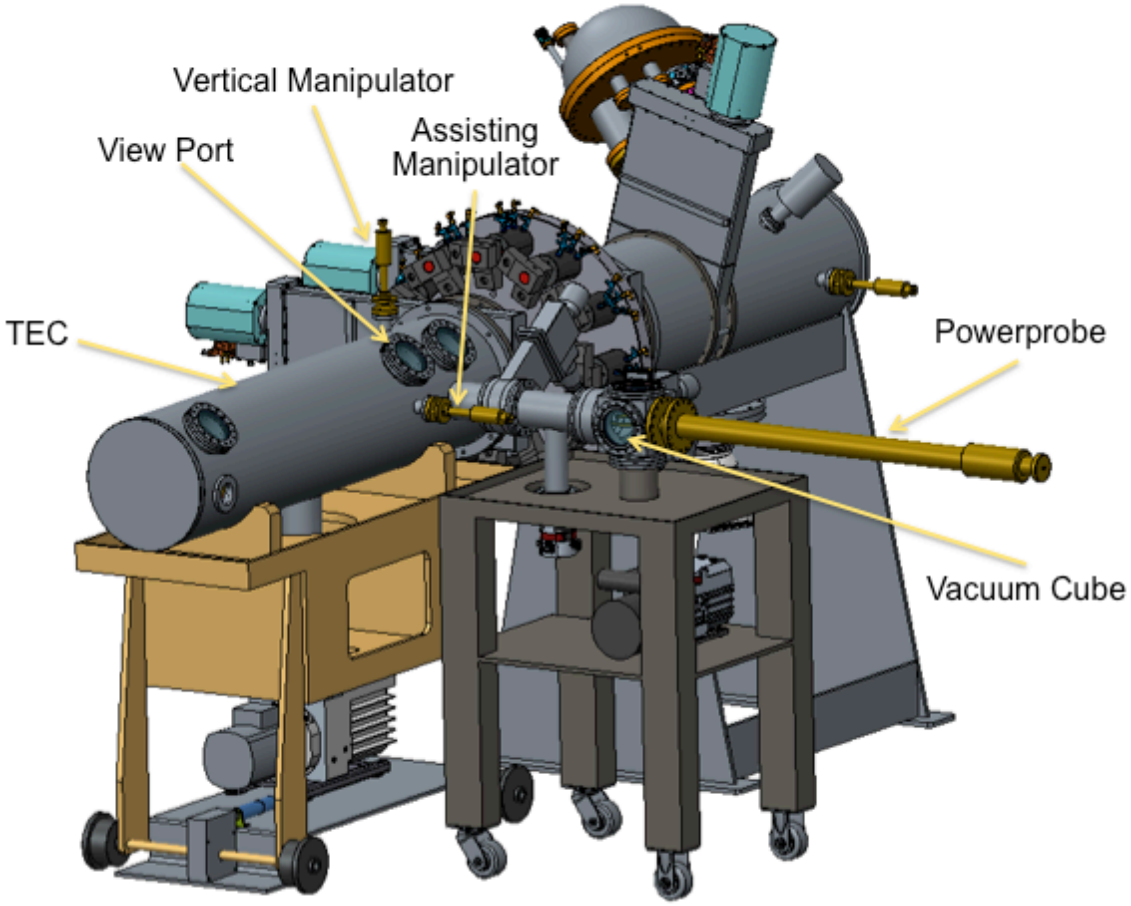

Fig. 36. Vacuum cart interfacing with TEC during target change out

For transfer of target to/from TEC, the vacuum cart flange is attached to the gate valve on the TEC port. The target holder is in retracted position with the target puck centered directly in front of the TEC port (See Fig. 35) For the 15° target, the vertical manipulator with its pincer fingers located on the notches of the target puck rotates the puck counter clockwise to release it from the target puck holder. Once released, the vertical manipulator will lift the target puck about 2cm above the target puck holder. The powerprobe then extends it arm below the elevated puck. The vertical manipulator then lowers and transfers the target puck to the recessed plate of the powerprobe. The power probe then retracts the target into the vacuum cube.

When the target has to be replaced with a new target, the vacuum cart interfaces with the glove box (see Fig. 37). Opening the gate valves, the target puck is introduced into the glove box. The glove box is used to minimize contamination from handling irradiated targets. There is very low radiation that the operator has to worry about during handling of these individual targets (~ 5 mrem/hr) in a glove box. Since the ORNL ACL's for extremities is 30 rem/yr (less than DOE ACL of 50 rem/yr) there is very little danger of an operator being exposed to large radiation levels.

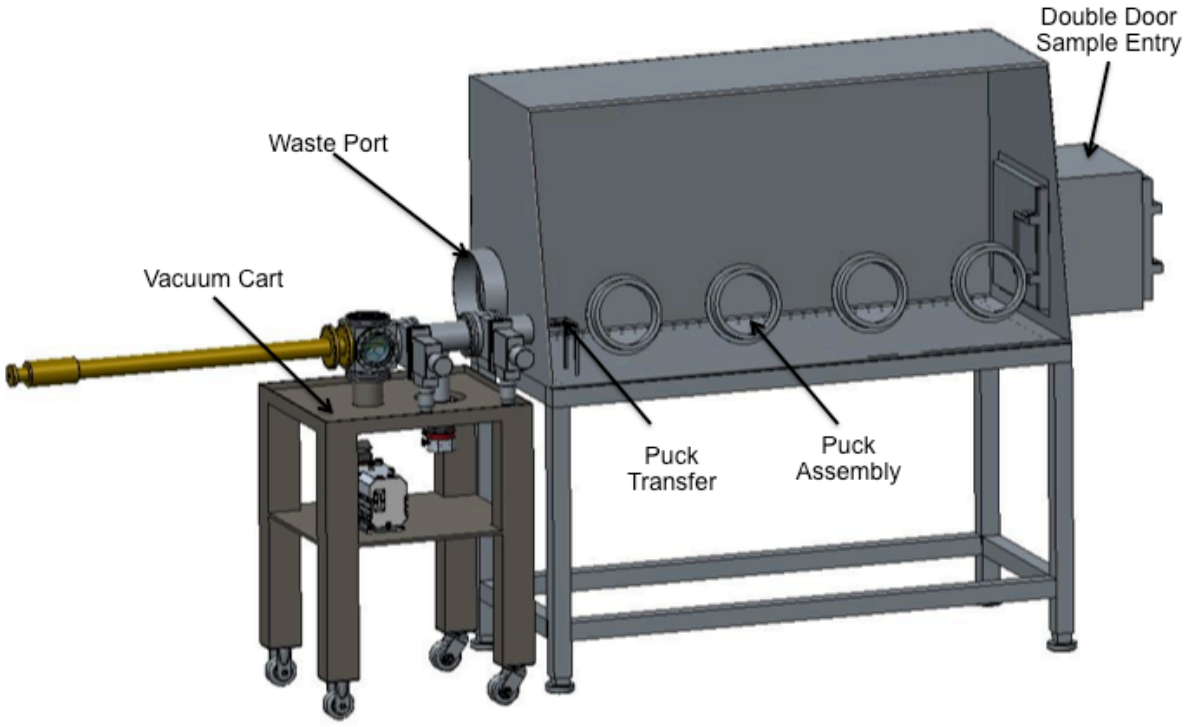

Fig. 37. Vacuum cart and Glove Box interface

The glove box is where the target puck gets assembled. The operator will introduce the sample transfer containers (with individualized IDs) through the double door. The operator opens the transfer containers and removes the target. Visual inspection of the sample is performed to see that there is no obvious damage to the target. The operator using specialized tools will assemble the target puck from target, grafoil, tungsten retainer, and the target securing base. The telescoping powerprobe's sample plate is extended on to the small stage directly in front of the port. The operator places the assembled target puck on to the recessed plate on the powerprobe. The powerprobe is then retracted and placed in the vacuum cube. Similarly, when removing an already plasma exposed sample, the target is reassembled into its transfer container. Care should be taken to ensure that the ID on the target sample and the transfer container match.

3.6.1 Contamination Control

The targets that are handled inside the glove box are radioactive. Although the activation level is not high (< 5 mrem/hr per sample), there is the potential for contamination. The Glove Box will be kept at a vacuum of 8-38 mm of water during handling of the activated samples. The exhaust from the glove box will go through a HEPA filter before venting it to the room ventilation system. Workers, wearing gloves and protective clothing, will be handling the samples from the shield storage cabinet to the Glove Box and back. After every transfer, the workers will perform a body scan to ensure there is no spread of contamination. Since the handling of the target inside the glove boxes is performed through gloves, there is no possibility of contamination unless there is a break in the gloves. Periodic wipe down of the glove box will be performed with a wet towel to keep the contamination low inside the Glove Box. This will also help reduce cross contamination between samples.

Connections are made between the vacuum cart and the glove box during sample transfer. Hence after every transfer, the surfaces of the flanges will be cleaned to ensure no spread of contamination. Similar steps will be taken during connection of the vacuum cart to the TEC chamber.

3.7 PROTOTYPING OF THE TARGET

The target puck was initially 3D printed on ABS+ material to see if the concept for compressing the grafoill worked. Since it was proved to be an adequate concept, all the parts of the target puck including the target were fabricated using W16.5 (readily available off the shelf).
Fig. 38 shows both the prototype ABS+ part and the tungsten parts. The grafoil could be compressed by rotating the locking ring using the target assembly tool. All parts fit well and the next stage of testing will be to see the heat conduction through different layers of material when exposed to a large heat source (blow torch) on the target and target puck surfaces. Integrated thermocouples will be integrated into the design for measuring temperatures of various regions.

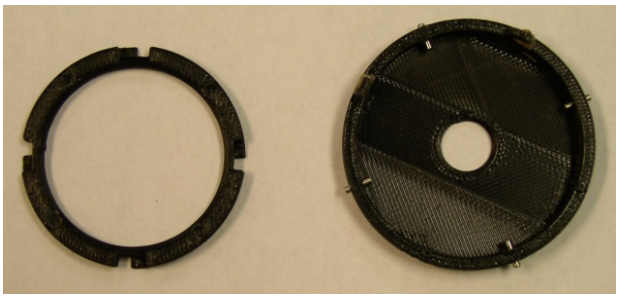

3D printed Retaining Ring and Target Puck

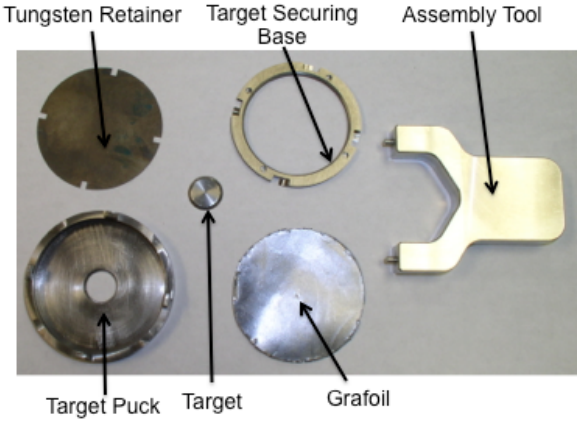

Fig. 38. 3D Printed and Fabricated Target Puck

4. ENRICHED TUNGSTEN MATERIAL PROCESSING

Using enriched ^{182}W would enable research to study the displacement by atoms due to neutron irradiation without leading to transmutation products. At high neutron irradiation doses and in particular for fusion prototypic neutron irradiation by 14 MeV neutrons significant concentrations of Re and Os can accumulate, which will influence the material properties significantly. Those transmutation products will also enhance the activation and lead to higher dose rates after the neutron irradiation. Hence using ^{182}W enriched tungsten might offer also the opportunity of fast experiment cycles without lengthy cool down periods before the neutron irradiated sample can be used for experiments in MPEX.

Enriched ^{182}W is commercially available in powder form. As part of this LDRD one research task was related to a feasibility study to manufacture a surrogate powder to a tungsten sample in the size of a sample to be irradiated in HFIR and then exposed to plasma in MPEX. The manufacturing process had the following requirements:

- Minimize the waste material during the manufacturing, since the enriched tungsten is very expensive

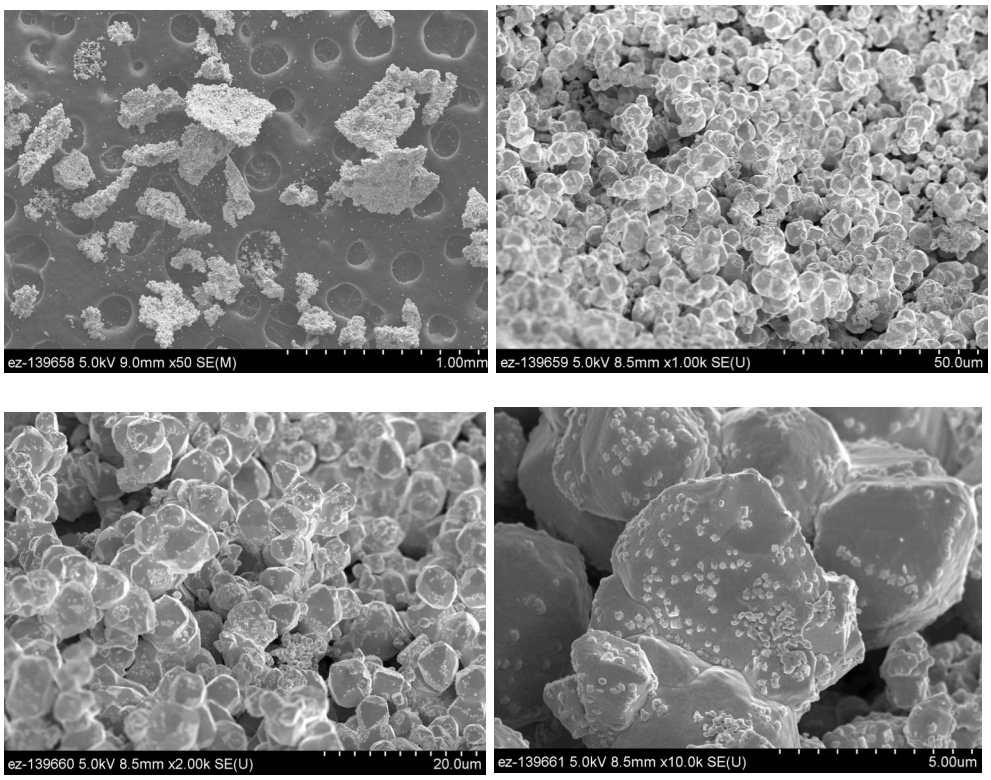

Fig. 39. SEM analysis of W-182 powder

- Produce mechanical material properties comparable to other tungsten material samples

The process development for the tungsten isotope sheet material was subdivided into several individual tasks:

- Characterization of the enriched ^{182}W powder by SEM
- Selection of a surrogate tungsten powder with natural isotope distribution by SEM

- Sintering of material samples
    - Mixing the surrogate powder with binder
    - Press powder into compact
    - Load compact into graphite die
    - Hot press material to increase density
- Work harden material samples
    - Can compact into stainless die
    - Material working by the equal channel angular extrusion method, which does minimize the material waste
    - Analysis (metallography) of material after extrusion
    - Warm rolling of tungsten samples to 1.25 mm thickness to obtain grain elongation
    - Remove cladding using abrasion or chemical treatment
- EDM cut samples to appropriate diameter and machine to final thickness

Fig. 39 shows the SEM analysis of the of the enriched ^{182}W isotope powder. It shows that the ^{182}W powder consists of both soft and hard agglomerates. A surrogate powder was identified and purchased from Global Tungsten Inc., which is closer in size to the ^{182}W powder than the tungsten powder from GE. A tungsten test pellet was pressed from a GE tungsten to determine the quantity needed for pressing compacts. The final pellet was 350 grams to produce a 1.01 by 1.036 by 1.81" long bar. The bar was 58.6 % of theoretical density. The size seems compatible with what is needed after sintering and canning. After the cold pressing was tested with GE powder, the sintering process was tested with the surrogate powder from Global W Inc. Global W was mixed with 1% binder of acrawax and cold pressed. Fig. 40 left shows a cold pressed tungsten bar, which was pressed to a density of 55%. The sample was then subsequently sintered (see Fig. 40 right) to a density of 67% only.

Since this density does not meet the requirements, the process was altered and hot pressing of tungsten pellets was pursued. A special graphite die was manufactured to obtain pellet sizes of interest. It should be noted that this is important, since the purpose of qualifying a material manufacturing process is related to minimize waste during the process. Fig. 39 left shows the graphite die for the hot pressing.

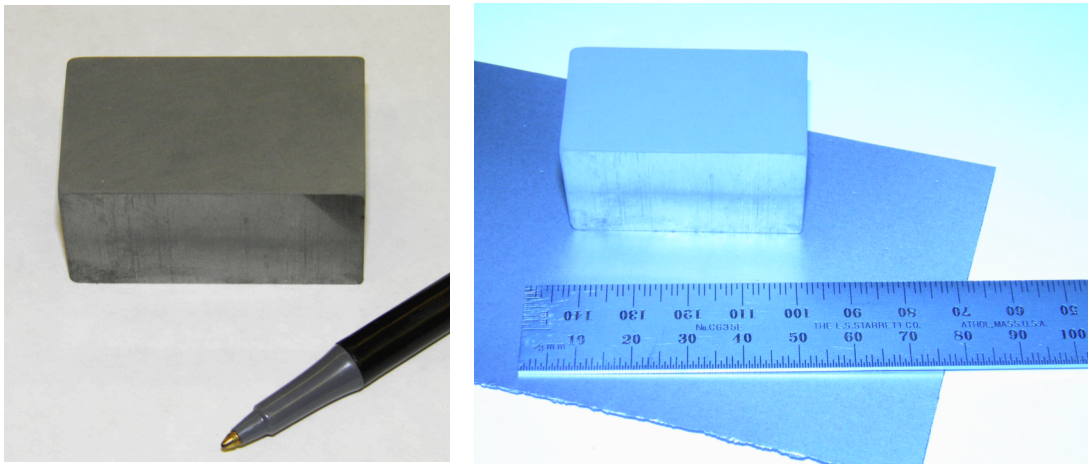

Fig. 40. Cold pressed tungsten to 55% density and sintered tungsten to 67% density

The tungsten samples were then hot-pressed to 1900 C°. A density of 93% was achieved with this hot pressing (See Fig. 39 right). After the hot pressing a WC layer was observed on the surface. Detailed

XRD on the tungsten surface revealed 1.5% WC only.

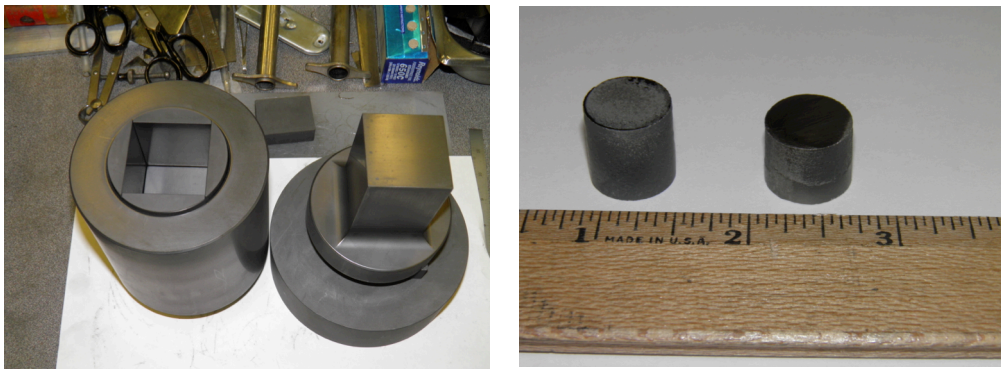

Fig. 41. Graphite die and tungsten pellets after hot-pressing to density of 90% (left) and 93% (right).

The pellets were then canned into stainless steel containers before the equal channel angular extrusion (ECAE) was performed at Shearform Inc. After the extrusion the can was cut into sections and the cross sections were polished for metallography. Fig. 42 shows the cross section. The tungsten was broken up into several pieces within the can (see Fig. 41). This was an unexpected result. Previous positive results from Shearform were related to close to 100% dense tungsten. The samples manufactured from the

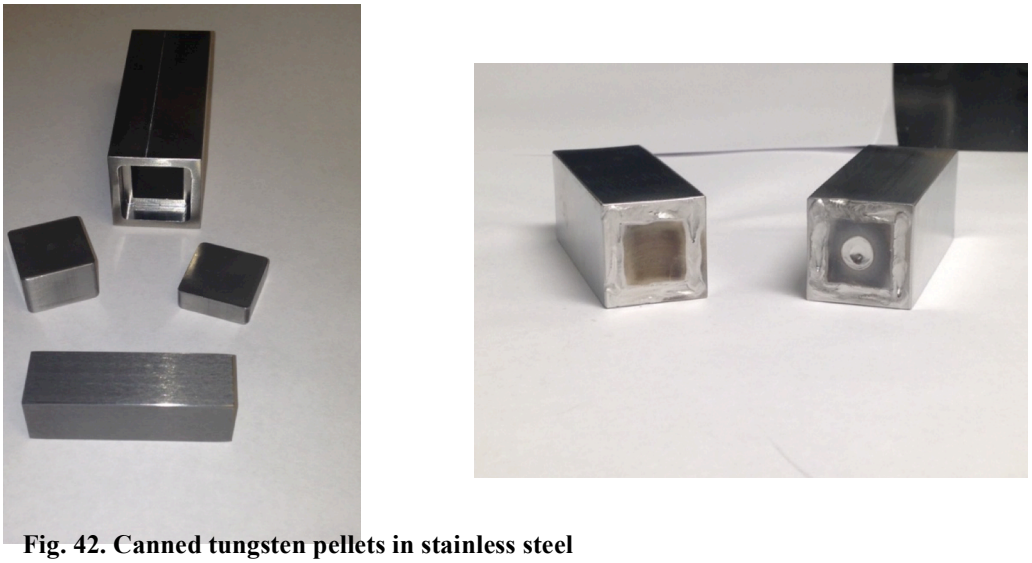

Fig. 42. Canned tungsten pellets in stainless steel

Global W powder as surrogate for the ^{182}W were suboptimal with densities just around 92%. Future attempts should focus on getting a better surrogate W powder, which can be densified to close to 100%.

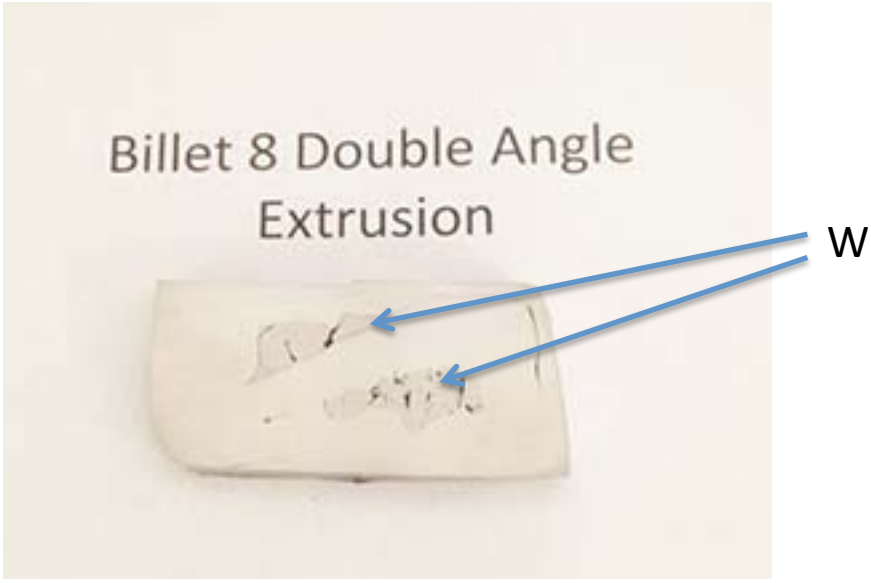

Fig. 43: Broken tungsten sections in a matrix of steel.

5. REFERENCES

1. Greenwald Panel FESAC Report, October 2007.
2. J. RAPP, et al. "The Development of Plasma-Material Interaction Facilities for the Future of Fusion Technology," *Fusion Science and Technology*, 64, August 2013.
3. P. GARIN et al., "IFMIF specifications from the users point of view", *Fusion Engineering and Design* **86**, 611, 2011.
4. R. E. STOLLER and L. R. GREENWOOD, *J. Nucl. Mater.* **271–272** (1999) 57–62.
5. A. HORSEWELL, et al, *J. Nucl. Mater.* **179–181** (1991) 924–927.
6. S.J. ZINKLE, M. VICTORIA, K. ABE, *J. Nucl. Mater.* **307-311** (2002) 31-42.
7. R. D. CHEVERTON and T. M. SIMS, "HFIR Core Nuclear Design," ORNL-4621, Oak Ridge National Laboratory (1971).
8. ORNL NEUTRON SCIENCES, "The High Flux Isotope Reactor at ORNL," Oak Ridge National Laboratory, http://neutrons.ornl.gov/facilities/HFIR/ (current as of Oct. 8, 2014).
9. N. XOUBI and R. T. PRIMM III, "Modeling of the High Flux Isotope Reactor Cycle 400," ORNL/TM-2004/251, Oak Ridge National Laboratory (2005).
10. R. J. ELLIS et al, "Cross Section Generation and Physics Modeling in a Feasibility Study of the Conversion of the High Flux Isotope Reactor Core to Use Low-Enriched Uranium Fuel," *Proc. of the PHYSOR-2006 International Conference on Advances in Reactor Physics: Advances in Nuclear Analysis and Simulation,* Vancouver, Canada, September 2006, American Nuclear Society (2007).
11. J. L. MCDUFFEE et al, "Proposed Fuel Pin Irradiation Facilities for the High Flux Isotope Reactor," Paper 8424, *Proc. ICAPP '08,* Anaheim, California, June 8–12, 2008, American Nuclear Society (2009).
12. R. J. ELLIS et al, "Analysis of a Fast Spectrum Irradiation Facility in the High Flux Isotope Reactor," *Proceedings of the PHYSOR-2008 International Conference on the Physics of Reactors, Nuclear Power: A Sustainable Resource,* Casino-Kursaal Conf. Center, Interlaken, Switzerland, September 14–19, 2008, Paul Scherrer Institut (2011).
13. D. E. PEPLOW, "A Computational Model of the High Flux Isotope Reactor for the Calculation of Cold Source, Beam Tube, and Guide Hall Nuclear Parameters," ORNL/TM-2004/237, Oak Ridge National Laboratory (Nov. 2004).
14. G. M. WRIGHT et al., "Hydrogenic retention in irradiated tungsten exposed to high-flux plasma," *Nuclear Fusion*, **50**, 075006, June 8, 2010.
15. M.H. J. 'T HOEN et al., "Saturation of deuterium retention in self-damaged tungsten exposed to high-flux plasmas," *Nuclear Fusion*, **52**, 023008, January 16, 2012.
16. X-5 MONTE CARLO TEAM, "MCNP - A General Monte Carlo N-Particle Transport Code, Version 5, Volume I: Overview and Theory," LA-UR-03-1987, Los Alamos National Laboratory (Apr. 2003, Revised Oct. 3, 2005).
17. "SCALE: A Comprehensive Modeling and Simulation Suite for Nuclear Safety Analysis and Design," ORNL/TM-2005/39, Version 6.1, Oak Ridge National Laboratory (June 2011), Available from the Radiation Safety Information Computational Center as CCC-785.
18. M. D. DEHART and S. M. BOWMAN, "Reactor Physics Methods and Analysis Capabilities in Scale," *Nuclear Technology*, **174,** *2*, 196–213 (2011).
19. G. L. BELL et al, "Summary of FY12 HFIR Irradiation Testing Activities," ORNL/TM-2012/454, Oak Ridge National Laboratory (Sept. 2012).
20. M. OKUNIEWSKI et al, "Microstructural Evolution of a Uranium-Zirconium Alloy at Low Fluences," presented at the Material Society 2013 TMS Annual Mtg. & Exhibition, San Antonio, Texas, April, 2013.
21. D. CHANDLER, Oak Ridge National Laboratory, "Update of the full neutron spectrum flux levels in the HFIR fast flux target region at midplane," Personal Communication (2014).
22. M. J. NORGETT et al, "A Proposed Method of Calculating Displacement Dose Rates," *Nuclear Engineering and Design*, **33**, 50–54, 1975.

23. R. E. STOLLER (ORNL), "Primary Radiation Damage Formation," *Comprehensive Nuclear Materials*, Chapter 11 p. 293–332, Elsevier Ltd., Amsterdam, Netherlands (2012).
24. R. E. MACFARLANE and A. C. KAHLER, "Methods for Processing ENDF/B-VII with NJOY" (Unclassified Report), LA-UR-10-04652, Los Alamos National Laboratory (July 2010), *Nuclear Data Sheets*, Vol. 111, p. 2739–2890 (Oct. 2010).
25. E. A. READ and C. R. E. DE OLIVEIRA, "A Functional Method for Estimating DPA Tallies in Monte Carlo Calculations of Light Water Reactors," *Proc. Int. Conf. on Mathematics and Computational Methods Applied to Nuclear Science and Engineering* (M&C 2011), Rio de Janeiro, RJ, Brazil, May 8–12, 2011, American Nuclear Society (2011).
26. P. D. EDMONDSON, et al., "Small-scale characterization of irradiated nuclear materials: Part I – Microstructure," *Journal of Nuclear Materials*, (2014), http://dx.doi.org/10.1016/j.jnucmat.2014.11.067
27. R. N. STUART et al, "A Computer Simulation of the Effect of Temperature on the Threshold Atomic Displacement Energy in Tungsten Metal," *Radiation Effects*, **30**, *3* (1976).
28. F. MAURY et al, (1978) "Frenkel pair creation and stage I recovery in W crystals irradiated near threshold," *Radiation Effects: Incorporating Plasma Science and Plasma Technology*, **38:**1-2, 53-65, DOI: 10.1080/00337577808233209
29. R. J. ELLIS, J. RAPP, "Neutron-Irradiated Samples as Test Materials for MPEX", Fus. Sci. Techol., November (2015) dx.doi.org/10.13182/FST14-909.

APPENDIX A. ACTIVITIES BY NUCLIDE FOR FIVE LIKELY MATERIALS IRRADIATED IN HFIR AND COOLED FOR AT LEAST TWO YEARS

APPENDIX A. ACTIVITIES BY NUCLIDE FOR FIVE LIKELY MATERIALS IRRADIATED IN HFIR AND COOLED FOR AT LEAST TWO YEARS

The following tables (Table A1 to A5) tabulate the activities of five likely MPEX sample materials, after irradiation in HFIR for 10 cycles (to a nominal displacement damage level of 10 DPA). The tables show the activities of the main nuclides in the irradiated material compositions as a function of cooling time from the time of discharge until at least two years later. The nuclides are ordered according to large-to-small activities at the two-year cooling (highlighted in blue) column. After two years of cooling, the most active nuclide for each of the irradiated materials is ^{185}W.
These activities are in units of Ci per gram of initial sample material. Each irradiated sample disk initially had a mass of about 2.1 g.

Table A 1 Activities (Ci) as function of cooling time per gram of 99% enriched ^{182}W material irradiated in HFIR for 10 cycles

99% ^{182}W	0.0 h	2.0 h	24.0 h	48.0 h	168.0 h	336.0 h	600.0 h	1100.0 h	2100.0 h	4320.0 h	8760.0 h	17520 h	26280 h
w185	1.66E+01	1.66E+01	1.65E+01	1.63E+01	1.56E+01	1.46E+01	1.32E+01	1.09E+01	7.40E+00	3.15E+00	5.72E-01	1.97E-02	6.78E-04
w181	4.07E-02	4.07E-02	4.04E-02	4.02E-02	3.91E-02	3.75E-02	3.53E-02	3.13E-02	2.47E-02	1.45E-02	5.04E-03	6.25E-04	7.75E-05
re188	9.04E+00	8.34E+00	3.44E+00	1.34E+00	7.31E-02	5.94E-02	5.32E-02	4.33E-02	2.86E-02	1.14E-02	1.82E-03	4.84E-05	1.29E-06
w188	6.75E-02	6.75E-02	6.68E-02	6.62E-02	6.30E-02	5.87E-02	5.27E-02	4.28E-02	2.83E-02	1.13E-02	1.80E-03	4.79E-05	1.28E-06
ir192	2.59E-03	2.59E-03	2.56E-03	2.54E-03	2.42E-03	2.27E-03	2.05E-03	1.68E-03	1.14E-03	4.78E-04	8.41E-05	2.73E-06	8.87E-08
ta182	1.98E-04	1.98E-04	1.97E-04	1.96E-04	1.90E-04	1.82E-04	1.71E-04	1.50E-04	1.17E-04	6.68E-05	2.19E-05	2.41E-06	2.66E-07
os185	3.24E-05	3.24E-05	3.22E-05	3.19E-05	3.08E-05	2.92E-05	2.69E-05	2.31E-05	1.70E-05	8.54E-06	2.17E-06	1.46E-07	9.75E-09
ir194	4.89E-02	4.55E-02	2.06E-02	8.71E-03	1.17E-04	3.57E-07	7.92E-08	7.86E-08	7.76E-08	7.54E-08	7.11E-08	6.33E-08	5.64E-08
re186	1.72E+01	1.70E+01	1.43E+01	1.19E+01	4.67E+00	1.27E+00	1.63E-01	3.35E-03	1.43E-06	1.15E-08	1.15E-08	1.15E-08	1.15E-08
re184	1.77E-06	1.76E-06	1.73E-06	1.70E-06	1.55E-06	1.37E-06	1.13E-06	7.82E-07	3.95E-07	1.19E-07	3.45E-08	7.45E-09	1.67E-09
hf181	3.53E-06	3.53E-06	3.47E-06	3.42E-06	3.15E-06	2.81E-06	2.35E-06	1.67E-06	8.44E-07	1.86E-07	9.04E-09	2.31E-11	5.91E-14
os191	8.64E-02	8.66E-02	8.61E-02	8.34E-02	6.69E-02	4.88E-02	2.98E-02	1.17E-02	1.79E-03	2.78E-05	6.72E-09	4.93E-16	3.61E-23
ir191m	8.64E-02	8.66E-02	8.61E-02	8.34E-02	6.69E-02	4.88E-02	2.98E-02	1.17E-02	1.79E-03	2.78E-05	6.72E-09	4.93E-16	3.61E-23
ir193m	6.88E-03	6.84E-03	6.44E-03	6.03E-03	4.34E-03	2.74E-03	1.33E-03	3.37E-04	2.17E-05	4.92E-08	2.53E-13	9.30E-24	0.00E+00
hf179m	4.13E-06	0.00E+00	0.00E+00	0.00E+00	0.00E+00	0.00E+00	0.00E+00	0.00E+00	0.00E+00	0.00E+00	0.00E+00	0.00E+00	0.00E+00
ta180	2.47E-06	2.08E-06	3.21E-07	4.17E-08	1.55E-12	9.72E-19	1.74E-28	0.00E+00	0.00E+00	0.00E+00	0.00E+00	0.00E+00	0.00E+00
ta182m	1.65E-05	0.00E+00	0.00E+00	0.00E+00	0.00E+00	0.00E+00	0.00E+00	0.00E+00	0.00E+00	0.00E+00	0.00E+00	0.00E+00	0.00E+00
ta183	5.21E-02	5.15E-02	4.55E-02	3.97E-02	2.01E-02	7.77E-03	1.74E-03	1.03E-04	3.56E-07	1.24E-12	1.49E-23	0.00E+00	0.00E+00
w183m	1.98E+02	2.63E-03	2.32E-03	2.02E-03	1.03E-03	3.96E-04	8.88E-05	5.23E-06	1.82E-08	6.30E-14	7.58E-25	0.00E+00	0.00E+00
w185m	8.15E-02	1.91E-23	0.00E+00	0.00E+00	0.00E+00	0.00E+00	0.00E+00	0.00E+00	0.00E+00	0.00E+00	0.00E+00	0.00E+00	0.00E+00
w187	7.11E+00	6.71E+00	3.56E+00	1.78E+00	5.56E-02	4.34E-04	2.12E-07	1.13E-13	3.25E-26	0.00E+00	0.00E+00	0.00E+00	0.00E+00
w189	9.48E-03	3.99E-06	0.00E+00	0.00E+00	0.00E+00	0.00E+00	0.00E+00	0.00E+00	0.00E+00	0.00E+00	0.00E+00	0.00E+00	0.00E+00
re188m	2.43E-01	2.77E-03	1.17E-24	0.00E+00	0.00E+00	0.00E+00	0.00E+00	0.00E+00	0.00E+00	0.00E+00	0.00E+00	0.00E+00	0.00E+00
re189	2.58E-02	2.44E-02	1.30E-02	6.58E-03	2.15E-04	1.78E-06	9.54E-10	6.10E-16	2.50E-28	0.00E+00	0.00E+00	0.00E+00	0.00E+00
os189m	8.63E-01	6.80E-01	5.08E-02	3.69E-03	2.89E-05	2.39E-07	1.33E-10	1.38E-12	1.55E-13	1.20E-15	7.27E-20	0.00E+00	0.00E+00
os190m	5.70E-06	1.28E-09	0.00E+00	0.00E+00	0.00E+00	0.00E+00	0.00E+00	0.00E+00	0.00E+00	0.00E+00	0.00E+00	0.00E+00	0.00E+00
os191m	1.44E-01	1.29E-01	4.03E-02	1.13E-02	1.98E-05	2.73E-09	2.34E-15	7.58E-27	0.00E+00	0.00E+00	0.00E+00	0.00E+00	0.00E+00
os193	8.83E-04	8.43E-04	5.08E-04	2.93E-04	1.85E-05	3.86E-07	8.86E-10	8.88E-15	8.93E-25	0.00E+00	0.00E+00	0.00E+00	0.00E+00
ir192m	5.64E-02	0.00E+00	0.00E+00	0.00E+00	0.00E+00	0.00E+00	0.00E+00	0.00E+00	0.00E+00	0.00E+00	0.00E+00	0.00E+00	0.00E+00
ir194m	7.87E-05	0.00E+00	0.00E+00	0.00E+00	0.00E+00	0.00E+00	0.00E+00	0.00E+00	0.00E+00	0.00E+00	0.00E+00	0.00E+00	0.00E+00
pt193m	1.33E-04	1.31E-04	1.13E-04	9.62E-05	4.32E-05	1.41E-05	2.42E-06	8.63E-08	1.09E-10	4.06E-17	5.58E-30	0.00E+00	0.00E+00
pt195m	4.02E-05	3.96E-05	3.38E-05	2.84E-05	1.20E-05	3.57E-06	5.34E-07	1.46E-08	1.09E-11	1.23E-18	0.00E+00	0.00E+00	0.00E+00
total	2.50E+02	4.98E+01	3.82E+01	3.16E+01	2.06E+01	1.61E+01	1.36E+01	1.10E+01	7.49E+00	3.19E+00	5.80E-01	2.04E-02	7.59E-04

Table A 2. Activities (Ci) as function of cooling time per gram of natural W material irradiated in HFIR for 10 cycles

nat_W	0.0 h	2.0 h	24.0 h	48.0 h	168.0 h	336.0 h	600.0 h	1100.0 h	2100.0 h	4320.0 h	8760.0 h	17520 h	26280 h
w185	4.12E+01	4.12E+01	4.08E+01	4.04E+01	3.86E+01	3.62E+01	3.27E+01	2.70E+01	1.84E+01	7.82E+00	1.42E+00	4.88E-02	1.68E-03
re188	5.88E+02	5.42E+02	2.24E+02	8.69E+01	4.88E+00	3.98E+00	3.57E+00	2.90E+00	1.92E+00	7.65E-01	1.22E-01	3.24E-03	8.63E-05
w188	4.52E+00	4.52E+00	4.48E+00	4.44E+00	4.22E+00	3.94E+00	3.53E+00	2.87E+00	1.90E+00	7.57E-01	1.21E-01	3.21E-03	8.55E-05
ir192	1.78E-01	1.78E-01	1.76E-01	1.74E-01	1.66E-01	1.56E-01	1.41E-01	1.16E-01	7.81E-02	3.28E-02	5.77E-03	1.88E-04	6.09E-06
w181	1.08E-02	1.07E-02	1.07E-02	1.06E-02	1.03E-02	9.92E-03	9.32E-03	8.27E-03	6.52E-03	3.84E-03	1.33E-03	1.65E-04	2.05E-05
pt193	6.00E-05	6.00E-05	6.03E-05	6.06E-05	6.15E-05	6.19E-05	6.21E-05	6.21E-05	6.20E-05	6.18E-05	6.13E-05	6.05E-05	5.97E-05
ir194	3.39E+00	3.15E+00	1.43E+00	6.03E-01	8.07E-03	2.48E-05	5.52E-06	5.48E-06	5.41E-06	5.25E-06	4.95E-06	4.41E-06	3.93E-06
os194	5.56E-06	5.56E-06	5.56E-06	5.55E-06	5.55E-06	5.53E-06	5.51E-06	5.48E-06	5.41E-06	5.25E-06	4.95E-06	4.41E-06	3.93E-06
os185	2.26E-04	2.26E-04	2.25E-04	2.23E-04	2.15E-04	2.04E-04	1.88E-04	1.61E-04	1.18E-04	5.97E-05	1.52E-05	1.02E-06	6.81E-08
ta182	5.28E-05	5.28E-05	5.25E-05	5.22E-05	5.06E-05	4.85E-05	4.54E-05	4.00E-05	3.11E-05	1.78E-05	5.82E-06	6.42E-07	7.08E-08
re186	5.90E+01	5.81E+01	4.89E+01	4.06E+01	1.60E+01	4.34E+00	5.58E-01	1.15E-02	4.92E-06	5.92E-08	5.92E-08	5.92E-08	5.92E-08
re184	5.88E-06	5.87E-06	5.78E-06	5.67E-06	5.18E-06	4.56E-06	3.75E-06	2.61E-06	1.32E-06	3.96E-07	1.16E-07	2.50E-08	5.59E-09
hf181	3.39E-06	3.38E-06	3.33E-06	3.28E-06	3.02E-06	2.69E-06	2.25E-06	1.60E-06	8.09E-07	1.78E-07	8.66E-09	2.22E-11	5.67E-14
os191	5.90E+00	5.91E+00	5.88E+00	5.69E+00	4.57E+00	3.33E+00	2.03E+00	7.95E-01	1.22E-01	1.90E-03	4.59E-07	3.36E-14	2.47E-21
ir191m	5.90E+00	5.91E+00	5.88E+00	5.69E+00	4.57E+00	3.33E+00	2.03E+00	7.95E-01	1.22E-01	1.90E-03	4.59E-07	3.36E-14	2.47E-21
ir193m	4.74E-01	4.71E-01	4.44E-01	4.16E-01	2.99E-01	1.89E-01	9.14E-02	2.32E-02	1.49E-03	3.39E-06	1.74E-11	6.40E-22	0.00E+0

													0
ir190	8.23E-06	8.19E-06	7.76E-06	7.32E-06	5.45E-06	3.61E-06	1.89E-06	5.55E-07	4.78E-08	2.07E-10	3.87E-15	1.82E-24	0.00E+00
hf179m	1.09E-06	0.00E+00	0.00E+00	0.00E+00	0.00E+00	0.00E+00	0.00E+00	0.00E+00	0.00E+00	0.00E+00	0.00E+00	0.00E+00	0.00E+00
ta182m	6.07E-06	0.00E+00	0.00E+00	0.00E+00	0.00E+00	0.00E+00	0.00E+00	0.00E+00	0.00E+00	0.00E+00	0.00E+00	0.00E+00	0.00E+00
ta183	1.39E-02	1.37E-02	1.21E-02	1.06E-02	5.36E-03	2.07E-03	4.64E-04	2.74E-05	9.50E-08	3.29E-13	3.96E-24	0.00E+00	0.00E+00
w183m	6.04E+01	7.00E-04	6.18E-04	5.39E-04	2.73E-04	1.06E-04	2.37E-05	1.40E-06	4.84E-09	1.68E-14	2.02E-25	0.00E+00	0.00E+00
w185m	1.64E-01	3.83E-23	0.00E+00	0.00E+00	0.00E+00	0.00E+00	0.00E+00	0.00E+00	0.00E+00	0.00E+00	0.00E+00	0.00E+00	0.00E+00
w187	4.43E+02	4.18E+02	2.21E+02	1.11E+02	3.46E+00	2.70E-02	1.32E-05	7.06E-12	2.02E-24	0.00E+00	0.00E+00	0.00E+00	0.00E+00
w189	6.36E-01	2.68E-04	0.00E+00	0.00E+00	0.00E+00	0.00E+00	0.00E+00	0.00E+00	0.00E+00	0.00E+00	0.00E+00	0.00E+00	0.00E+00
re188m	1.58E+01	1.80E-01	7.59E-23	0.00E+00	0.00E+00	0.00E+00	0.00E+00	0.00E+00	0.00E+00	0.00E+00	0.00E+00	0.00E+00	0.00E+00
re189	1.70E+00	1.61E+00	8.59E-01	4.33E-01	1.41E-02	1.17E-04	6.29E-08	4.02E-14	1.65E-26	0.00E+00	0.00E+00	0.00E+00	0.00E+00
os189m	5.19E+01	4.10E+01	3.07E+00	2.27E-01	1.90E-03	1.58E-05	8.75E-09	9.51E-11	1.07E-11	8.29E-14	5.00E-18	0.00E+00	0.00E+00
os190m	3.71E-04	8.34E-08	0.00E+00	0.00E+00	0.00E+00	0.00E+00	0.00E+00	0.00E+00	0.00E+00	0.00E+00	0.00E+00	0.00E+00	0.00E+00
os191m	9.76E+00	8.78E+00	2.74E+00	7.70E-01	1.35E-03	1.86E-07	1.59E-13	5.15E-25	0.00E+00	0.00E+00	0.00E+00	0.00E+00	0.00E+00
os193	6.12E-02	5.84E-02	3.52E-02	2.03E-02	1.28E-03	2.68E-05	6.14E-08	6.15E-13	6.19E-23	0.00E+00	0.00E+00	0.00E+00	0.00E+00
ir192m	3.87E+00	0.00E+00	0.00E+00	0.00E+00	0.00E+00	0.00E+00	0.00E+00	0.00E+00	0.00E+00	0.00E+00	0.00E+00	0.00E+00	0.00E+00
ir194m	5.44E-03	0.00E+00	0.00E+00	0.00E+00	0.00E+00	0.00E+00	0.00E+00	0.00E+00	0.00E+00	0.00E+00	0.00E+00	0.00E+00	0.00E+00
pt191	3.03E-06	2.97E-06	2.36E-06	1.85E-06	5.36E-07	9.48E-08	6.24E-09	3.61E-11	1.20E-15	1.39E-25	0.00E+00	0.00E+00	0.00E+00
pt193m	9.22E-03	9.09E-03	7.85E-03	6.69E-03	3.01E-03	9.80E-04	1.68E-04	6.00E-06	7.61E-09	2.82E-15	3.88E-28	0.00E+00	0.00E+00
pt195m	2.80E-03	2.76E-03	2.36E-03	1.98E-03	8.36E-04	2.49E-04	3.72E-05	1.02E-06	7.57E-10	8.61E-17	1.11E-30	0.00E+00	0.00E+00
pt197	3.38E-05	3.16E-05	1.47E-05	6.37E-06	9.73E-08	2.79E-10	2.82E-14	7.66E-22	0.00E+00	0.00E+00	0.00E+00	0.00E+00	0.00E+00
pt197m	1.81E-06	7.57E-07	5.18E-11	1.48E-15	0.00E+00	0.00E+00	0.00E+00	0.00E+00	0.00E+00	0.00E+00	0.00E+00	0.00E+00	0.00E+00
au199	9.90E-06	9.72E-06	7.94E-06	6.36E-06	2.11E-06	4.50E-07	3.96E-08	3.98E-10	4.02E-14	5.41E-23	0.00E+00	0.00E+00	0.00E+00
total	**1.30E+03**	**1.13E+03**	**5.60E+02**	**2.97E+02**	**7.68E+01**	**5.55E+01**	**4.47E+01**	**3.45E+01**	**2.25E+01**	**9.38E+00**	**1.67E+00**	**5.57E-02**	**1.95E-03**

Table A 3. Activities (Ci) as function of cooling time per gram of 10 wt%Ta-W material irradiated in HFIR for 10 cycles

Ta10-W	**0.0 h**	**2.0 h**	**24.0 h**	**48.0 h**	**168.0 h**	**336.0 h**	**600.0 h**	**1100.0 h**	**2100.0 h**	**4320.0 h**	**8760.0 h**	**17520 h**	**26280 h**
w185	3.86E+01	3.86E+01	3.82E+01	3.79E+01	3.62E+01	3.39E+01	3.06E+01	2.53E+01	1.72E+01	7.33E+00	1.33E+00	4.57E-02	1.57E-03
ta182	5.47E-01	5.47E-01	5.44E-01	5.41E-01	5.25E-01	5.03E-01	4.71E-01	4.15E-01	3.23E-01	1.85E-01	6.03E-02	6.65E-03	7.33E-04
re188	5.35E+02	4.93E+02	2.04E+02	7.91E+01	4.44E+00	3.62E+00	3.24E+00	2.64E+00	1.74E+00	6.96E-01	1.11E-01	2.95E-03	7.85E-05
w188	4.12E+00	4.11E+00	4.08E+00	4.04E+00	3.84E+00	3.58E+00	3.21E+00	2.61E+00	1.73E+00	6.89E-01	1.10E-01	2.92E-03	7.77E-05
ir192	1.62E-01	1.62E-01	1.60E-01	1.59E-01	1.51E-01	1.42E-01	1.28E-01	1.05E-01	7.11E-02	2.98E-02	5.25E-03	1.71E-04	5.54E-06
w181	9.79E-03	9.78E-03	9.73E-03	9.68E-03	9.40E-03	9.04E-03	8.48E-03	7.53E-03	5.93E-03	3.50E-03	1.21E-03	1.51E-04	1.87E-05
pt193	5.46E-05	5.46E-05	5.49E-05	5.52E-05	5.59E-05	5.64E-05	5.65E-05	5.65E-05	5.64E-05	5.62E-05	5.58E-05	5.51E-05	5.43E-05
ir194	3.08E+00	2.87E+00	1.30E+00	5.49E-01	7.35E-03	2.25E-05	5.02E-06	4.99E-06	4.92E-06	4.78E-06	4.51E-06	4.02E-06	3.58E-06
os194	5.06E-06	5.06E-06	5.06E-06	5.06E-06	5.05E-06	5.04E-06	5.02E-06	4.99E-06	4.92E-06	4.78E-06	4.51E-06	4.02E-06	3.58E-06
ta179	4.06E-06	4.06E-06	4.06E-06	4.05E-06	4.03E-06	4.00E-06	3.96E-06	3.87E-06	3.71E-06	3.37E-06	2.78E-06	1.90E-06	1.30E-06
os185	2.08E-04	2.08E-04	2.06E-04	2.05E-04	1.97E-04	1.87E-04	1.73E-04	1.48E-04	1.09E-04	5.48E-05	1.39E-05	9.32E-07	6.25E-08
re186	5.47E+01	5.39E+01	4.54E+01	3.77E+01	1.48E+01	4.03E+00	5.18E-01	1.07E-02	4.57E-06	5.45E-08	5.45E-08	5.45E-08	5.45E-08
re184	5.47E-06	5.46E-06	5.37E-06	5.27E-06	4.81E-06	4.24E-06	3.48E-06	2.42E-06	1.22E-06	3.68E-07	1.07E-07	2.32E-08	5.19E-09
hf181	1.73E-03	1.73E-03	1.70E-03	1.67E-03	1.54E-03	1.38E-03	1.15E-03	8.17E-04	4.13E-04	9.11E-05	4.42E-06	1.13E-08	2.89E-11
os191	5.37E+00	5.38E+00	5.35E+00	5.18E+00	4.16E+00	3.03E+00	1.85E+00	7.24E-01	1.11E-01	1.73E-03	4.18E-07	3.06E-14	2.24E-21
ir191m	5.37E+00	5.38E+00	5.35E+00	5.18E+00	4.16E+00	3.03E+00	1.85E+00	7.24E-01	1.11E-01	1.73E-03	4.18E-07	3.06E-14	2.24E-21
ir193m	4.31E-01	4.29E-01	4.04E-01	3.78E-01	2.72E-01	1.72E-01	8.32E-02	2.11E-02	1.36E-03	3.08E-06	1.59E-11	5.83E-22	0.00E+00
ir190	7.49E-06	7.45E-06	7.06E-06	6.66E-06	4.96E-06	3.29E-06	1.72E-06	5.05E-07	4.35E-08	1.88E-10	3.52E-15	1.66E-24	0.00E+00
hf179m	1.29E-06	0.00E+00	0.00E+00	0.00E+00	0.00E+00	0.00E+00	0.00E+00	0.00E+00	0.00E+00	0.00E+00	0.00E+00	0.00E+00	0.00E+00
ta180	8.62E-03	7.27E-03	1.12E-03	1.46E-04	5.41E-09	3.40E-15	6.09E-25	0.00E+00	0.00E+00	0.00E+00	0.00E+00	0.00E+00	0.00E+00
ta182m	1.09E-02	0.00E+00	0.00E+00	0.00E+00	0.00E+00	0.00E+00	0.00E+00	0.00E+00	0.00E+00	0.00E+00	0.00E+00	0.00E+00	0.00E+00
ta183	1.46E+02	1.44E+02	1.27E+02	1.11E+02	5.63E+01	2.18E+01	4.88E+00	2.87E-01	9.98E-04	3.46E-09	4.16E-20	0.00E+00	0.00E+00
w183m	6.48E+01	7.35E+00	6.49E+00	5.67E+00	2.87E+00	1.11E+00	2.49E-01	1.47E-02	5.09E-05	1.76E-10	2.12E-21	0.00E+00	0.00E+00
w185m	1.54E-01	3.62E-23	0.00E+00	0.00E+00	0.00E+00	0.00E+00	0.00E+00	0.00E+00	0.00E+00	0.00E+00	0.00E+00	0.00E+00	0.00E+00
w187	4.02E+02	3.80E+02	2.01E+02	1.01E+02	3.14E+00	2.46E-02	1.20E-05	6.42E-12	1.84E-24	0.00E+00	0.00E+00	0.00E+00	0.00E+00
w189	5.78E-01	2.43E-04	0.00E+00	0.00E+00	0.00E+00	0.00E+00	0.00E+00	0.00E+00	0.00E+00	0.00E+00	0.00E+00	0.00E+00	0.00E+00
re188m	1.43E+01	1.63E-01	6.91E-23	0.00E+00	0.00E+00	0.00E+00	0.00E+00	0.00E+00	0.00E+00	0.00E+00	0.00E+00	0.00E+00	0.00E+00
re189	1.55E+00	1.46E+00	7.82E-01	3.94E-01	1.29E-02	1.07E-04	5.72E-08	3.66E-14	1.50E-26	0.00E+00	0.00E+00	0.00E+00	0.00E+00
os189m	4.73E+01	3.73E+01	2.79E+00	2.06E-01	1.73E-03	1.44E-05	7.96E-09	8.65E-11	9.70E-12	7.54E-14	4.55E-18	0.00E+00	0.00E+00
os190m	3.38E-04	7.59E-08	0.00E+00	0.00E+00	0.00E+00	0.00E+00	0.00E+00	0.00E+00	0.00E+00	0.00E+00	0.00E+00	0.00E+00	0.00E+00
os191m	8.88E+00	7.99E+00	2.49E+00	7.00E-01	1.22E-03	1.69E-07	1.45E-13	4.69E-25	0.00E+00	0.00E+00	0.00E+00	0.00E+00	0.00E+00
os193	5.57E-02	5.32E-02	3.20E-02	1.84E-02	1.16E-03	2.44E-05	5.59E-08	5.60E-13	5.63E-23	0.00E+00	0.00E+00	0.00E+00	0.00E+00
ir192m	3.52E+00	0.00E+00	0.00E+00	0.00E+00	0.00E+00	0.00E+00	0.00E+00	0.00E+00	0.00E+00	0.00E+00	0.00E+00	0.00E+00	0.00E+00

ir194m	4.96E-03	0.00E+00	0.00E+00	0.00E+00	0.00E+00	0.00E+00	0.00E+00	0.00E+00	0.00E+00	0.00E+00	0.00E+00	0.00E+00	0.00E+00
pt191	2.76E-06	2.70E-06	2.15E-06	1.68E-06	4.88E-07	8.63E-08	5.68E-09	3.28E-11	1.10E-15	1.26E-25	0.00E+00	0.00E+00	0.00E+00
pt193m	8.39E-03	8.28E-03	7.15E-03	6.09E-03	2.74E-03	8.92E-04	1.53E-04	5.46E-06	6.92E-09	2.57E-15	3.53E-28	0.00E+00	0.00E+00
pt195m	2.55E-03	2.51E-03	2.15E-03	1.81E-03	7.61E-04	2.27E-04	3.39E-05	9.25E-07	6.89E-10	7.83E-17	1.01E-30	0.00E+00	0.00E+00

Table A 4. Activities (Ci) as function of cooling time per gram of W-La_2O_3 material irradiated in HFIR for 10 cycles

W-La_2O_3	**0.0 h**	**2.0 h**	**24.0 h**	**48.0 h**	**168.0 h**	**336.0 h**	**600.0 h**	**1100.0 h**	**2100.0 h**	**4320.0 h**	**8760.0 h**	**17520 h**
w185	4.07E+01	4.07E+01	4.03E+01	4.00E+01	3.82E+01	3.58E+01	3.23E+01	2.67E+01	1.82E+01	7.73E+00	1.40E+00	4.83E-02
re188	5.81E+02	5.36E+02	2.21E+02	8.59E+01	4.82E+00	3.93E+00	3.52E+00	2.86E+00	1.89E+00	7.55E-01	1.20E-01	3.20E-03
w188	4.47E+00	4.47E+00	4.43E+00	4.38E+00	4.17E+00	3.89E+00	3.49E+00	2.84E+00	1.87E+00	7.48E-01	1.19E-01	3.17E-03
ir192	1.76E-01	1.75E-01	1.74E-01	1.72E-01	1.64E-01	1.54E-01	1.39E-01	1.14E-01	7.72E-02	3.24E-02	5.70E-03	1.85E-04
w181	1.06E-02	1.06E-02	1.06E-02	1.05E-02	1.02E-02	9.80E-03	9.20E-03	8.17E-03	6.44E-03	3.79E-03	1.32E-03	1.63E-04
pt193	5.93E-05	5.93E-05	5.96E-05	5.99E-05	6.07E-05	6.12E-05	6.14E-05	6.13E-05	6.12E-05	6.10E-05	6.06E-05	5.98E-05
ir194	3.35E+00	3.11E+00	1.41E+00	5.96E-01	7.98E-03	2.45E-05	5.45E-06	5.41E-06	5.34E-06	5.19E-06	4.89E-06	4.36E-06
os194	5.49E-06	5.49E-06	5.49E-06	5.49E-06	5.48E-06	5.47E-06	5.45E-06	5.41E-06	5.34E-06	5.19E-06	4.89E-06	4.36E-06
os185	2.24E-04	2.24E-04	2.22E-04	2.21E-04	2.13E-04	2.02E-04	1.86E-04	1.59E-04	1.17E-04	5.90E-05	1.50E-05	1.01E-06
ta182	5.22E-05	5.21E-05	5.19E-05	5.15E-05	5.00E-05	4.79E-05	4.49E-05	3.96E-05	3.08E-05	1.76E-05	5.75E-06	6.34E-07
ce139	1.48E-05	1.48E-05	1.48E-05	1.47E-05	1.43E-05	1.38E-05	1.31E-05	1.18E-05	9.55E-06	5.99E-06	2.36E-06	3.76E-07
re186	5.83E+01	5.74E+01	4.84E+01	4.02E+01	1.58E+01	4.29E+00	5.52E-01	1.14E-02	4.86E-06	5.85E-08	5.85E-08	5.85E-08
re184	5.82E-06	5.81E-06	5.71E-06	5.61E-06	5.12E-06	4.51E-06	3.71E-06	2.58E-06	1.30E-06	3.92E-07	1.14E-07	2.47E-08
ce141	8.66E-02	8.64E-02	8.48E-02	8.30E-02	7.46E-02	6.43E-02	5.09E-02	3.26E-02	1.34E-02	1.87E-03	3.61E-05	1.51E-08
pr144	2.26E-05	2.98E-07	2.42E-08	2.42E-08	2.39E-08	2.35E-08	2.28E-08	2.17E-08	1.96E-08	1.57E-08	9.99E-09	4.11E-09
pr144m	1.56E-05	3.81E-10	2.31E-10	2.31E-10	2.28E-10	2.24E-10	2.18E-10	2.07E-10	1.87E-10	1.50E-10	9.54E-11	3.92E-11
hf181	3.34E-06	3.34E-06	3.29E-06	3.24E-06	2.98E-06	2.66E-06	2.22E-06	1.58E-06	8.00E-07	1.76E-07	8.56E-09	2.19E-11
os191	5.83E+00	5.84E+00	5.81E+00	5.62E+00	4.51E+00	3.29E+00	2.01E+00	7.86E-01	1.21E-01	1.87E-03	4.53E-07	3.32E-14
ir191m	5.83E+00	5.84E+00	5.81E+00	5.62E+00	4.51E+00	3.29E+00	2.01E+00	7.86E-01	1.21E-01	1.87E-03	4.53E-07	3.32E-14
pr143	1.12E-04	1.12E-04	1.12E-04	1.09E-04	8.83E-05	6.21E-05	3.54E-05	1.22E-05	1.45E-06	1.29E-08	1.02E-12	8.12E-21
ir193m	4.68E-01	4.66E-01	4.39E-01	4.11E-01	2.95E-01	1.86E-01	9.03E-02	2.29E-02	1.48E-03	3.35E-06	1.72E-11	6.33E-22
ir190	8.13E-06	8.09E-06	7.67E-06	7.23E-06	5.39E-06	3.57E-06	1.87E-06	5.48E-07	4.72E-08	2.04E-10	3.83E-15	1.80E-24
n 16	4.33E-05	0.00E+00	0.00E+00	0.00E+00	0.00E+00	0.00E+00	0.00E+00	0.00E+00	0.00E+00	0.00E+00	0.00E+00	0.00E+00
la140	9.02E+00	8.71E+00	5.97E+00	3.95E+00	5.01E-01	2.78E-02	2.96E-04	5.46E-08	3.34E-11	2.19E-13	9.40E-18	0.00E+00
la141	1.88E-02	1.32E-02	2.70E-04	3.87E-06	2.36E-15	2.96E-28	0.00E+00	0.00E+00	0.00E+00	0.00E+00	0.00E+00	0.00E+00
ce139m	7.60E-05	0.00E+00	0.00E+00	0.00E+00	0.00E+00	0.00E+00	0.00E+00	0.00E+00	0.00E+00	0.00E+00	0.00E+00	0.00E+00
ce143	1.34E-04	1.28E-04	8.07E-05	4.88E-05	3.93E-06	1.16E-07	4.56E-10	1.27E-14	9.80E-24	0.00E+00	0.00E+00	0.00E+00
pr140	1.14E-06	1.30E-11	1.07E-11	8.74E-12	3.12E-12	7.40E-13	7.71E-14	1.06E-15	2.01E-19	0.00E+00	0.00E+00	0.00E+00
pr142	1.98E-02	1.85E-02	8.31E-03	3.48E-03	4.49E-05	1.02E-07	7.10E-12	9.53E-20	0.00E+00	0.00E+00	0.00E+00	0.00E+00
pr142m	6.93E-03	2.33E-05	0.00E+00	0.00E+00	0.00E+00	0.00E+00	0.00E+00	0.00E+00	0.00E+00	0.00E+00	0.00E+00	0.00E+00
hf179m	1.08E-06	0.00E+00	0.00E+00	0.00E+00	0.00E+00	0.00E+00	0.00E+00	0.00E+00	0.00E+00	0.00E+00	0.00E+00	0.00E+00
ta182m	5.99E-06	0.00E+00	0.00E+00	0.00E+00	0.00E+00	0.00E+00	0.00E+00	0.00E+00	0.00E+00	0.00E+00	0.00E+00	0.00E+00
ta183	1.37E-02	1.36E-02	1.20E-02	1.05E-02	5.30E-03	2.05E-03	4.59E-04	2.70E-05	9.38E-08	3.25E-13	3.91E-24	0.00E+00
w183m	5.97E+01	6.91E-04	6.10E-04	5.33E-04	2.70E-04	1.04E-04	2.34E-05	1.38E-06	4.78E-09	1.66E-14	2.00E-25	0.00E+00
w185m	1.62E-01	3.79E-23	0.00E+00	0.00E+00	0.00E+00	0.00E+00	0.00E+00	0.00E+00	0.00E+00	0.00E+00	0.00E+00	0.00E+00
w187	4.37E+02	4.13E+02	2.19E+02	1.09E+02	3.42E+00	2.67E-02	1.30E-05	6.97E-12	2.00E-24	0.00E+00	0.00E+00	0.00E+00
w189	6.28E-01	2.64E-04	0.00E+00	0.00E+00	0.00E+00	0.00E+00	0.00E+00	0.00E+00	0.00E+00	0.00E+00	0.00E+00	0.00E+00
re188m	1.56E+01	1.78E-01	7.50E-23	0.00E+00	0.00E+00	0.00E+00	0.00E+00	0.00E+00	0.00E+00	0.00E+00	0.00E+00	0.00E+00
re189	1.68E+00	1.59E+00	8.49E-01	4.28E-01	1.40E-02	1.16E-04	6.21E-08	3.97E-14	1.63E-26	0.00E+00	0.00E+00	0.00E+00
os189m	5.13E+01	4.05E+01	3.03E+00	2.24E-01	1.88E-03	1.56E-05	8.64E-09	9.40E-11	1.05E-11	8.19E-14	4.94E-18	0.00E+00
os190m	3.67E-04	8.24E-08	0.00E+00	0.00E+00	0.00E+00	0.00E+00	0.00E+00	0.00E+00	0.00E+00	0.00E+00	0.00E+00	0.00E+00
os191m	9.64E+00	8.67E+00	2.71E+00	7.60E-01	1.33E-03	1.83E-07	1.57E-13	5.09E-25	0.00E+00	0.00E+00	0.00E+00	0.00E+00
os193	6.04E-02	5.77E-02	3.48E-02	2.00E-02	1.26E-03	2.64E-05	6.06E-08	6.08E-13	6.11E-23	0.00E+00	0.00E+00	0.00E+00
ir192m	3.82E+00	0.00E+00	0.00E+00	0.00E+00	0.00E+00	0.00E+00	0.00E+00	0.00E+00	0.00E+00	0.00E+00	0.00E+00	0.00E+00
ir194m	5.38E-03	0.00E+00	0.00E+00	0.00E+00	0.00E+00	0.00E+00	0.00E+00	0.00E+00	0.00E+00	0.00E+00	0.00E+00	0.00E+00
pt191	2.99E-06	2.93E-06	2.34E-06	1.82E-06	5.29E-07	9.37E-08	6.17E-09	3.56E-11	1.19E-15	1.37E-25	0.00E+00	0.00E+00
pt193m	9.11E-03	8.99E-03	7.76E-03	6.61E-03	2.97E-03	9.68E-04	1.66E-04	5.93E-06	7.52E-09	2.79E-15	3.83E-28	0.00E+00
pt195m	2.77E-03	2.73E-03	2.33E-03	1.96E-03	8.26E-04	2.46E-04	3.68E-05	1.00E-06	7.48E-10	8.50E-17	1.10E-30	0.00E+00
pt197	3.34E-05	3.12E-05	1.45E-05	6.29E-06	9.62E-08	2.76E-10	2.79E-14	7.57E-22	0.00E+00	0.00E+00	0.00E+00	0.00E+00
pt197m	1.79E-06	7.48E-07	5.12E-11	1.47E-15	0.00E+00	0.00E+00	0.00E+00	0.00E+00	0.00E+00	0.00E+00	0.00E+00	0.00E+00
au199	9.78E-06	9.60E-06	7.84E-06	6.29E-06	2.08E-06	4.44E-07	3.92E-08	3.93E-10	3.97E-14	5.35E-23	0.00E+00	0.00E+00
total	**1.29E+03**	**1.13E+03**	**5.59E+02**	**2.98E+02**	**7.65E+01**	**5.50E+01**	**4.42E+01**	**3.41E+01**	**2.23E+01**	**9.28E+00**	**1.65E+00**	**5.51E-02**

Table A 5. Activities (Ci) as function of cooling time per gram of WRe material irradiated in HFIR for 10 cycles

WRe	**0.0 h**	**2.0 h**	**24.0 h**	**48.0 h**	**168.0 h**	**336.0 h**	**600.0 h**	**1100.0 h**	**2100.0 h**	**4320.0 h**	**8760.0 h**	**17520 h**	**26280 h**
w185	3.38E+01	3.37E+01	3.35E+01	3.31E+01	3.17E+01	2.97E+01	2.68E+01	2.21E+01	1.51E+01	6.41E+00	1.16E+00	4.00E-02	1.38E-03
re188	6.19E+02	5.71E+02	2.35E+02	9.06E+01	4.14E+00	3.26E+00	2.92E+00	2.37E+00	1.57E+00	6.26E-01	9.96E-02	2.65E-03	7.07E-05
w188	3.70E+00	3.70E+00	3.67E+00	3.63E+00	3.46E+00	3.22E+00	2.89E+00	2.35E+00	1.55E+00	6.20E-01	9.86E-02	2.63E-03	7.00E-05
ir192	5.11E-01	5.11E-01	5.06E-01	5.02E-01	4.79E-01	4.48E-01	4.04E-01	3.32E-01	2.25E-01	9.43E-02	1.66E-02	5.39E-04	1.75E-05
pt193	2.21E-04	2.21E-04	2.22E-04	2.23E-04	2.26E-04	2.28E-04	2.28E-04	2.28E-04	2.28E-04	2.27E-04	2.25E-04	2.22E-04	2.19E-04
w181	8.49E-03	8.49E-03	8.44E-03	8.39E-03	8.16E-03	7.84E-03	7.36E-03	6.53E-03	5.15E-03	3.03E-03	1.05E-03	1.31E-04	1.62E-05
ir194	1.05E+01	9.78E+00	4.44E+00	1.87E+00	2.51E-02	7.98E-05	2.01E-05	2.00E-05	1.97E-05	1.92E-05	1.81E-05	1.61E-05	1.44E-05
os194	2.03E-05	2.03E-05	2.03E-05	2.03E-05	2.02E-05	2.02E-05	2.01E-05	2.00E-05	1.97E-05	1.92E-05	1.81E-05	1.61E-05	1.43E-05
os185	1.15E-03	1.15E-03	1.14E-03	1.13E-03	1.09E-03	1.04E-03	9.56E-04	8.20E-04	6.02E-04	3.03E-04	7.71E-05	5.17E-06	3.46E-07

ta182	4.19E-05	4.18E-05	4.16E-05	4.14E-05	4.01E-05	3.85E-05	3.60E-05	3.17E-05	2.47E-05	1.41E-05	4.61E-06	5.09E-07	5.61E-08
re186	5.46E+01	5.38E+01	4.53E+01	3.76E+01	1.48E+01	4.02E+00	5.17E-01	1.06E-02	4.63E-06	1.31E-07	1.31E-07	1.31E-07	1.31E-07
re184	7.21E-06	7.20E-06	7.08E-06	6.95E-06	6.35E-06	5.59E-06	4.60E-06	3.20E-06	1.62E-06	4.86E-07	1.42E-07	3.07E-08	6.87E-09
hf181	2.71E-06	2.70E-06	2.66E-06	2.62E-06	2.41E-06	2.15E-06	1.80E-06	1.28E-06	6.47E-07	1.43E-07	6.92E-09	1.77E-11	4.53E-14
ir191m	1.65E+01	1.66E+01	1.65E+01	1.59E+01	1.28E+01	9.32E+00	5.68E+00	2.22E+00	3.41E-01	5.30E-03	1.28E-06	9.41E-14	6.90E-21
os191	1.65E+01	1.66E+01	1.65E+01	1.59E+01	1.28E+01	9.32E+00	5.68E+00	2.22E+00	3.41E-01	5.30E-03	1.28E-06	9.41E-14	6.90E-21
ir193m	1.40E+00	1.39E+00	1.31E+00	1.22E+00	8.80E-01	5.55E-01	2.69E-01	6.83E-02	4.40E-03	9.97E-06	5.13E-11	1.89E-21	0.00E+00
ir190	2.41E-05	2.40E-05	2.27E-05	2.14E-05	1.60E-05	1.06E-05	5.53E-06	1.62E-06	1.40E-07	6.05E-10	1.13E-14	5.33E-24	0.00E+00
ta182m	4.78E-06	0.00E+00	0.00E+00	0.00E+00	0.00E+00	0.00E+00	0.00E+00	0.00E+00	0.00E+00	0.00E+00	0.00E+00	0.00E+00	0.00E+00
ta183	1.10E-02	1.09E-02	9.60E-03	8.38E-03	4.25E-03	1.64E-03	3.68E-04	2.17E-05	7.53E-08	2.61E-13	3.14E-24	0.00E+00	0.00E+00
w183m	4.83E+01	5.55E-04	4.90E-04	4.28E-04	2.17E-04	8.37E-05	1.88E-05	1.11E-06	3.84E-09	1.33E-14	0.00E+00	0.00E+00	0.00E+00
w185m	1.34E-01	3.15E-23	0.00E+00	0.00E+00	0.00E+00	0.00E+00	0.00E+00	0.00E+00	0.00E+00	0.00E+00	0.00E+00	0.00E+00	0.00E+00
w187	3.62E+02	3.42E+02	1.81E+02	9.06E+01	2.83E+00	2.21E-02	1.08E-05	5.78E-12	1.66E-24	0.00E+00	0.00E+00	0.00E+00	0.00E+00
w189	5.20E-01	2.19E-04	0.00E+00	0.00E+00	0.00E+00	0.00E+00	0.00E+00	0.00E+00	0.00E+00	0.00E+00	0.00E+00	0.00E+00	0.00E+00
re188m	1.66E+01	1.89E-01	8.00E-23	0.00E+00	0.00E+00	0.00E+00	0.00E+00	0.00E+00	0.00E+00	0.00E+00	0.00E+00	0.00E+00	0.00E+00
re189	1.65E+00	1.56E+00	8.31E-01	4.19E-01	1.37E-02	1.13E-04	6.08E-08	3.89E-14	1.59E-26	0.00E+00	0.00E+00	0.00E+00	0.00E+00
os189m	1.02E+02	8.01E+01	5.90E+00	3.87E-01	1.84E-03	1.53E-05	9.02E-09	2.79E-10	3.13E-11	2.43E-13	1.47E-17	0.00E+00	0.00E+00
os190m	8.44E-04	1.89E-07	0.00E+00	0.00E+00	0.00E+00	0.00E+00	0.00E+00	0.00E+00	0.00E+00	0.00E+00	0.00E+00	0.00E+00	0.00E+00
os191m	2.68E+01	2.41E+01	7.52E+00	2.11E+00	3.69E-03	5.09E-07	4.36E-13	1.41E-24	0.00E+00	0.00E+00	0.00E+00	0.00E+00	0.00E+00
os193	1.99E-01	1.90E-01	1.14E-01	6.58E-02	4.15E-03	8.68E-05	1.99E-07	2.00E-12	2.01E-22	0.00E+00	0.00E+00	0.00E+00	0.00E+00
ir192m	1.10E+01	0.00E+00	0.00E+00	0.00E+00	0.00E+00	0.00E+00	0.00E+00	0.00E+00	0.00E+00	0.00E+00	0.00E+00	0.00E+00	0.00E+00
ir194m	1.69E-02	0.00E+00	0.00E+00	0.00E+00	0.00E+00	0.00E+00	0.00E+00	0.00E+00	0.00E+00	0.00E+00	0.00E+00	0.00E+00	0.00E+00
pt191	1.02E-05	9.97E-06	7.95E-06	6.20E-06	1.80E-06	3.19E-07	2.10E-08	1.21E-10	4.05E-15	4.67E-25	0.00E+00	0.00E+00	0.00E+00
pt193m	3.11E-02	3.06E-02	2.65E-02	2.26E-02	1.01E-02	3.30E-03	5.68E-04	2.02E-05	2.56E-08	9.51E-15	1.31E-27	0.00E+00	0.00E+00
pt195m	1.01E-02	9.97E-03	8.50E-03	7.15E-03	3.02E-03	8.99E-04	1.34E-04	3.66E-06	2.73E-09	3.11E-16	4.02E-30	0.00E+00	0.00E+00
pt197	1.47E-04	1.38E-04	6.40E-05	2.77E-05	4.24E-07	1.22E-09	1.23E-13	3.34E-21	0.00E+00	0.00E+00	0.00E+00	0.00E+00	0.00E+00
pt197m	7.86E-06	3.29E-06	2.25E-10	6.44E-15	0.00E+00	0.00E+00	0.00E+00	0.00E+00	0.00E+00	0.00E+00	0.00E+00	0.00E+00	0.00E+00
au198	3.56E-06	3.49E-06	2.76E-06	2.13E-06	5.90E-07	9.77E-08	5.78E-09	2.73E-11	6.04E-16	2.80E-26	0.00E+00	0.00E+00	0.00E+00
au199	4.63E-05	4.54E-05	3.71E-05	2.97E-05	9.86E-06	2.10E-06	1.85E-07	1.86E-09	1.88E-13	2.53E-22	0.00E+00	0.00E+00	0.00E+00
au200	1.48E-06	2.65E-07	4.58E-11	1.88E-11	2.20E-13	4.35E-16	2.45E-20	0.00E+00	0.00E+00	0.00E+00	0.00E+00	0.00E+00	0.00E+00
total	**1.33E+03**	**1.16E+03**	**5.52E+02**	**2.94E+02**	**8.39E+01**	**5.98E+01**	**4.52E+01**	**3.17E+01**	**1.91E+01**	**7.77E+00**	**1.38E+00**	**4.62E-02**	**1.80E-03**

APPENDIX B. DOSE EQUIVALENT RATES (MREM/HR) FOR SEVERAL MPEX MATERIAL SAMPLES AS A FUNCTION OF COOLING TIME, THAT WERE IRRADIATED IN THE HFIR CENTRAL FLUX TRAP FOR 10 CYCLES

APPENDIX B. DOSE EQUIVALENT RATES (MREM/HR) FOR SEVERAL MPEX MATERIAL SAMPLES AS A FUNCTION OF COOLING TIME, THAT WERE IRRADIATED IN THE HFIR CENTRAL FLUX TRAP FOR 10 CYCLES.

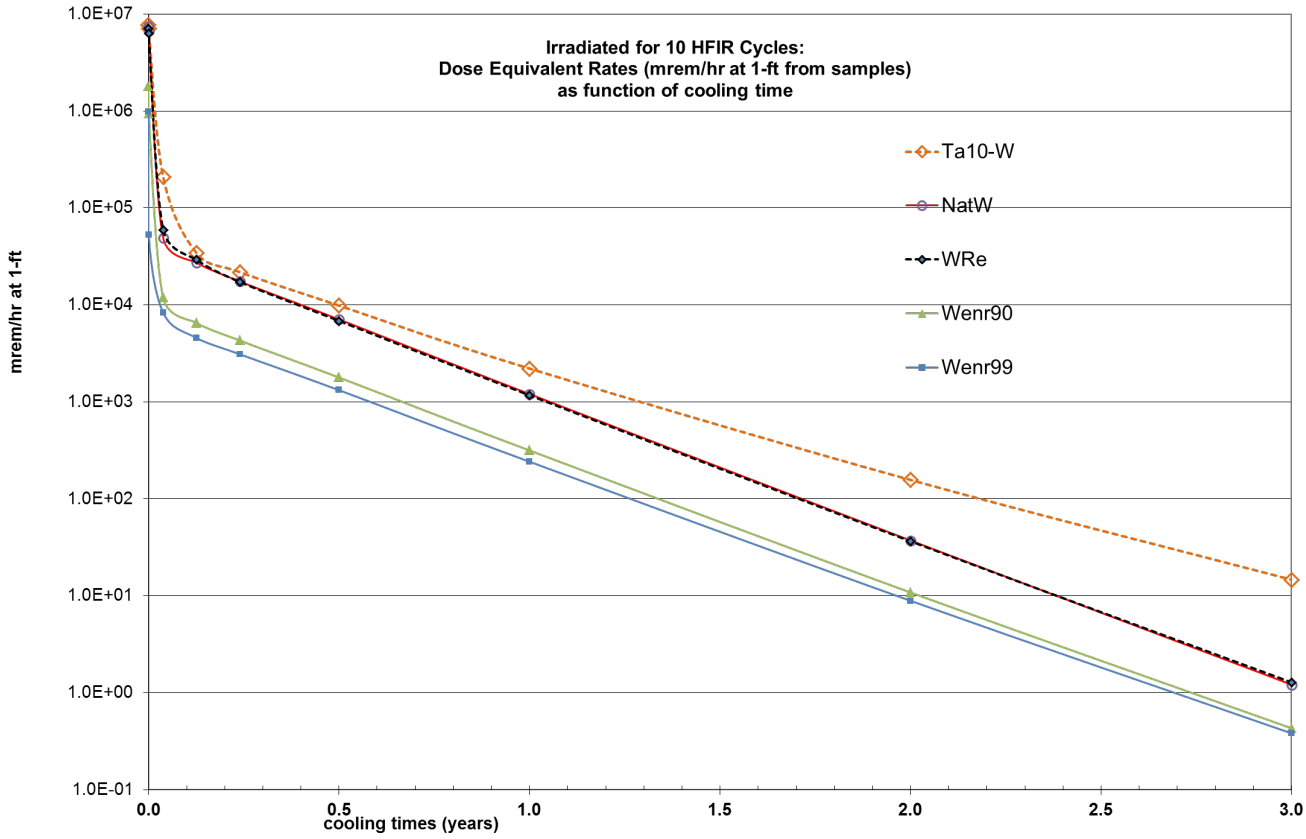

	cooling time, yrs =>	0	2.300E-04	3.836E-02	1.256E-01	2.397E-01	5.000E-01	1	2	3
ta10-w	nat W with 10 wt% Ta	7.78E+06	7.06E+06	2.08E+05	3.45E+04	2.18E+04	9.83E+03	2.21E+03	1.57E+02	1.46E+01
natw	nat W	7.50E+06	6.72E+06	4.90E+04	2.73E+04	1.75E+04	7.09E+03	1.20E+03	3.72E+01	1.21E+00
wre	nat W with 20.1 wt% Re	7.10E+06	6.35E+06	5.95E+04	2.93E+04	1.72E+04	6.84E+03	1.17E+03	3.64E+01	1.28E+00
wenr90	W enr to 90wt% W-182	1.78E+06	9.46E+05	1.18E+04	6.53E+03	4.29E+03	1.78E+03	3.15E+02	1.08E+01	4.29E-01
wenr99	W enr to 99wt% W-182	9.79E+05	5.29E+04	8.31E+03	4.57E+03	3.10E+03	1.32E+03	2.41E+02	8.87E+00	3.81E-01
			mrem/hr at 1-ft per disk							

APPENDIX C. Differences in SNS and HFIR Irradiations

APPENDIX C. DIFFERENCES IN SNS AND HFIR IRRADIATIONS

For a comparison of the relative effects of irradiating tungsten samples in the flux trap region of HFIR and in a target site in SNS, a series of dose rate and radionuclide activity calculations were completed for two similar irradiation scenarios: 1) the SNS irradiation scenario (spallation neutrons and residual high-energy protons) was calculated for two years at the center of the SNS target location designated "rod_3 cm" with a nominal beam power of 1.4 MW [19] and 2) the corresponding HFIR neutron irradiation was taken to be 14 HFIR cycles (equivalent to seven cycles per year in HFIR, for two years). The irradiation time duration for this comparison was taken to be two full years for both SNS and HFIR, for consistency between the simulation models.

In Table C 1, the most active radionuclides in the tungsten samples (and the percentage differences in their activities) are tabulated for the SNS [19] and for the HFIR irradiations. As shown in Table C 1, the radionuclide compositions of the irradiated tungsten samples are very different for the two irradiations because the reaction channels are very different for neutron irradiations in HFIR and neutron/proton irradiations in SNS. The DPA damage level for the natural tungsten samples is similar in the HFIR irradiation (14 DPA) and in the SNS irradiation (13 DPA).

Table C 1. Differences in radionuclide composition (in terms of percentage of total activity) for natural tungsten samples irradiated for two years in HFIR and in SNS. The 12 topmost active radionuclides are listed for each case, at zero cooling and after 1-year cooling periods.

SNS: Zero Cooling		HFIR: Zero Cooling		SNS: 1-Yr Cooling		HFIR: 1-Yr Cooling	
W-187	45.5	Re-188	42.5	W-185	21.0	W-185	89.5
W-183m	24.0	W-187	27.5	W-181	19.9	Re-188	4.80
W-185	5.35	Os-189m	6.32	H-3	16.7	W-188	4.75
Re-188	2.65	Re-186	6.07	Ta-179	12.4	Ir-192	0.916
W-185m	1.60	W-183m	4.61	Lu-173	7.07	W-181	0.0602
W-181	1.41	W-185	4.15	Lu-172	4.93	Pt-193	0.0193
Re-186	0.991	Os-191m	2.24	Hf-172	4.88	Ir-194	0.00158
Ta-178	0.385	Os-191	1.42	Sm-145	2.00	Os-194	0.00158
W-179	0.384	Ir-191m	1.42	Pm-143	1.79	Os-185	0.00126
Ta-177	0.357	Re-188m	1.14	Dy-159	1.48	Ta-182	0.000351
Ta-183	0.353	Ir-194	1.03	Ce-139	1.06	Os-191	0.000082
Yb-169	0.310	Ir-192m	0.961	Ta-182	0.972	Ir-191m	0.000082

radionuclide compositions for the two irradiation samples are so different in these two irradiation environments, the gamma source strengths and spectra from the two tungsten samples yield different trends in the dose rates. Table C 2 presents comparisons in the rem/hr dose rates, at a distance of 1 ft (about 30 cm) from the SNS and HFIR samples at various cooling times. To provide appropriate results for comparison, the dose rates are presented in rem/hr and are for tungsten samples of 1 cm^3 (about 19.3 g in mass). Note that this simulation sample size is much larger than the sample size considered for the HFIR disk sample irradiation results presented in the neutronics section.

Table C 2. Dose rate comparisons for tungsten sample irradiations in HFIR and SNS. For this comparison, the dose rates are in rem/hr for 1 cm^3 of tungsten sample (approx. 19 g of tungsten). This comparison was for two full years of irradiation in SNS and HFIR.

Cooling time	Zero	6 months	1 year
Enriched W (90 wt% W-182) in HFIR	12600	21.4	4.0
Natural W in HFIR	49300	64.6	10.6
Natural W in SNS	2990	21.0	12.0

In comparing the behavior of natural tungsten irradiated in HFIR or in SNS for two years, it is apparent that the dose rate from the HFIR sample is much higher at shorter cooling times but will be less than that from SNS after one year of cooling.

Similar length irradiations in HFIR and SNS were seen to produce about the same level of DPA damage in the irradiated samples. The dose rates for the samples from HFIR were found to be significantly higher for short cooling times but less than those for the SNS-irradiated samples after a cooling time of one year. The use of tungsten enriched in ^{182}W (90–99 wt%) significantly reduces the sample activity and dose rate.

APPENDIX D. MPEX SYSTEM SAFETY ISSUES OPERATING NEAR A MAGNETIC FIELD

APPENDIX D. MPEX SYSTEM SAFETY ISSUES OPERATING NEAR A MAGNETIC FIELD

The MPEX system operates under a maximum super conducting magnetic field of 2.25 Tesla. There are areas near the MPEX system with a field of 2000 Gauss where human presence is needed while the field is 'ON'. Since the field cannot be shut down unless it is in undergoing scheduled/unscheduled maintenance or target change out is taking place, a human may have to work in the close proximity to such magnetic field.

Disconnecting water lines for target cooling, change out of the target under certain scenarios, and checking out diagnostic tools are possible reason for a person to be near such magnetic fields.

Based on data from American Conference on Governmental Industrial Hygienists following are the recommended exposure limits.

Significant Sources – Direct current intensive processes (e.g., aluminum extraction & chlor-alkali plants), magnetic resonance imaging (MRI)* in healthcare, and nuclear magnetic resonance (NMR) facilities with superconducting magnets in analytical labs, Electromagnets and large magnets enclosed in equipment such as lab etchers.
*Also a radiofrequency (RF) radiation exposure source for patients

Biological Effects – No specific target organ(s) identified. Possible displacement and /or functional impairment of ferro-magnetic medical implants, including cardiac pacemakers and implantable cardioverter-defibrillators (ICDs), potential for magneto-hydrodynamic effects (changes in hydrostatic pressure and electrical potentials across vessels in the human vasculature) on blood flow. Body movement in the stray fields near MRIs can produce adverse effects on neurocognitive performance and balance.

Exposure Guidelines ACGIH 2012 TLVs	**Ceiling Value**
Whole Body (general workplace)	2 Tesla (T)
Whole Body (special worker training and controlled workplace environment)	8 T
Limbs	20 T
Medical device wearers	0.5 mT

Ancillary Hazards – Magnet weights require substantial structural support. Ferromagnetic (metal) objects (e.g., tools, gas cylinders, pocketknives, key rings, etc.) can be accelerated with great force and speed towards large magnets causing personal injury. Objects striking superconducting magnets can cause them to quench (become resistive); the rapid vaporization of the cryogenic liquid(s) in the magnets can displace air in the laboratory creating an asphyxiation hazard.

Control Measures – Isolation / controlled access to MRI and NMR units to keep embedded medical device wearers outside of 5 gauss (0.5 mT) magnetic field line and prevent ferro-magnetic objects from getting inside that line. Signage will be placed to warn potential entrants into areas occupied by the above units of the cited hazards about the potential damage to magnetic media (credits cards, hard disk drives, ID cards, etc.). Superconducting magnets should have the asphyxiation hazard evaluated.

Worker Safety for MPEX workers:

1) A boundary of 5Cgauss or (0.5mT) for exposure will be delimited around the MPEX area to warn

employees of strong magnetic field presence.

2) Due to this high field, employees entering this area to perform work will have to wear company cloths (cotton) with no magnetic (ferromagnetic) tools. Watches, phones, pens, etc. will have to left outside the magnetized area.
3) Tools that are taken into the area needs to undergo prior approval before being taken inside
4) 316 series stainless steel or equivalent tools are preferred inside the magnetic field due to their low magnetic permeability.
5) Magnetic data storage disks, credit cards, proximity cards etc. should not be taken inside the magnetic field boundary since the potential exist for them to be destroyed.
6) Personnel wearing pacemakers are no allowed inside the magnetic field boundary

References and Additional Information

American Conference of Governmental Industrial Hygienists (ACGIH): Static Magnetic Fields TLV Documentation (2012).

AIHA Nonionizing Radiation Guide Series – General Concepts for Nonionizing Radiation Protection

Peter H. Wald and Greg M. Stave (eds.): Physical and Biological Agents of the Workplace, 2nd Edition. New York: John Wiley & Sons, 2002.

R.T. Hitchcock, C.E. Moss, W.E. Murray, R.M. Patterson, and R. James Rockwell: Chapter 22, Nonionizing Radiation in The Occupational Environment: Its Evaluation, Control, and Management, 2nd Edition. Fairfax, VA: AIHA, 2003.

APPENDIX E. Alternative approach for linear motion of the target into PMI chamber

APPENDIX E. ALTERNATIVE APPROACH FOR LINEAR MOTION OF THE TARGET INTO PMI CHAMBER

Initial design for the linear actuation of the target was a telescoping tube (see **Error! Reference source not found.**). The tube was pushed in and out by a large bellows at the back of the TEC chamber. Since there are two gate valves and a hydraulic clamping system between PMI chamber and TEC, the telescoping tube have to translate about 1.6 m before the target reaches the intended location inside the PMI chamber. Since bellows can only extend about 40% of its nominal length, to obtain a 1.6 m stroke, the bellows have to be 4 m long. This requires a very large bellow for actuation, which will be very difficult to incorporate into the design while also making it impossible for the TEC chamber to be on a rail for transport into an adjacent room.

The cooling lines for the target in this design were incorporated into the telescoping tube. To obtain the linear translation of the tube, the cooling lines were coiled in a helical fashion inside the tube. The tubes then would extend and contract inside the telescoping tube during the actuation. The cooling waterlines were for cooling the target were attached to the end of the telescoping tube. This design did not incorporate a 15° target and no provisions were provided for changing the target periodically. The entire tungsten piece had to be removed for changing the sample. The new design incorporates a cable tray/hose carrier method compared to the helical coolant lines used in this earlier version.

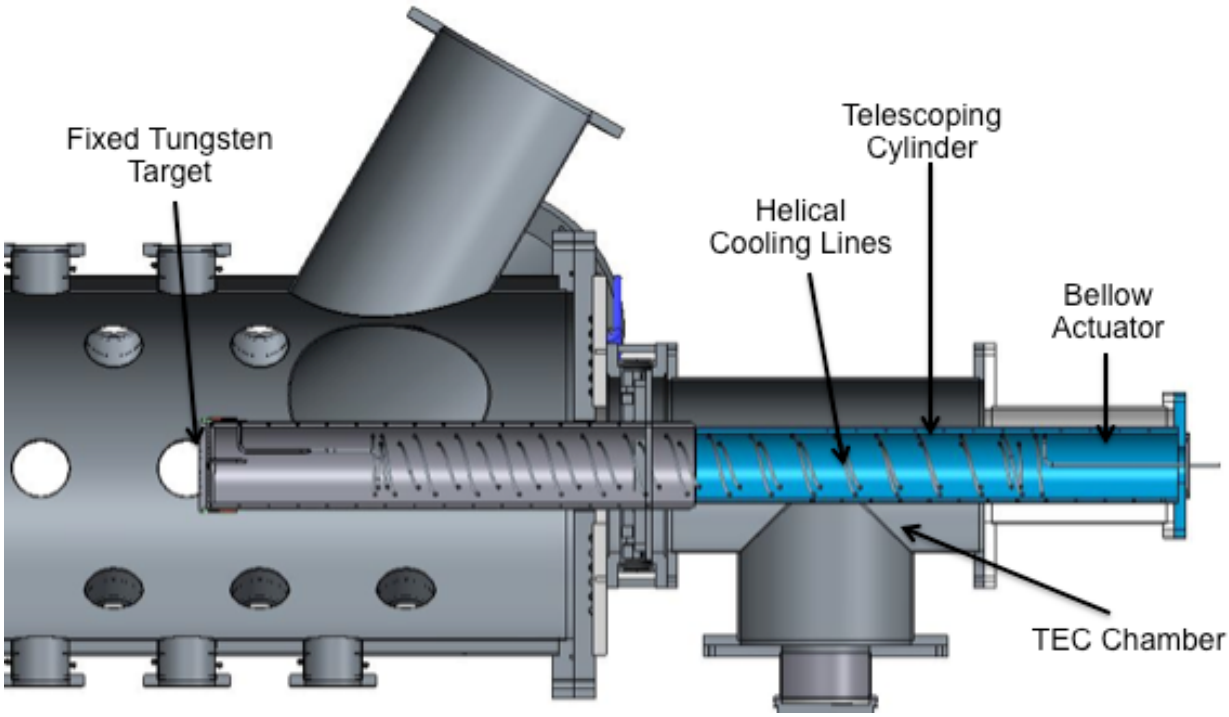

Fig. J 1 Earlier Design of the Telescoping Tubular Actuator